Impact of biophysical cues on brain organoid growth and development

by

Camille Cassel de Camps
Department of Biomedical Engineering

McGill University
Montréal, Québec, Canada
August 2023

A thesis submitted to McGill University in partial fulfillment of the requirements to the degree of Doctor of Philosophy

Abstract

Accumulating evidence illustrates the importance of biophysical cues such as mechanical properties and stresses in embryonic development of organs, as well as disease progression. Researchers in the tissue engineering field are increasingly calling for the incorporation of these cues into strategies for biophysical guidance of engineered tissue development, both for generating improved experimental models as well as generating tissue for regenerative medicine purposes. However, studies of the influence of such biophysical cues on brain organoids are limited. Brain organoids are self-organizing, 3D tissue-engineered models of the human brain that are grown from stem cells and mimic certain aspects of embryonic brain development. These important models are the current state-of-the-art in neuroscience, enabling studies in human models that are impossible with other systems. This thesis explores the effects of several biophysical cues on brain organoid growth and development, namely matrix stiffness and geometry, overall and at the organoid periphery. First, the material properties of the hydrogel used to encapsulate brain organoids were modified to change the physical nature of the organoid microenvironment. Stiffer hydrogels yielded smaller midbrain organoids with increased neuronal maturation, and altered internal microarchitectures; specifically, characteristic developmental structures known as neural rosettes were smaller and fewer. Next, to manipulate overall geometry of pre-formed organoids, a compressive hydrogel molding platform was developed. Using this platform, breast cancer spheroids were molded into simple shapes, and brain organoids were molded into rings, by shaping the organoid around a post to fuse with itself. Tissue markers suggested these ring-shaped organoids differentiated as expected within these devices, indicating the platform could be used to mold tissue building blocks into a variety of shapes. Lastly, a system was engineered to create assembloids from brain organoids with passively shaped peripheries, and investigate the influence of the peripheral geometry. The results suggested that axonal projections from midbrain organoids exhibited target-seeking behaviour, and that geometry influences cell migration out of cerebral organoids. The platform could be used to observe such cellular behaviours in culture models of neural circuit formation. Overall, these new tools and insights could lead to integration of biophysical cues into brain

organoid strategies, which may improve them as experimental models, and yield further knowledge into developmental processes.

Résumé

Des preuves de plus en plus nombreuses illustrent l'importance des indices biophysiques tels que les propriétés mécaniques et les contraintes dans le développement embryonnaire des organes, ainsi que dans la progression des maladies. Les chercheurs dans le domaine de l'ingénierie tissulaire demandent de plus en plus l'incorporation de ces indices dans les stratégies de guidage biophysique du développement des tissus artificiels, à la fois pour générer des modèles expérimentaux améliorés et pour générer des tissus à des fins de médecine régénérative. Cependant, les études sur l'influence de ces signaux biophysiques sur les organoïdes cérébraux sont limitées. Les organoïdes cérébraux sont des modèles de cerveau humain auto-organisés, fabriqués en 3D à partir de cellules souches et reproduisant certains aspects du développement du cerveau embryonnaire. Ces modèles importants constituent l'état de l'art actuel en neurosciences, permettant des études sur des modèles humains impossibles à réaliser avec d'autres systèmes. Cette thèse explore les effets de plusieurs indices biophysiques sur la croissance et le développement des organoïdes cérébraux, à savoir la rigidité et la géométrie de la matrice, globalement et à la périphérie de l'organoïde. Tout d'abord, les propriétés matérielles de l'hydrogel utilisé pour encapsuler les organoïdes cérébraux ont été modifiées afin de changer la nature physique du microenvironnement des organoïdes. Des hydrogels plus rigides ont produit des organoïdes de cerveau moyen plus petits avec une maturation neuronale accrue et des microarchitectures internes modifiées ; en particulier, les structures de développement caractéristiques connues sous le nom de rosettes neurales étaient plus petites et moins nombreuses. Ensuite, pour manipuler la géométrie globale des organoïdes préformés, une plateforme de moulage d'hydrogel compressif a été mise au point. Grâce à cette plateforme, des sphéroïdes de cancer du sein ont été moulés dans des formes simples et des organoïdes cérébraux ont été moulés en anneaux, en façonnant l'organoïde autour d'un poteau pour qu'il fusionne avec lui-même. Les marqueurs tissulaires suggèrent que ces organoïdes en forme d'anneau se sont différenciés comme prévu à l'intérieur de ces dispositifs, ce qui indique que la plateforme pourrait être utilisée pour mouler des édifices tissulaires dans une variété de formes. Enfin, un système a été conçu pour créer des assembloïdes à partir d'organoïdes cérébraux avec des périphéries de forme passive, et pour étudier l'influence de la géométrie périphérique. Les

résultats suggèrent que les projections axonales des organoïdes du mésencéphale présentent un comportement de recherche de cible et que la géométrie influence la migration des cellules hors des organoïdes cérébraux. La plateforme pourrait être utilisée pour observer de tels comportements cellulaires dans des modèles de culture de formation de circuits neuronaux. Dans l'ensemble, ces nouveaux outils et connaissances pourraient conduire à l'intégration de repères biophysiques dans les stratégies des organoïdes cérébraux, ce qui pourrait les améliorer en tant que modèles expérimentaux et permettre d'approfondir les connaissances sur les processus de développement.

Acknowledgements

It is no secret that doing PhD is a challenging journey, and it is by no means a solo endeavour. I would like to thank all the people who helped me get to this point, in all the ways that they did, providing support, advice, and laughter.

Thank you to my supervisor, Chris Moraes, for taking a chance on a life sciences student who hadn't taken a physics class in 6 years. Thank you for your scientific enthusiasm, your much-needed support, and guidance.

Thank you to Tom Durcan for welcoming me into my second lab home, providing guidance and words of encouragement, and telling me that everything would work out in the end.

Thank you to all the labmates I have had the pleasure of working with and getting to know over the years. In the Moraes lab, to Sarah, my first lab friend. To Wontae, always ready to help when I asked (which was a lot). To Steph, for your frank and grounded words of advice. To Ray, for commiserating over stem cells and quietly being there for me. To Nikita, for our late-night labwork and chats, and your paramedic entertainment. To Chen, my first student, for your TED talks, the coffee, and surprisingly helpful advice. To Christina, for your kind presence and generosity, support in the form of shared panic, telling each other to go home, and baked goods. To Sabra, for your guidance in the final stages. To Ben for your calming presence, and Susie for your kindness, and both for the treats. To the undergrads of summer 2023, for reminding me what it was like in the beginning. And to all the other labmates who I crossed paths with over the years, who helped me or shared good times, thank you.

At the Neuro, to Vi, Meghna, Paula, and Maria, who were my organoid support crew. To Chanshuai, Narges, Carol, and Cecilia for all your help, and Vince and Valerio for making me laugh. Thank you to all the lab members who made this a place I looked forward to.

All in all, thank you to all lab members for your help in and outside of the lab, and for putting up with my antics as I transitioned from an excited and eager, but naïve, first year student to a, hopefully, wiser terminal stage PhD candidate.

Thank you to all the wonderful people I met in the BBME program, and to all my friends. I am so incredibly grateful for your friendship and support – especially to Ana and Giulia, who saw me through many ups and downs.

To my family, I absolutely could not have done this without you, thank you for everything – my parents Diane and Paul, for all the support in all the ways, my sister Celeste for being there, and my uncle Craig for all the snacks.

Thank you to Harry Styles and Taylor Swift for being the constant soundtrack to my last year (and then some) of intense labwork, and to my labmates for putting up with my music choices until you couldn't anymore. I would also like to acknowledge ChatGPT for waiting until the very end of my PhD to remind me that I am dispensable.

In much the same way that this thesis does not contain all the work of the past 5 years, these acknowledgments cannot truly cover all the people I met and the support they provided – so to all those mentioned here as well as those who aren't, thank you, with immense gratitude. These were undoubtedly some of the hardest but also best years of my life, and it is thanks to the people I met that I made it through, and had so much fun along the way.

This work was supported by funding from the National Sciences and Engineering Council, the Healthy Brains, Healthy Lives initiative, and the Vadasz Scholar McGill Engineering Doctoral Award.

Copyright acknowledgments

Table of Contents

Preface

This thesis is written in the manuscript-based format, with modifications made based on examiner request. It contains two published articles (Chapter 3 and 4), and one manuscript in preparation (Chapter 5).

First author publications originating from this thesis

1. Hydrogel Mechanics Influence the Growth and Development of Embedded Brain Organoids
   C Cassel de Camps, S Aslani, N Stylianesis, H Nami, NV Mohamed, TM Durcan, C Moraes
   ACS Appl Bio Mater 5 (2022). https://doi.org/10.1021/acsabm.1c01047

2. Compressive molding of engineered tissues via thermoresponsive hydrogel devices
   C Cassel de Camps, S Mok, E Ashby, C Li, P Lépine, TM Durcan, C Moraes
   Lab Chip (2023). https://doi.org/10.1039/D3LC00007A

3. Microfabricated dynamic brain organoid cocultures to assess the effects of surface geometry on assembloid formation
   C Cassel de Camps, S Rostami, V Xu, C Li, P Lépine, TM Durcan, C Moraes
   Manuscript in preparation

Additional publications

1. Applying hiPSCs and biomaterials towards an understanding and treatment of traumatic brain injury
   M Lacalle-Aurioles, **C Cassel de Camps**, CE Zorca, LK Beitel, TM Durcan
   Front Cell Neurosci 14, 594304 (2020). https://doi.org/10.3389/fncel.2020.594304

2. Pro-invasive mechanoresponses of patient derived triple negative breast cancer associated fibroblasts are AhR-dependent and correlate with disease state
   G Brewer, P Savage, AN Fortier, H Zhao, A Pacis, YCD Wang, D Zuo, M de Nobrega, A

Pedersen, **C Cassel de Camps**, M Souleimanova, V Muñoz Ramos, I Ragoussis, M Park, C Moraes

Manuscript in preparation

Original contributions to knowledge

This thesis explores the impact of multiple biophysical cues in the microenvironment on brain organoids. Specifically, the stiffness of the surrounding 3D environment, triggerable geometric constraint, and passive geometric constraint at the interface of coculture.

First, I modify the stiffness of the extracellular matrix used to support brain organoid growth, to probe how this would influence their development. This was the first time this question was investigated in this model system, and I found that brain organoid growth, development, and maturation were affected. Organoids grown in stiff matrices were smaller and rounder, and developed fewer and smaller neural rosettes, which are characteristic structures in brain organoids mimicking *in vivo* embryonic brain development. In addition, I found an increased proportion of mature neurons in these organoids. These results demonstrate that the stiffness of the surrounding matrix impacts brain organoid self-organizing capacity, which is a defining feature of organoid cultures, and therefore stiffness must be recognized as a critical factor to facilitate or manipulate this crucial process.

Next, I develop a platform to mold growing brain organoids into new geometries. The platform uses a thermoresponsive hydrogel to apply a shape to cultured tissues on-demand. This is a novel application of this material, capitalizing on its thermoresponsive properties in a way that had not been done before, and is a novel application of hydrogel actuators to apply 3D forces to 3D tissues in culture. I show that brain organoids can be grown long-term in these devices, and determine the factors necessary to mold brain organoids into rings, fusing with themselves to produce cohesive units. I find that this culture system allows brain organoids to differentiate as usual and does not interfere with expected developmental programming, demonstrating the suitability of the platform for molding organoids into building blocks for applications in bioassembly.

Finally, I develop coculture devices to position and passively shape growing brain organoids to explore the impact of geometry on the interaction of distinct organoid types. I design a platform to facilitate coculture of these different organoids with separate media, and optimize a PDMS casting technique to enable fabrication of these complex devices. I use these devices to implement controlled assembly of distinct brain organoid types to form assembloid

cultures, and observe that geometry influences cell migration from the organoid. I find that this platform allows growth and observation of axonal projections, which target nearby organoids. These results demonstrate its utility as a system to explore axonal target-seeking in studies of neural circuitry development, the interaction between different tissue types with defined positions and geometries, and assembloid formation.

These findings demonstrate several distinct ways that biophysical cues in the external microenvironment can be employed to manipulate brain organoid growth, development, maturation, external shape and internal architecture, and facilitate extension of single organoids to assembloid cultures.

Contribution of authors

Manuscript 1 (Chapter 3): Hydrogel Mechanics Influence the Growth and Development of Embedded Brain Organoids

Camille Cassel de Camps – designed and conducted experiments, data analysis, drafted and edited manuscript

Saba Aslani – performed preliminary rheology experiments

Nicholas Stylianesis – performed rheology experiments

Harris Nami – developed and tested CellProfiler pipeline for immunofluorescence analysis

Nguyen-Vi Mohamed – provided guidance, supervision

Thomas M. Durcan – project conceptualization, resources, supervision, edited the manuscript

Christopher Moraes – project conceptualization, resources, supervision, edited the manuscript

Manuscript 2 (Chapter 4): Compressive molding of engineered tissues via thermoresponsive hydrogel devices

Camille Cassel de Camps – project conceptualization, designed and conducted experiments, data analysis, drafted and edited manuscript

Stephanie Mok – project conceptualization, designed and conducted experiments, data analysis, edited manuscript

Emily Ashby – designed and conducted experiments, data analysis

Chen Li – designed some molds used for casting PNIPAM devices

Paula Lépine – generated organoids for some experiments

Thomas M. Durcan – resources, supervision, edited the manuscript

Christopher Moraes – project conceptualization, resources, supervision, edited the manuscript

Manuscript 3 (Chapter 5): Microfabricated dynamic brain organoid cocultures to assess the effects of surface geometry on assembloid formation

Camille Cassel de Camps – project conceptualization, designed and conducted experiments, data analysis, drafted and edited manuscript

Sabra Rostami – generated organoids for some experiments

Vanessa Xu – performed imaging of organoids growing in devices

Chen Li – assisted with mold design and PDMS casting techniques

Paula Lépine – generated organoids for some experiments

Thomas M. Durcan – resources, supervision

Christopher Moraes – project conceptualization, resources, supervision, edited the manuscript

List of figures

Chapter 1

1 Introduction

1.1 Rationale

Biophysical cues such as mechanics, forces, and geometry are crucial during organ and tissue morphogenesis, as supported by studies of development and tissue cultures. Human brain development is complex, and difficult to study. As a result, at present in neuroscience fields, brain organoids are the state-of-the-art *in vitro* human tissue-scale models. These are self-organizing, 3D tissue-engineered models of the human brain that are grown from stem cells and mimic certain aspects of embryonic brain development[1–4]. Brain organoids allow highly translational modeling not possible with 2D cell culture or non-human animals, and can enable exploration of uniquely human complexities *in vitro*; organoid models present exciting opportunities to study both healthy and diseased brain development, including currently untreatable diseases[2,3,5]. However, studies investigating the aforementioned biophysical cues in the context of brain organoids are limited, despite evidence highlighting their importance.

1.2 Thesis objectives

This thesis aims to explore the impact of several biophysical cues on brain organoid growth and development, and develop new platforms to enable this investigation. Ultimately, success of this objective could lend insights to improve brain organoids as experimental models for understanding human brain development, and neurological disease.

The specific aims of this thesis are to:

1. Explore the impact of matrix mechanics on brain organoid growth and development.
2. Create a platform to manipulate organoid shape, molding brain organoids into rings, and assess the impact of this forced geometry.
3. Develop a system to form assembloids from brain organoids with shaped peripheries, and investigate the influence of the peripheral geometry on cell behaviours.

Specifically, this work explores the biophysical cues of material stiffness, and two forms of geometry, global and peripheral, on brain organoids at the micro- and macroscale. Overall, the

technologies developed contribute new tools to the tissue engineering field, and the knowledge gained could inform strategies for studies of these biophysical cues *in vitro*.

Chapter 2

The following chapter begins with an overview of brain organoids as experimental models, including their advantages and limitations. Assembloid cocultures are discussed as an extension of organoid technology. Finally, mechanical and biophysical cues and their contributions to development are reviewed.

2 Literature review

The human brain is remarkably complex, and remarkably difficult to study. Tissue samples required to explore brain development throughout embryonic and later life stages are scarce, and raise ethical concerns[1,6–8]. Studying the human brain in children and adults presents numerous logistical challenges, in addition to ethical issues; the brain is surrounded by the blood-brain-barrier and skull, it is extremely delicate, and biopsies are practically impossible[8]. Furthering our understanding of the brain in spite of these challenges is of paramount importance due to the prevalence of neurodevelopmental, neurological, and neuropsychiatric diseases and disorders, and the high impact they impose on people's lives, healthcare systems, and social infrastructures worldwide[8,9].

2.1 Brain organoids

As a result of these challenges, neuroscience research traditionally uses *in vitro* cell cultures or animals as models, both of which have their own strengths, as well as limitations and drawbacks. Newer models employ tissue engineering strategies that enable *in vitro* development and culture of 3D human tissues. Brain organoids are 3D self-organizing cell cultures, grown from an initial aggregate of stem cells that is differentiated into neural tissue over weeks to months. When grown from human stem cells, these organoids are experimental models of the human brain that recapitulate multiple aspects of embryonic brain development. The cell types that develop match the cell types in the developing human brain, including some that are unique to humans (e.g., outer radial glia)[5,10–14], and these cells self-organize in the organoid to form neuroepithelial structures reminiscent of the neural tube and brain ventricles. These characteristic structures in organoids are called neural rosettes, and they consist of cells centred around fluid-filled lumens with accurate axial polarity and developmental patterning, mirroring their *in vivo* counterparts[3,10,11,15]. Neural progenitor cells are localized right next to the lumen, forming a

ventricular zone, and exhibit interkinetic nuclear migration during mitosis[11,15]. As progenitors divide, they give rise to neurons, which migrate away from the lumen as they differentiate and mature, and form functional synapses that participate in spontaneous or stimulated activity[16]. All these phenomena are seen in the ventricular zone in the embryo, the zone surrounding the ventricular lumen[2,15]. Organoids also reproduce inside-out neuronal layering as is seen in the human cerebral cortex, where neurons are generated in waves that migrate towards the brain surface one after the other, forming six layers of different types of neurons, all of which have been found in brain organoids[5,15].

To grow brain organoids, first 3D aggregates of stem cells are formed, called embryoid bodies (EBs), and cultured in suspension. Although there are some differences depending on the protocol, in general the EBs are led first towards the ectoderm germ layer, which is the germ layer that gives rise to the brain in embryo. They are then progressively induced towards a neural fate by timed addition of soluble factors, such as signalling molecules and growth factors[3]. Minimal media formulations, i.e. with fewer small molecules, allow intrinsic patterning to proceed and give rise to cerebral organoids, modeling the whole brain, whereas use of specific patterning factors for directed differentiation can produce a variety of brain region-specific organoids, such as forebrain, midbrain, hindbrain, striatal, hypothalamic, hippocampal, cerebellar[1,3,5,17–22]. Often organoids are embedded in an extracellular matrix (ECM) extract consisting of ECM proteins as well as growth factors that forms a hydrogel around the organoid, which provides structural support for their 3D growth and development of architectural orientation[3,23,24].

Brain organoids can be cultured for long periods of time, months to even years, and progress through developmental phases matching those of the young human brain[12,25], typically growing up to a size of ~4 mm in diameter[19,26]. They mature through stages, modeling first the embryonic brain and then the fetal brain[5,16], and even the early postnatal brain in longer term cultures, featuring multiple developmental milestones that occur during gestation and after birth[6,27]. The generation of different types of neurons and glial cells occurs in a specific temporal order, and brain organoids accurately reproduce this, with timing matching the *in vivo* human embryo[11,16,25,28]. Single cell transcriptomics show that brain organoids follow the genetic

programming of the developing human brain, corresponding to fetal and then postnatal tissue at different stages of organoid development[1,25,27,29]. All in all, the cell types, spatial organization, and behaviours of those cells, and the developmental timeline of human brain organoids parallels that of the human brain as it develops in the embryo[10,28].

2.1.1 Advantages

Brain organoids have certain advantages over traditional 2D cell cultures and animal models[24,26,28,30,31]. Body tissues and organs are 3D, and have dimensionality, topography, organized cell-cell contacts, and extracellular matrix contacts that are lacking in 2D cultures, where cells are grown in monolayers on plastic dishes. The diffusion of soluble factors, like signaling molecules or drugs, is therefore very different in cell monolayers versus living tissues. As organoids are 3D tissues, they are more similar to organs than 2D cell cultures in all these ways, and contain multiple cell types spatially organized in cytoarchitectures reminiscent of the *in vivo* organ, consequently yielding higher translational potential as model systems[18,24,32]. For example, one study on cystic fibrosis used patient-derived intestinal organoids that enabled a novel chemical-induced swelling assay, where drug correction of the disease phenotype was variable in organoids derived from different patients[33]; this assay was possible due to the lumenized structure of the organoids, and could not have been performed with 2D monolayer cultures. In the brain organoid field, stem cells derived from a patient with microcephaly produced cerebral brain organoids that were much smaller than controls; using this model system, researchers were able to identify and test a mechanism that contributes to the disorder, which is difficult to model in mice[2]. Brain organoids have also been used for drug screening, showing important differences in efficacy in monolayer versus organoid cultures[34], and one study screening for neurotoxicity found that organoids predicted toxicity with accuracy far superior to animal models[35,36]. In many use cases, brain organoids offer greater experimental power than 2D cell cultures, while still affording many of the advantages that cell cultures have over animal models – as they are still *in vitro* cultures, organoids are amenable to easy observation, manipulation and controllability, and many standard assays, and present minimal ethical issues and low costs, enabling higher throughput than animals[18,24,26,32].

Brain organoids' ability to follow intrinsic developmental programming allows the differentiation of multiple cell types in a single culture, and their capacity to self-organize means these cells model human development in ways that are not possible with 2D cultures, or in animal models[24,26,28,30–32]. The human brain is unique, and distinct from animal models in numerous ways, with differences in its morphogenesis and development, the corresponding timelines and component cell types, as well as neurological diseases[24,28,30,32]. In fact, brain organoids have been used to model some of these differences; they can be grown from animal stem cells and compared to human organoids, and uniquely human features are seen only in those grown with human cells[11]. For example, human cerebral organoids develop specific human characteristics not seen in mice, or mouse cerebral organoids, such as an inner fibre layer and an outer subventricular zone containing outer radial glia, an important cell type in human brain development[2,3,5,10,11,15]. Comparing human brain organoids to those generated from non-human primate species (chimpanzee, macaque), multiple differences were observed, such as in the gene expression levels in some cells, and timing of generation of different types of neurons, recapitulating the species-specific timing seen *in vivo*[11,37]. Brain organoids allow modeling of these uniquely human features and developmental processes, and these processes can now be studied, probed, and manipulated to improve our understanding of human brain development[24,28,32,38]. They have even been used to study evolution[1,39].

In addition, the neurological and psychiatric diseases that affect humans are often not found naturally in typical animal models, and those that can be reproduced in some way are done so with varying degrees of success and utility[28,30]. Brain organoids have been used to model Alzheimer's disease[40,41], Parkinson's disease[42,43], autism spectrum disorder[44], schizophrenia[45], and a variety of other syndromes and pathologies[2,21,28,30,46] with clinical relevance. One study on schizophrenia found differences in the spatial organization of multiple neuron types in brain organoids grown with cells derived from patients with schizophrenia compared to controls, and were able to link the observed cortical malformation to a specific gene[45]. These findings contribute evidence towards understanding the cause and mechanism of schizophrenia, which are still open scientific questions[45]. Brain organoids have also been used to model infection with Zika virus, demonstrating viral infection of neural progenitors, causing cell death and resulting in

multiple morphological features of microcephaly (smaller organoid size, thinner neuronal layer, larger ventricles/lumens)[5,26]. Typical animal models like rodents do not accurately reproduce this pathology, so these organoid studies highlight the potential of human brain organoids, providing definitive evidence that Zika virus was causing microcephaly during the epidemic of 2015-16[5,24,26,47]. Since brain organoids can be generated from patient-derived cells, they can also be used to explore disorders with complex, undefined genetic bases[28,30]. With brain organoids, researchers can model and study human brain development and disease in ways not possible before – in either traditional cell cultures or animal models, or even human samples or participants – and explore uniquely human processes and conditions, and test drugs or manipulate a variety of factors all in an *in vitro* human system.

2.1.2 Limitations

Although remarkable in their potential, brain organoid models of course possess a number of limitations. From a biological perspective, high variability and low reproducibility have been considered major challenges in the field[5,10,24,28,48]. Variations are seen in size, morphology, internal organization and distribution of cell types from sample-to-sample, batch-to-batch, and between different cell lines, presenting challenges for analyses and drawing robust conclusions[5,12,26,28,48]. Phenotypic differences must be large enough to be detectable[3], which somewhat limits the possible applications of organoid models[5]. However, multiple studies have shown that brain region-specific organoids, generated by additional specific patterning signals in the media, are generally less variable than whole-brain cerebral organoids[9,26,49]. For example, via addition of soluble factors to pattern organoids towards forebrain identity, combined with use of miniaturized bioreactors, forebrain organoids were produced with much greater homogeneity compared to whole-brain cerebral organoids[5]. Variability in gross organoid morphology and morphology of internal cytoarchitecture was reduced, and robust expression of forebrain markers with a consistent timeline of neuronal differentiation, which was similar between different cell lines, was observed[5]. In dorsal forebrain organoids, single-cell RNA sequencing demonstrated very high reproducibility in cellular composition and developmental trajectory between organoids within and between batches and cell lines[10].

Due to their three-dimensional nature and size, brain organoids develop a necrotic core as they grow, as oxygen and nutrients cannot penetrate into the centre of the dense tissue[2,5,50]. Based on diffusion limitations, this may happen once organoids reach 500-800 μm in diameter[51]. This also lessens the generation of new cells and interferes with architectural organization, a drawback for longer term studies[1,50]. It has been suggested that the variability in nutrient availability contributes to the variability seen in organoid growth patterns[3]. This is the reason for introducing media movement in brain organoid protocols, using shaker plates or stirred bioreactors to improve oxygen and nutrient diffusion[3,5,10]. Studies have also tried increasing the oxygen saturation in incubators and using oxygen-permeable culture dishes to combat hypoxia, and even cutting or slicing growing organoids into pieces throughout culture to avoid necrotic core formation[15,50,52,53]. Others have started with fewer cells to form smaller initial aggregates, and added additional signaling factors to reduce the number of dead cells[10,12]. Taking this even further, there is work attempting to vascularize organoids to facilitate internal circulation, discussed further below. Despite all these different approaches, necrosis in the organoid centre remains a challenge in the field.

As brain organoids are grown from an embryonic stage, and follow a similar developmental time course to the human brain, they are quite a "young" model in terms of the human ages they represent[24]. With optimization of brain organoid protocols enabling longer term culture and, accordingly, further degrees of maturation, numerous studies have shown that they model quite well the embryonic and fetal stages of the human brain[5,16,28]. However, additional work is needed to reach post-natal stages, and ideally much later stages to model diseases and neurodegenerative disorders that manifest during adulthood[9,24,54]. Notwithstanding this limitation, studies have shown that brain organoids do in fact have value in studying some of these disorders, such as Alzheimer's disease[24,41,55].

Organoids are evidently not true brains, and although they have certain levels of organization, they lack further levels as well as the complexity of a real brain since they do not develop in the context of the embryo; as such, they are not exposed to all *in vivo* cues and morphogen gradients that pattern the brain with respect to the body axes[3,28]. One study devised a strategy to integrate one such patterning gradient into brain organoids, forming an organizing

centre directly within the organoid itself: cells secreting a signaling molecule (Sonic Hedgehog) at one end of the organoid created a gradient that patterned the forebrain organoid along dorsoventral and anteroposterior axes, with major forebrain subdivisions correctly positioned with respect to one another[56]. However, this method has not been adapted into standard protocols. Brain organoids also lack specific local and long-range connections matching the wiring of the real brain; although some models have been shown to produce spontaneous neural activity, they do not exhibit reproducible, stereotypical circuit organization[24,28,57]. Another consequence of not developing inside an embryo, the other germ layers are not present, and so brain organoids do not contain some cell types that the brain in the body has, such as microglia, pericytes, or endothelial cells and their vasculature[24,54]. These cells and their effects are important for modeling certain diseases, and also may influence some aspects of neural development[24,58]. Efforts are being made to integrate these cells into brain organoid models[28], discussed further below.

From a technical perspective, there are limitations stemming from the nature of the protocol and its manual involvement. There are multiple technically challenging and tedious steps that make culturing and processing brain organoids labour-intensive[26,59], and make success user-dependent. These steps also create opportunities for inconsistencies that contribute to organoid variability[48], hampering their ability to be adopted as a standard model system for neurological studies[26]. Simply changing the media and manipulating small and fragile organoids for experiments and characterization requires a degree of practice and expertise beyond standard cell culture experience[26,59]. Even *with* that expertise, a high degree of sample loss is expected, which reduces throughput; scalability is certainly less than 2D cultures[6,26]. There have been efforts to address these ease-of-use challenges. For example, microfabricated microwell arrays were used to increase throughput of generating and maintaining midbrain organoids, reducing the manual labour involved as seeding and media changes could be performed for hundreds of organoids on each device at once; these devices also reduced organoid variability[59]. Similar results were achieved with cerebral organoids[60]. It has been suggested that using microengineered systems for automated culture would be another way to address these technical limitations[30,48]. One study that illustrates such an approach used microfluidic

electrospray technology to form embryoid bodies for brain organoids[61]. As with any model, brain organoids have numerous advantages and drawbacks; work on how to address their limitations is ongoing in the field, as this will only increase their remarkable potential.

2.2 Coculture systems

2.2.1 Assembloids

As noted above, using brain region-specific organoids is one way to combat the high variability seen in brain organoid cultures, as the more directed differentiation produces less variability than seen in whole brain cerebral organoids. However, one disadvantage of this approach is that many brain regions interact as they develop, with cells migrating and neurons projecting to form long-range connections between different areas[9 62]. One strategy that is being explored to study this *in vitro* is the use of so-called assembloids – formed from organoids of different types assembled together, which allows the cells to interact as the organoids grow and fuse. Assembloids are advantageous as they can use brain region-specific protocols, which are less variable, but they also enable interactions between the different regions represented by each organoid and their cell types[9,21,62,63]. This creates more complex models than single type organoids, as well as more realistic modeling of the developing brain and neurodevelopmental disorders as the interaction between the distinct organoids mimics the development of neuronal connections forming neural circuits as *in vivo*[62,64–66]. Assembloids generated from cortical and striatal organoids have been used to model the formation of cortico-striatal circuitry, with unidirectional axonal projection of neurons from cortical to striatal organoids as happens in the fetal brain[22]. Forebrain assembloids demonstrated unidirectional migration of interneurons from ventral to dorsal forebrain organoids, accurately modeling this aspect of brain development[21].

Assembloid cultures have been formed in several ways. One method is to position the two organoids next to each other on transwell inserts, and then leave them unperturbed for several days to allow them to fuse together[20]. Another similar method places the two organoids together into a microcentrifuge tube to keep them in close proximity until fusion takes place[20,22]. Embedding several organoids together in a Matrigel droplet has also been used as a way to achieve fusion[67]. One group has developed a more automated approach that uses microfluidics to sequentially flow pre-formed organoids into guiding holes in an on-chip array[61].

2.2.2 Other coculture systems

In assembloid approaches, the two types of organoids are formed separately first, each according to their own protocol and media formulations, and then combined, but this is just one type of coculture system. Other types of cocultures that have been explored for organoids add a secondary cell type as single cells to an already formed organoid, or mix different cell types together at the time of organoid formation to generate a combined multi-type organoid. For example, suspensions of microglia have been added to formed brain organoids, following which the microglia infiltrate the organoids[58,68,69]. Endothelial cells have been incorporated to create vascularized brain organoids via several techniques. One approach embedded brain organoids in Matrigel with endothelial cells[51]. Another mixed engineered stem cells, inducible to express a transcription factor driving endothelial cell differentiation, in with unmodified stem cells at the time of organoid formation and induced them after several days of culture[70]. A third approach first generated blood vessel organoids, then dissociated them into clumps and combined those with brain organoids[71]. While these vascularization approaches may improve nutrient and oxygen delivery to the organoid core, they add varying decreases of complexity to the culture protocol, which could be very limiting in terms of scale-up. A related approach to model the blood-brain barrier, although it does not contain neural tissue, mixed brain endothelial cells, pericytes and astrocytes together to form multi-component spheroids[72,73]. Tumour invasion has also been explored by culturing single glioma cells with brain organoids[74]. In some studies, cells are isolated from organoids and then used in 2D cocultures[63].

There are multiple different types of coculture systems that do not use organoids or 3D cultures. For example, transwell inserts that allow culturing of different cell types on the insert and in the well below have been used to create a model of the blood-brain barrier[75]. On-chip systems, where cells are grown in microfabricated devices containing channels in a variety of geometries, have been used to connect cultures of different cell types by media flow[48]. Neurons have been cocultured in chip devices where they have innervated muscle cells growing in a distinct chamber[76]. There is interest in combining organoids with organ-on-chip approaches, which might offer some improvements to standard organoid cocultures[31,48,77]. This has been achieved with liver organoids and endothelial cells to create vascularized liver organoids[78], and

also in three-part systems (liver, intestinal, and stomach organoids[78]; liver organoid, heart organoid, and lung construct[79]) where the multiple components could interact via shared media but did not physically contact each other. However, exploration of incorporating brain organoids into an on-chip approach is limited.

2.3 Mechanical & biophysical cues

As the biochemical factors that induce stem cells to differentiate into neural tissue are indispensable for the growth of brain organoids, research has largely focused on these cues. However, many protocols also highlight the importance of the ECM support material, provided most often in the form of Matrigel, which although does provide some chemical signalling molecules, is importantly thought to provide physical support for 3D organoid growth and expansion[3,5,12,24]. This is one type of factor in the biophysical microenvironment that can be manipulated, and there are several others that can be controlled as well. Indeed, mechanical properties of the microenvironment have emerged as critical parameters in tissue engineering[23,80,81].

Mechanics have been found to influence numerous cellular processes such as survival, proliferation, migration and differentiation[81–85], and evidence demonstrating the importance of mechanical factors in organ development and disease is growing[81,82,86–89]. Biophysical cues such as material stiffness, viscoelasticity, shape, and external or internally generated forces like tension and compression influence the morphogenesis of organs and organisms at the micro- and macro-architectural scale, from the *Drosophila* egg chamber[90] and wing[91] to the human heart and brain[82,92,93]. The complex shape-shifting process of morphogenesis is how organs develop into their functional capacities, evolving from one initial form into a completely different structure. As function is inextricably linked to form, correct form is necessary for proper organ function – accurate morphogenesis is therefore critical for healthy and functional tissues and organisms. Abnormalities in mechanical cues can cause disruptions in the process, resulting in defects and dysfunction in organs and whole organisms[94,95]. For example, mutations that affect dynamic stress profiles can cause neural tube defects via disrupted tissue biomechanics[96,97], increases in tissue stiffness can promote cancer progression[89,98–100], and there is evidence that

the stiffness of the human brain influences its embryonic development[82] and changes with aging and various disease states[82,101].

2.3.1 Stiffness/material properties

One common mechanical factor used to explore effects on cell behaviour is material properties of the culture substrate, in particular stiffness; this can be modified by using materials with different or variable properties, often polymers with differing degrees of crosslinking. For example, in a landmark study, mesenchymal stem cells were cultured on hydrogels of a range of stiffnesses and on the softest, they differentiated into neurons, on intermediate towards myoblasts, and on the stiffest towards osteoblasts[102]. Several studies have examined the impact of substrate stiffness on neural cultures using hydrogels. Neurons have been found to prefer softer substrates (e.g. ~0.5 kPa), whereas glia prefer stiffer ones (e.g. ~1kPa)[103–105]; likewise, neural stem cells differentiate better on softer substrates, which selectively promote neurogenesis[106], neuritogenesis[107], neurite branching[104] and extension[108]. Studies have suggested this is logical as the brain itself is very soft[23,101,105,109], thus the more compliant environments better match the properties of the *in vivo* organ.

Work on 2D substrate stiffness has been translated to 3D tissues by encapsulating organoids in hydrogels of varied mechanical properties, with stiffness affecting formation[110–112] and viability[113,114] of intestinal and pancreatic islet organoids, as well as their differentiation and maturation[111,112,114]. For example, intestinal organoid formation was more efficient in softer hydrogels[110], and resulted in higher viability than stiffer formulations[114]. Although the majority of the work in this field has focused on intestinal organoids, one study investigated the impact of hydrogel stiffness on the formation of neuroepithelial cysts from single murine stem cells, and observed that it influenced differentiation and proliferation[115]. The softest material best promoted proliferation, whereas intermediate stiffness best promoted early neural differentiation and polarized organization[115]; of note, this is much stiffer than found optimal in work with neural cells in 2D[103–107]. All together, this work shows that microenvironmental mechanics affect the growth and development of neural stem cells and neurons[103–108], as well as that of certain types of organoids[110–114]. This suggests that the mechanical environment of a brain

organoid would likely have an influence, although how growth and development would be affected was unknown.

2.3.2 Mechanical forces

Another set of mechanical cues important in organ development is forces. Gene expression plans and biochemical signaling cues such as morphogen gradients interact within a 3D tissue to create patterns and drive morphogenesis, but morphogenesis is ultimately a physical process, and necessarily involves mechanical factors and forces acting in 3D to produce shape changes[92,94,116,117]. Cell behaviours connect biochemical signaling to mechanics and force production, and vice versa[94,117]. Forces generated by the cells at the site of change are considered intrinsic forces, i.e. generated by the shape-changing tissue itself; in contrast, forces generated by neighboring cells or emerging within the tissue globally can be considered extrinsic forces[94,118–120]. For example, bending of the primitive heart structure (the heart tube) during embryonic development is driven by intrinsic forces, generated by changes in size of the cells that make up the bending tissue, affecting distributions of stress and strain[92]. In neurulation of the embryo, folding of the neural plate to form the neural tube involves both intrinsic forces[121,122], through changes in cell shape at hinge points, as well as extrinsic ones, through compressive forces exerted by the neighbouring nonneural ectoderm[121,123–125] that together bend and roll the initially flat tissue into a closed tube that develops into the brain and spinal cord (discussed below). Breakdowns in these mechanical processes where the neural tube fails to close properly result in neural tube defects, severe congenital malformations that are some of the most prevalent and disabling birth defects worldwide[122,126,127].

These forces acting in developing tissues feed back into the biochemical signaling pathways that drive them by instructing cells' behaviour, gene expression, fate specification and differentiation[117]. For example, numerous studies have found that applying deformations such as stretching, twisting, and shear affects the proliferation and differentiation of stem cells in monolayer culture[128]. For example, cyclic stretching could increase or decrease proliferation of mesenchymal stem cells (MSCs) depending on strain magnitude and duration[129], and, when combined with bending, increased their differentiation towards cardiomyocytes[130]. Dynamic compression improved differentiation of human dental pulp stem cells into odontoblasts, and

was likewise able to induce differentiation of MSCs[131]. These studies use techniques such as magnetic manipulation of beads attached to cells (magnetic twisting cytometry), stretching deformable cell culture substrates to produce strain, and fluid flow through bioreactors or microfluidic chips to apply different forces[48,128–130,132].

At the tissue level, much of the work done on elucidating and probing the forces involved in morphogenesis has used animal models (such as *Drosophila*, *C. elegans*, zebrafish, chick, axolotl, mouse) and tissue explants[87,92,94,124,125,133]. It makes use of techniques like ultraviolet (UV) laser ablation, single cell force spectroscopy, and micropipette aspiration, as well as physical mimics, for example testing gels in place of tissues, and computational simulations[87,94,118,134–137]. For example, UV laser ablation experiments have been used to investigate the development of tension in different tissues of the *Drosophila* embryo, and its contribution to morphogenetic events[138]. By culturing neural plate explants with varying amounts of surrounding tissue and observing the movements and shape changes of the explant, experiments have shown that both intrinsic and extrinsic forces are involved in producing tissue shape changes during neurulation that act to fold the neural plate and form the neural tube[124,125,139]. One explant study using Xenopus skin ectoderm found that oriented tissue strain generated by the mesoderm during gastrulation was critical in forming the global axis of planar polarity. Isolated ectoderm explants failed to properly develop this axis, but mechanical strain could be exogenously applied (using hydraulic suction into a capillary tube to apply strain and vary its parameters) to correctly orient planar cell polarity components and rescue development of polarity[140]. Worth noting, there are numerous differences between morphogenesis in animals and humans, as well as phenotypic differences in disease in animal models versus humans[133]. Although animal models provide extremely valuable insights, they are not capable of allowing study of every process and mechanism[133,141].

Some studies have begun to appear that apply mechanical forces to organoid cultures to explore their impact, using microengineered setups[48]. For example, the effects of fluid flow have been examined in on-chip approaches in kidney, pancreas and intestinal organoids, finding improvements in their structural and functional maturation[48,142–144]. One study devised a device to apply strains to neural tube organoids growing on a stretchable membrane, and found

enhanced growth and patterning[145]. This work points to the importance of mechanical forces not only in development *in vivo* but also in 3D systems *in vitro*, like developing organoid tissues[48].

2.3.3 Shape/geometry

Another group of biophysical factors important in tissue morphogenesis and function is shape, via physical boundaries that provide geometrical cues[30]. The shape and structure of an organism and its organs affect their developing function[126,146]; for example, the branched architecture of the lung allows it to perform maximal O_2/CO_2 exchange (due to the large surface area the branching provides)[147], and the pattern of branching in the developing airway epithelium is strikingly stereotyped[148], which is suggestive of its importance. In the brain, the reduction of folding seen in the cerebral cortex in lissencephaly ("smooth brain") is associated with cognitive deficits[13].

As function necessitates form, there has long been interest in how one may bring about the other[126,146,149]. In various contexts, studies have looked at how manipulating cell shape impacts cell function. Geometric confinement of stem cells to 2D circular micropatterns of particular sizes enables self-organization and reproducible differentiation into spatially organized embryonic germ layers[150]. Similar micropatterns, again size-dependently, enhanced differentiation of stem cells towards pancreatic lineages[151]. Such approaches have also promoted organization and improved reproducibility of developing neural structures, namely neural rosettes formed in monolayer cultures[152,153]. One study that brings this shape aspect to 3D organoid technology used polymer microfilaments to provide a floating scaffold for embryoid body formation, guiding them to form elongated neuroepithelium as they differentiated into brain organoids, resulting in enhanced neural induction[154]. The initial geometry of 3D mammary epithelial cultures has been shown to influence the branching, proliferation, or invasion of normal or tumour cells, as dictated by sites of high stress formed by the geometry[155–157].

As tissue shape is not static but dynamic during morphogenesis, as the very word implies, producing dynamic geometries is of interest. There are some approaches that, although not necessarily designed for studies of morphogenesis, achieve dynamic geometry in culture in a variety of contexts. One group used a cellulose fibre scaffold combined with collagen gel to culture cells in a sheet that can be manually rolled up to create a 3D tissue culture, which allows

for unrolling at the time of analysis (called TRACER: tissue roll for analysis of cellular environment and response)[158]. Another example achieved shape change over time by growing brain organoids in a physically restrictive environment such that tissues outgrew the space in which they were confined, forcing wrinkles or folds[159]. Finally, several studies have used "tissue origami" approaches, which generally start with 2D cell layers that are folded to produce 3D cultures. One study seeded two different cell types on alginate-coated microplates, followed by enzymatic degradation of the alginate which released the cells, inducing folding[160]. The other made use of contractile fibroblast clusters seeded inside an ECM gel to induce deformation of the matrix, and thereby the cells seeded on top, over time[161]. One study combined a shape memory wire with a collagen matrix to support cell growth around the wire; an electrical current triggered the shape change of the wire into a pre-programmed coil[162].

2.4 Conclusion

All these biophysical cues influence a variety of cell behaviours, and are important in the morphogenesis and development of organs and organisms, contributing critically to proper functional development, as well as to disease pathophysiology. Given the accumulating data, it is logical that they would also influence the development of tissues *in vitro*, and therefore important to integrate these mechanical factors into tissue engineering strategies to achieve functional tissues for experimental models and regenerative medicine applications[48].

At present in neuroscience fields, brain organoids are the at the leading-edge of *in vitro* human tissue-scale models. These self-organizing, 3D tissue-engineered models of the human brain are grown from stem cells and mimic certain features of embryonic brain development[1–4]. Brain organoids facilitate improved translational modeling not possible with 2D cell culture or non-human animals, and enable exploration of uniquely human complexities *in vitro*, including both healthy and diseased brain development[2,3,5].

Multiple examples summarized here demonstrate the diverse effects of mechanical properties, force application, and geometry in various contexts ranging from 2D cell monolayers to 3D tissues such as explants and organoids. With advances in tissue engineering, there is growing interest in translating this to engineered tissues *in vitro* – both to enhance our understanding of the processes at work in development and to create more refined experimental

models[48,93,160,163]. Of note, some work has been conducted on neural cells and tissues demonstrating the impact of certain mechanical factors, but there is ample room in the field to further explore the influence of biophysical cues on brain organoids.

Further investigation into these biophysical cues would provide valuable insights into their impact on cell behaviours, organ development and function, and pathological processes. New tools and platforms designed to integrate and study these cues would deepen our understanding, and could expand the potential of brain organoids. This would likely result in more realistic models, and may enable the study of the morphogenetic events that lead to functional organs. Given the importance of morphogenesis in tissue and organ development and its medical relevance, engineering platforms to enable mimicry of this complex process in human tissues *in vitro* would unlock new opportunities. Such platforms could enhance our understanding of how morphogenetic transformations take place, facilitate studies of both healthy and pathogenic processes, and potentially generate more functional engineered tissues for regenerative medicine.

Chapter 3

Mechanical properties have been shown to be important in organ development as well as in tissue engineering, influencing growth and development of the tissue and the differentiation of the comprising cells. Stiffness of the surrounding microenvironment is one such factor that has been extensively studied in many systems, with a variety of effects. Substrate stiffness has also been shown to impact 2D neural cultures, but its influence on brain organoids had not been studied. Therefore, stiffness was the first biophysical cue I chose to explore in the context of human brain organoids. Most brain organoid protocols use Matrigel as a supporting matrix, but its mechanical properties are not tunable. In this manuscript, we combined alginate, a well-established biomaterial in the tissue engineering field, with Matrigel to tune the elastic modulus of the hydrogel independently from chemical components and adhesive properties. This allowed us to explore how hydrogel stiffness influenced the encapsulated brain organoids. We characterize the mechanical properties of composite Matrigel-alginate hydrogels, and the impact on brain organoid growth and gross morphology, as well as microarchitecture and maturation. This work was published in *ACS Applied Bio Materials* by the American Chemical Society in January 2022.

The findings provide evidence that matrix stiffness affects brain organoid growth and self-organizing capacity, highlighting the importance of appropriate mechanical properties to support the optimal development of brain organoids and their ability to follow characteristic intrinsic programming. This is necessary to consider as brain organoids are increasingly used as models of human brain development and disease. These results also suggest the potential in further studying how biophysical cues could be used to manipulate brain organoid development.

3 Hydrogel Mechanics Influence the Growth and Development of Embedded Brain Organoids

Camille Cassel de Camps[1], Saba Aslani[2], Nicholas Stylianesis[3], Harris Nami[2], Nguyen-Vi Mohamed[2], Thomas M. Durcan[2*], Christopher Moraes[1,3,4,5*]

1. Department of Biomedical Engineering, McGill University, Montréal, H3A 2B4 QC Canada
2. The Neuro's Early Drug Discovery Unit (EDDU), McGill University, 3801 University Street, Montréal, H3A 2B4 QC Canada
3. Department of Chemical Engineering, McGill University, Montréal, H3A 0C5 QC Canada
4. Rosalind and Morris Goodman Cancer Research Centre, McGill University, Montréal, H3A 1A3 QC Canada
5. Division of Experimental Medicine, McGill University, Montréal, H4A 3J1, QC Canada

* co-corresponding authors: chris.moraes@mcgill.ca; thomas.durcan@mcgill.ca

3.1 Abstract

Brain organoids are three-dimensional, tissue-engineered neural models derived from induced pluripotent stem cells that enable studies of neurodevelopmental and disease processes. Mechanical properties of the microenvironment are known to be critical parameters in tissue engineering, but the mechanical consequences of the encapsulating matrix on brain organoid growth and development remain undefined. Here, Matrigel® was modified with an interpenetrating network (IPN) of alginate, to tune the mechanical properties of the encapsulating matrix. Brain organoids grown in IPNs were viable, with characteristic formation of neuroepithelial buds. However, organoid growth was significantly restricted in the stiffest matrix tested. Moreover, stiffer matrices skewed cell populations towards mature neuronal phenotypes, with fewer and smaller neural rosettes. These findings demonstrate that mechanics of the culture environment are important parameters in brain organoid development, and show that the self-organizing capacity and subsequent architecture of brain organoids can be modulated by forces arising from growth-induced compression of the surrounding matrix. This study therefore suggests that carefully designing the mechanical properties of organoid encapsulation materials is a potential strategy to direct organoid growth and maturation towards desired structures.

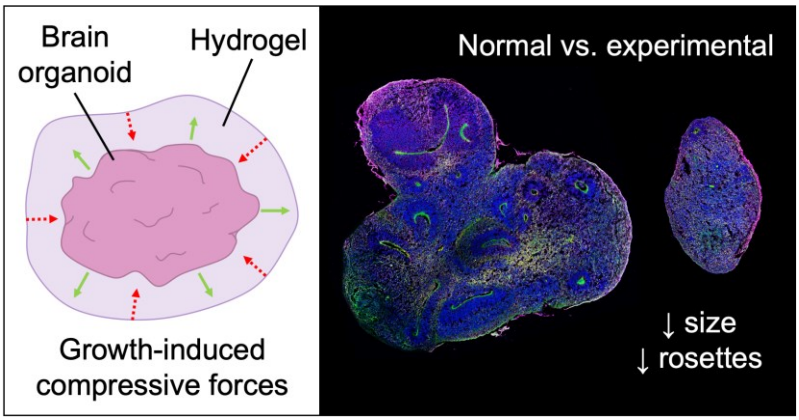

Figure 3.0. Graphical abstract.

3.2 Introduction

Brain organoids are 3D neural tissue models that facilitate studies of human developmental and disease processes in culture, in a manner that more closely resembles the human brain than traditional models. Derived from human induced pluripotent stem cells (iPSCs), these tissues are self-organizing and recapitulate aspects of human embryological development[2,3,5,11,15], and are emerging as valuable tools to study neurological diseases[2,5,13,44]. Given the ethical and logistical challenges of studying the human brain[164,165], brain organoids present new opportunities to better understand human brain development and pathogenesis[38,166] in a dish.

To support their growth, organoids are typically encapsulated in an extracellular matrix (ECM)[80,105], such as Matrigel®, which provides microenvironmental cues that influence organoid growth and development[2–4]. Mechanical properties of the cell and tissue microenvironment are known to be critical parameters in tissue engineering, and these properties can be tailored to direct biology and influence cell behavior[23,80,81]. In general, mechanics have been demonstrated to affect numerous processes, from cell survival, proliferation, and migration, to differentiation and disease progression[81–83,85]. In the context of the brain, several studies have investigated how mechanics affect neurons or neural stem cells in 2D by varying substrate stiffness. The brain is one of the softest organs in the body, with an elastic modulus in the range of 0.5 to 25 kPa, depending on the region and the measurement technique[23,101,105,109], and environments that match this stiffness better induce neurogenesis and favour neuronal growth[103–108]. Matrix mechanics have been shown to influence tissue formation[110,111], viability[113,114], differentiation

and maturation[111,114] of intestinal organoids/spheroids and pancreatic islet organoids[112]. The formation of neuroepithelial cysts from single stem cells is also influenced by matrix stiffness[115]. However, the role of matrix stiffness on brain organoid growth and differentiation remains undefined.

Several challenges exist in defining the impact of matrix mechanics on organoid differentiation. The use of Matrigel for organoid growth is generally considered essential, but this basement membrane matrix extracted from Engelbreth–Holm–swarm tumors in mice is highly complex, and therefore challenging to modify directly[167–170]. While organoid culture in synthetically-defined and mechanically-tunable matrices is possible[23,80,105,114,170], these matrices often do not present Matrigel-like cues required for appropriate differentiation. To manipulate the properties of Matrigel without directly modifying the material, we incorporated alginate, a mechanically tunable polysaccharide that can be crosslinked with divalent cations to form interpenetrating hydrogel networks (IPNs). The mechanical properties of these IPNs can be easily tuned to yield a range of stiffnesses[114,171]. Alginate has been successfully combined with Matrigel for culture of mammary epithelial[172], breast cancer[173], and induced neuronal cells[174,175], and used on its own to support the growth of intestinal organoids[114]. Importantly, alginate neither presents cell-binding molecules nor adsorbs proteins, and therefore does not have cell-adhesive properties[114,172,176–180]. Using this composite IPN, we can manipulate mechanical properties, while maintaining the chemical and adhesive cues provided by Matrigel, to explore how microenvironmental mechanics affect brain organoids.

In this work, we characterize the mechanical properties of alginate-Matrigel IPNs and use them as an encapsulating material to grow and differentiate 3D brain organoids (**Fig. 3.1**). We demonstrate viable growth of brain organoids within different IPN matrices, and observe differences in the gross morphology of our organoids and their internal architecture depending on the stiffness of the matrix. Our findings illustrate that hydrogel mechanics are an important set of parameters in modulating brain organoid development and imply that the self-organizing capacity and development of brain organoids are influenced by external mechanics.

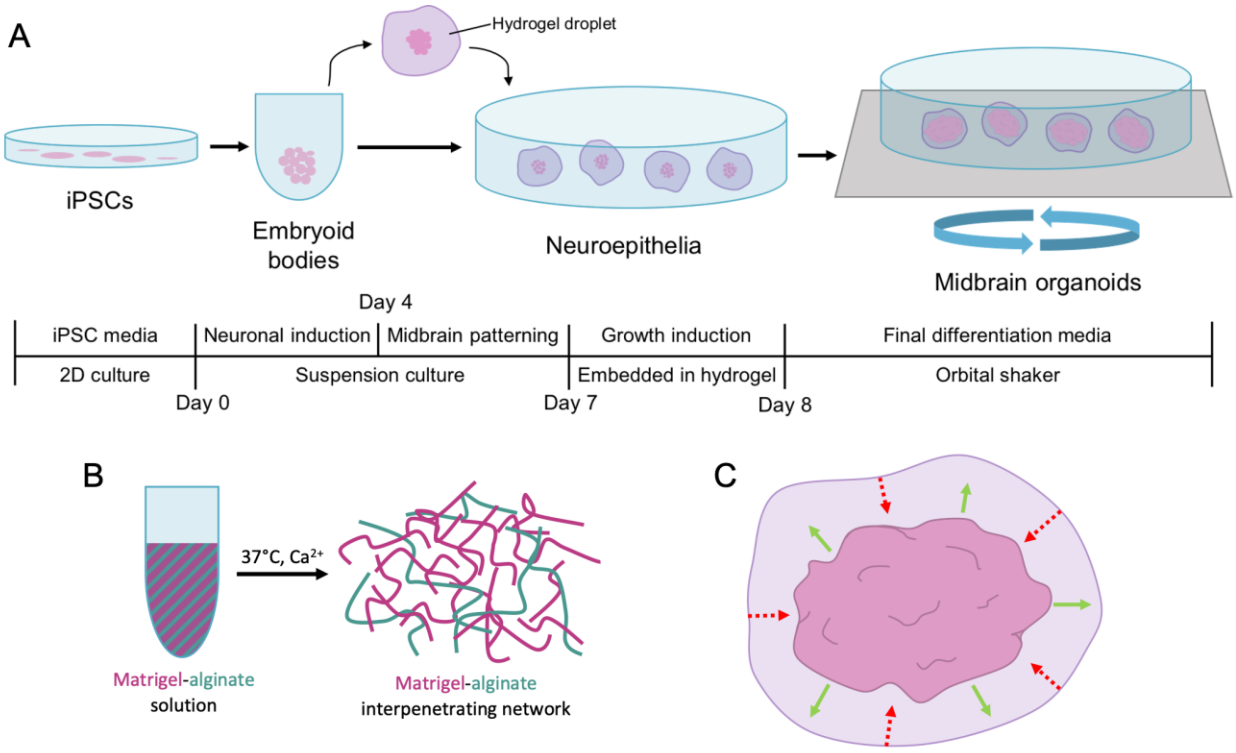

Figure 3.1. A Schematic of midbrain organoid generation procedure. **B** Formation of a Matrigel-alginate interpenetrating network from solution mixture via thermally triggered gelation and calcium crosslinking. **C** Model of growth-induced compressional forces within the encapsulating hydrogel as the organoid grows within the hydrogel scaffold (green arrows), which likely applies a reaction compressional force (red dashed arrows) that may influence the organoid's growth and development.

3.3 Materials and methods

Unless otherwise stated, all cell culture materials and supplies were purchased from Fisher Scientific (Ottawa, ON) and chemicals from Sigma Aldrich (Oakville, ON).

3.3.1 Hydrogel formation

The hydrogel formulations we used were based on preliminary work conducted in our lab, as we were aiming to have a range of stiffnesses in which to grow brain organoids.

2% w/v stock solutions of sodium alginate were prepared in deionized water or phosphate-buffered saline (PBS) without Ca^{2+} and Mg^{2+}, filtered through a 0.22 µm filter, and diluted for use as needed. Aliquots of growth factor reduced Matrigel (Corning 356230) were diluted to prepare the following solutions: undiluted (Matrigel 100%), diluted in PBS (without Ca^{2+} and Mg^{2+}) at 4°C (Matrigel 50%), and/or with alginate stock solutions to form IPN prepolymer solutions (Matrigel

50% + alginate 0.08%, and Matrigel 50% + alginate 1%). These pre-gel solutions were dispensed as desired for rheology and organoid embedding. Thermal gelation of the Matrigel components occurred within 5-20 min at 37°C, and the alginate IPN was formed by incubating for up to 1 hr with an excess volume of calcium chloride (1% w/v for rheometry, 0.1% w/v for cell culture; due to diffusion limitations of the rheometer setup and to avoid calcium cytotoxicity, respectively), added following Matrigel gelation in an appropriate media to the culture vessel and stage.

3.3.2 Rheological measurements

Rheological experiments were performed on an Anton Paar MCR 302 rheometer with a temperature-adjustable chromium oxide bottom plate fixture. 100 µL of gel solution was dispensed onto the bottom plate of a parallel plate geometry. An 8 mm diameter top plate was lowered to form a 1 mm gap, followed by thermal gelation for 5 min at 37℃. Calcium chloride solution was then dispensed onto the bottom plate to surround the sample for alginate gelation. Linear viscoelastic (LVE) regions of the gels were determined through shear-strain-controlled amplitude sweeps. Solution gelation behaviour was monitored using time-resolved dynamic oscillatory analysis at a fixed frequency (1 rad/s) and strain (0.5%), which was within the LVE regime of each gel as determined by amplitude sweeps. Reported mechanics were obtained after stabilization of gel mechanical properties. All measurements were performed in triplicate.

3.3.3 Scanning electron microscopy and analysis

Hydrogels were snap frozen in liquid nitrogen for 2 min and freeze-dried overnight, a method capable of maintaining pore sizes[181]. The dried samples were cut into halves and mounted on aluminum stubs with electrically conductive carbon adhesive tape. SEMs were obtained using a Hitachi SU3500 scanning electron microscope in the variable pressure mode at an accelerating voltage of 3-10 kV. The average pore size within each hydrogel sample was analyzed manually using ImageJ software[182], using a minimum of 30 randomly selected pores from 3 images.

3.3.4 Generation of 3D brain organoids from iPSCs

The control NCRM1 (male) iPSC line was obtained from the NIH biorepository, and the TD22 (male) control iPSC line was obtained through The Neuro's C-BIG repository[183]. Both lines underwent a four-step quality control workflow (results presented in Chen et al.[183]). The use of iPSCs in this research is approved by the McGill University Health Centre Research Ethics Board

(DURCAN_IPSC / 2019-5374). Both lines were maintained at 37°C with 5% CO_2 on Matrigel coated plates in mTeSR (StemCell Technologies) with daily media changes. Cells were passaged when 70% confluent using Gentle Cell Dissociation Reagent (StemCell Technologies). Areas of spontaneous differentiation were removed manually prior to passaging. Cerebral organoids were generated from human iPSCs (line NCRM1) according to the Lancaster protocol[3], with the following modifications: 10,000 cells/well were seeded in 96-well round bottom ultra-low attachment plates (Corning Costar), and then centrifuged for 10 min at 1200 rpm. The resulting embryoid bodies (EBs) were maintained for 6-10 days prior to embedding in 30 µL of one of four hydrogel matrices directly in the 96-well plate (as previously described[19], details on gelation of IPNs above). The four hydrogel matrices tested were: Matrigel 100%, Matrigel 50%, Matrigel 50% + alginate 0.08%, and Matrigel 50% + alginate 1%. Embedded organoids were then transferred to 6-well ultra-low attachment plates (Corning Costar) containing 4 mL media (without added $CaCl_2$), using cut 1000 µL pipette tips. After a static culture period of 4 days, plates were transferred to an orbital shaker at 70 rpm for the remainder of culture. Midbrain organoids were generated from the TD22 line using a previously published approach (Fig. 3-1)[19]. EBs were cultured in neuronal induction media (Day 1), without ROCK inhibitor (Day 2), and midbrain patterning media (Day 4-7). Hydrogel embedding was performed on Day 7 and organoids were cultured in tissue growth induction media. On Day 8, organoids were transferred to 6-well plates and cultured in final differentiation media. Partial media changes were performed every 2-3 days for the remainder of culture.

3.3.5 Live organoid analyses

Organoid viability was assessed by washing twice with PBS and staining with 2 µM calcein AM and ethidium homodimer-1 (Life Technologies) for 40 min at 37°C. Fluorescent analysis was performed on images collected with an Olympus IX73 spinning disc confocal microscope at low magnification. Gross organoid growth and morphology were assessed via live brightfield imaging on an EVOS transmitted light microscope (XL Core). Average Feret diameter was calculated using an ImageJ macro[184] where possible, or by freehand selection.

3.3.6 Immunostaining

Organoids were fixed in 4% paraformaldehyde at 4°C overnight, washed thrice for 15 min in PBS, and incubated in 20% sucrose at 4°C prior to cryosectioning into 12 μm thick slices in optimal cutting temperature mounting medium. Staining was performed as previously described[19], and sections were counterstained with Hoechst. The antibodies and stains used were: anti-tyrosine hydroxylase at 1:50 (rabbit polyclonal, Pel-Freez P40101), anti-microtubule-associated protein 2 (MAP2) at 1:400 (chicken polyclonal, EnCor Biotechnology CPCA-MAP2) anti-β-tubulin III (Tuj1) at 1:300 (chicken polyclonal, Millipore Sigma AB9354), anti-cleaved caspase-3 (CC3) at 1:100 (rabbit monoclonal, Cell Signaling Technology 9664), anti-Ki67 at 1:100 (mouse monoclonal, BD Pharmingen 556003), phalloidin for filamentous actin (F-actin) at 1:25 (Thermo Fisher Scientific F432), and Hoechst 33342 at 1:5000 (Invitrogen H3570). Tiled images were collected on a Leica TCS SP8 confocal microscope.

3.3.7 Image analysis

Images were analyzed in a CellProfiler[185] pipeline (**Fig. S3.1**) using an automated thresholding method, identifying nuclei based on the difference in intensity between the background and the borders of the nuclei. Nuclear segmentation by the pipeline was validated against manual counts. The area covered by staining for other markers was also quantified. The organoid area was quantified by a mask overlay based on the nuclei image. Immunofluorescent images were used to quantify neural rosettes as they allow for assessment of spatial patterns of protein expression[57,186]. Clearly demarcated F-actin rings or curves in which an apparent lumen could be observed were used to identify rosettes; rosettes were counted in 8 organoids per condition (1 tissue section per organoid, i.e., 8 individual organoid sections). Rosette length was characterized by tracing the apical side of the neuroepithelium with the segmented line tool with spline fit in ImageJ[182]; 3 organoids per condition were analyzed (1 tissue section per organoid).

3.3.8 Statistical analysis

R statistical software[187], or JASP[188] for rheological data, were used to calculate one-way ANOVAs between conditions, or two-way ANOVAs between conditions and time points, followed by Tukey post hoc comparisons, carried out at 95% significance.

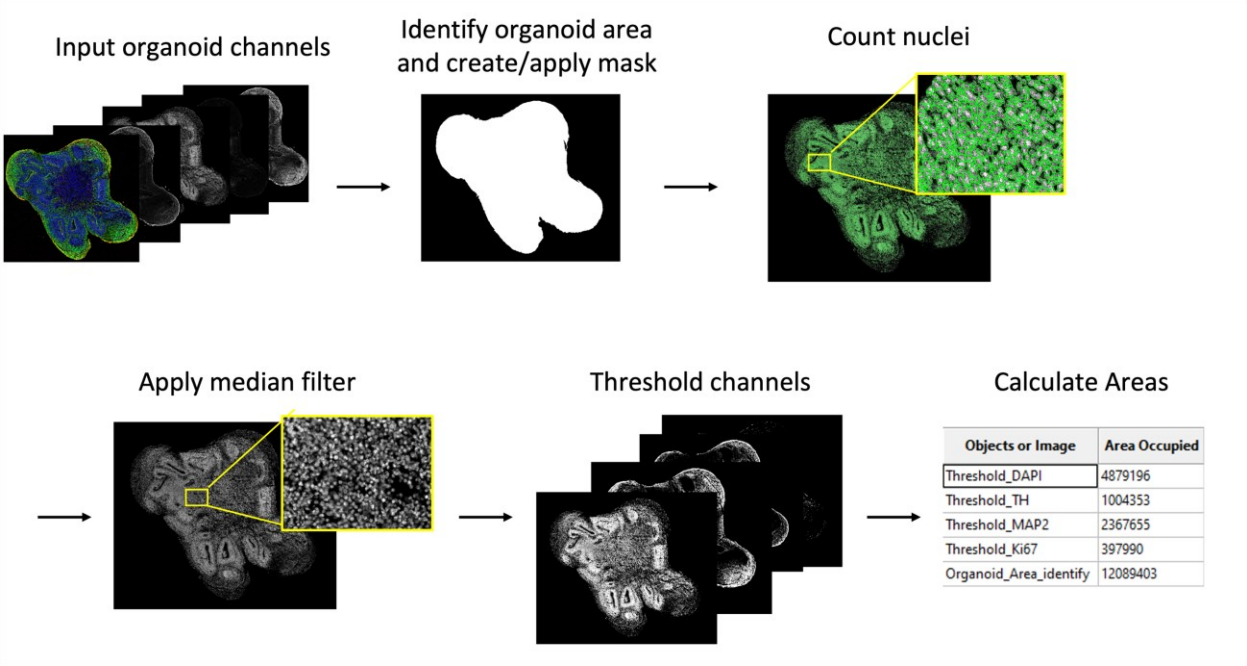

Figure S3.1. Schematic of CellProfiler pipeline used to analyze stained organoid images.

3.4 Results

3.4.1 Characterization of hydrogel IPN mechanical properties

To first verify that alginate could modulate the mechanical properties of the hydrogel IPNs, and to characterize the time needed to reach steady-state mechanical properties of the formed gels, isothermal oscillatory rheometry was applied to the various hydrogel formulations tested in this work. As expected, thermal gelation of the Matrigel component created low-modulus gels, and the addition of calcium ions induced immediate gel stiffening due to the alginate component. Gel moduli plateaued within 30-180 minutes (representative dataset in **Fig. 3.2A**), at which point mechanical characterization results were reported.

As expected, decreasing the Matrigel content reduced the gel storage modulus (Fig. 3.2B). Adding low concentrations of alginate (0.08%) did not significantly change the IPN storage modulus, while high concentrations of alginate (1%) significantly stiffened the matrix compared to similar concentrations of either Matrigel or alginate alone. The viscoelastic properties also changed significantly with sufficiently large alginate concentrations as shown by the loss modulus (Fig. 3-2C), but the phase angles (ratio between storage and loss modulus) were reasonably consistent across samples. As the mechanical properties of IPNs are not simply additive, the

alginate monomers likely affect Matrigel polymerization, and entanglement of alginate within the protein network may create distinct network architectures and hence mechanical properties. These findings are consistent with other studies of alginate-IPN hydrogels[189–192], and achieve a range of storage moduli physiologically relevant for soft tissues[82].

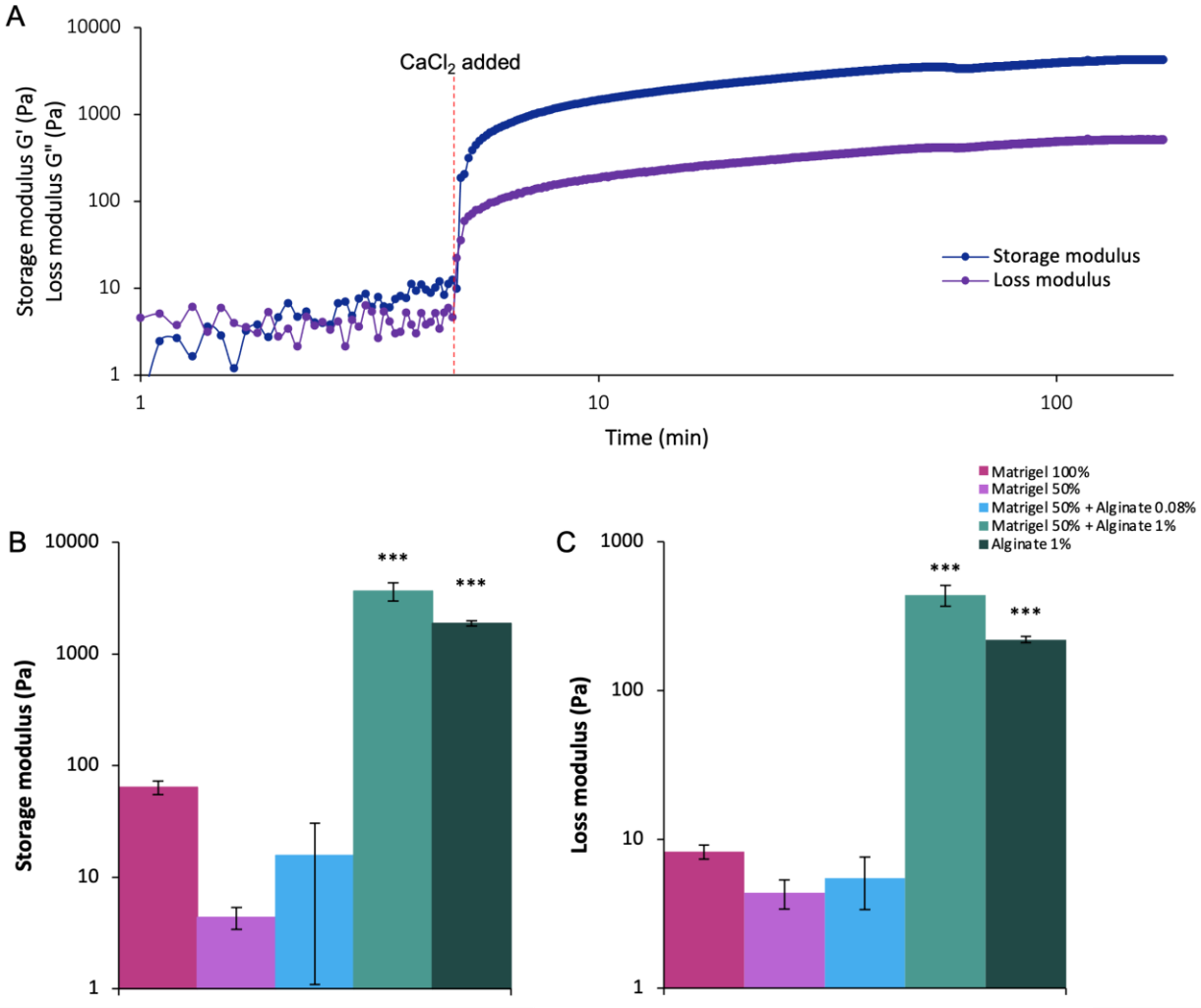

Figure 3.2. Alginate modulates stiffness of Matrigel-alginate composites to yield a range of mechanical properties. **A** Gelation time course of a typical Matrigel-alginate IPN (Matrigel 50% + alginate 1%). Dashed line indicates addition of calcium chloride solution. **B** Storage and **C** loss modulus measured via rheology (data presented as mean ± standard deviation; n = 3 gels per composition; ***p < 0.001 by one-way ANOVA with Tukey post hoc comparisons).

Given the interactions expected in global mechanical properties, we next sought to estimate hydrogel pore size in Matrigel and Matrigel-alginate IPNs (**Fig. S3.2**), as pore size can play a significant role in critical cellular processes related to transport and microenvironmental

sensing[80,193,194]. Direct observation of pores via scanning electron microscopy demonstrated a range of sizes between 5 and 50 µm, which is sufficient to allow extensive transport[180,195,196]. While 100% Matrigel had significantly smaller pores than any other conditions tested, no significant differences were found between 50% Matrigel doped with 1% alginate and the relevant control, 50% Matrigel, despite the increased mechanical stiffness of the IPN composite. Interestingly, pore size of the IPN was greater than the alginate-only component, as 50% Matrigel doped with 1% alginate had significantly larger pores than 1% alginate alone, further supporting our supposition that the two materials interact during thermal and calcium-driven polymerization.

These results together demonstrate that using the protocols described here, incorporating an alginate IPN within a 50% Matrigel network may be used to independently and significantly modulate mechanical properties by several fold, over a range known to influence organoid development[113,114], while maintaining consistent Matrigel content, and without a substantial change in pore size.

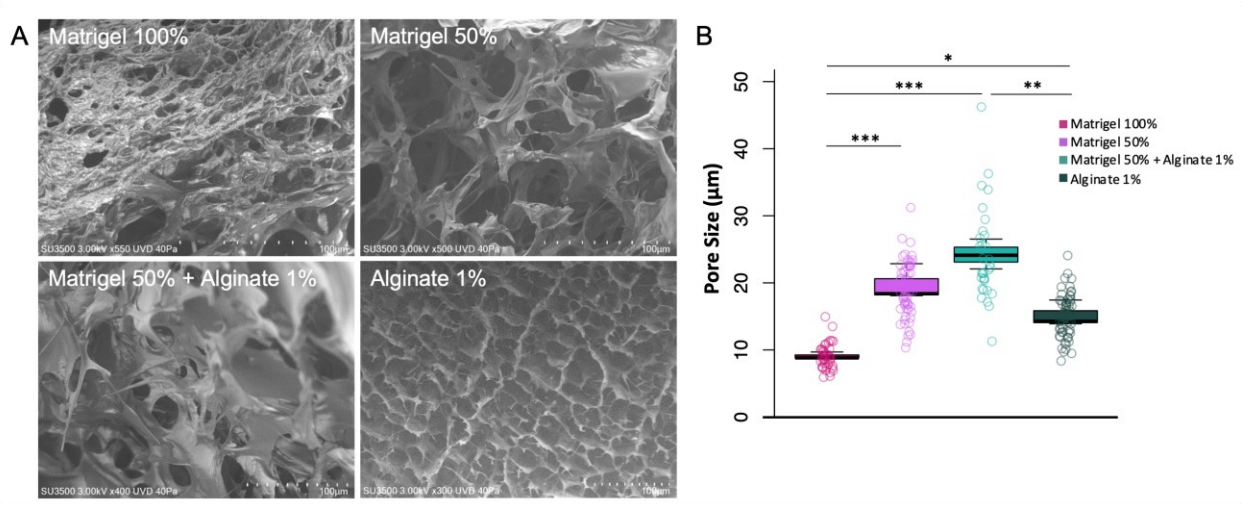

Figure S3.2. Pore size is comparable between 50% Matrigel and alginate-doped counterpart. **A** SEM images illustrating pore structure of hydrogels. **B** Pore sizes measured from SEM images (data presented as box and whisker plots; n = 3 images per gel type, n = at least 10 pores measured per image; *p < 0.05, **p < 0.01, ***p < 0.001 by one-way ANOVA with Tukey post hoc comparisons).

3.4.2 Effects of hydrogel mechanics on growth rate and gross organoid morphology

To verify that our hydrogel formulations do not affect organoid viability, we first conducted a live/dead assay of cerebral brain organoids as a model system. iPSCs were aggregated to form embryoid bodies (EBs), then encapsulated and grown for a further 3 days within Matrigel and alginate-Matrigel IPNs. No differences in short-term viability were observed between the various gel formulations tested (representative images in **Fig. S3.3**), confirming the expected cytocompatibility of these materials.

Next, midbrain organoids were generated and EBs (Fig. 3.3A) reached a consistent size of ~700 µm in diameter over 6 days (Fig. 3.3B). Once embedded in hydrogels, organoids were allowed to grow and develop for up to 2 months (Fig. 3.3C). In all hydrogel formulations, organoids consistently exhibited characteristic morphological traits including the development of neuroepithelial buds, and volumetric growth of the organoid within two weeks of embedding. Notably, organoids in the stiffest IPN tested (initial G' ~3.6 kPa, compared to the other matrices with initial G' <0.1 kPa) developed fewer buds. Furthermore, beyond two weeks, gross morphological differences developed with the stiffest IPN formulation, as organoids in the stiffest matrices grew to be rounder and significantly smaller than those in softer matrix formulations (Fig. 3.3D). Since hydrogel pore sizes are roughly equivalent between matrices, and the gel volumes are in the microliter range, it is unlikely that these morphological differences arise from metabolic transport limitations[197], but instead from the growth-induced compression caused by organoid growth into the surrounding mechanically rigid hydrogel network.

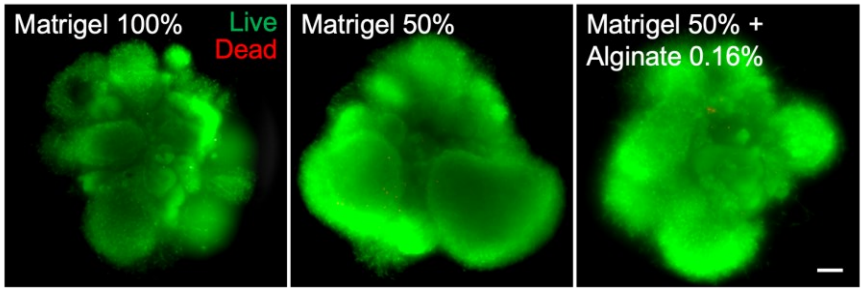

Figure S3.3. Live/dead staining with calcein AM (live) and ethidium homodimer-1 (dead) demonstrating viability of brain organoids after 3 days of growth in all hydrogels (n = 3 organoids). Organoids were generated with NCRM1 cells. Scale bar = 250 µm.

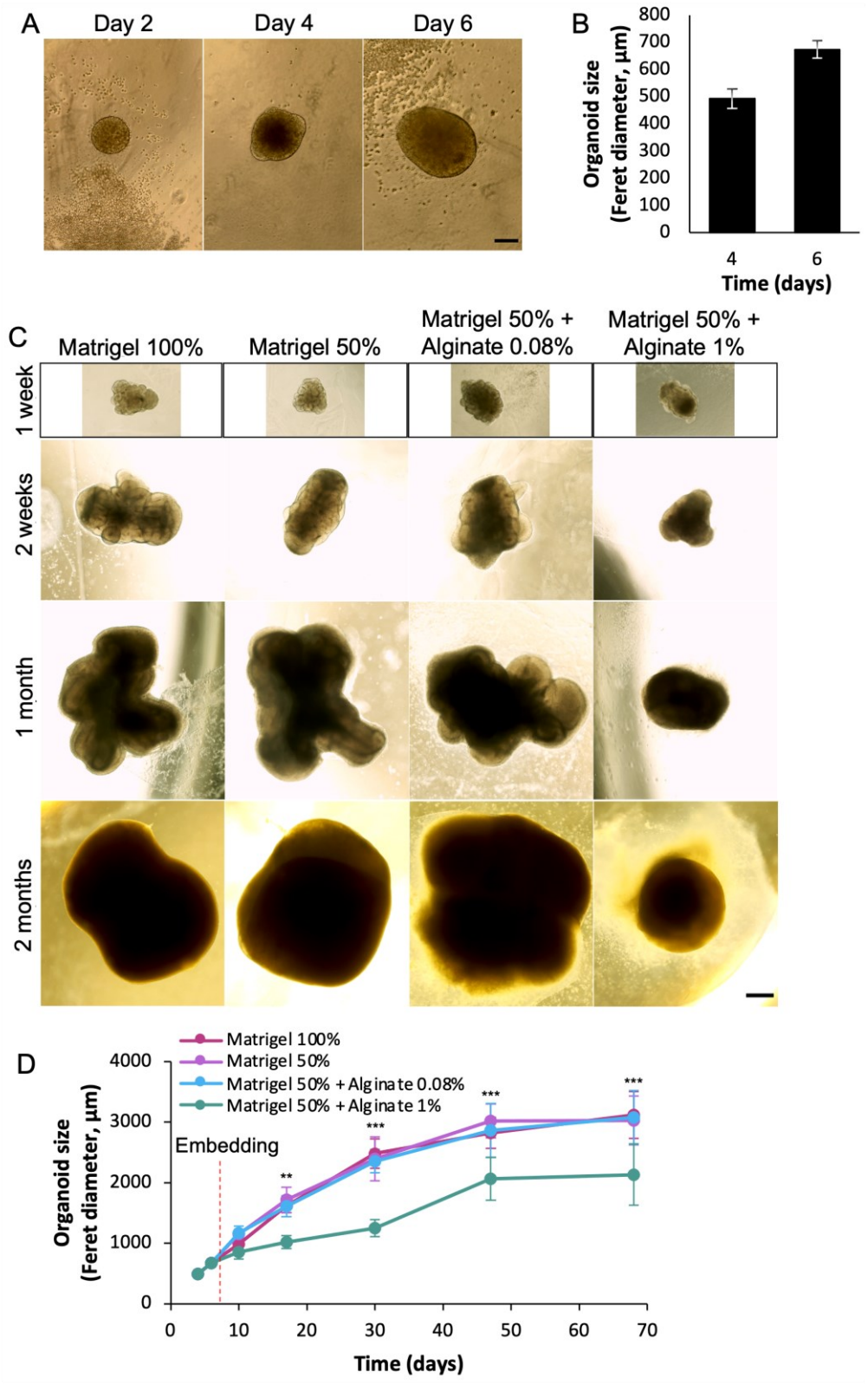

Figure 3.3. Organoid growth is restricted in stiffest composite. **A** Brightfield images of midbrain organoids during first week after seeding, before hydrogel embedding. Scale bar = 200 µm. **B**

Quantification of organoid growth pre-embedding demonstrating low size variability before introduction of hydrogels. **C** Brightfield images of midbrain organoid growth over time once embedded in hydrogels. Scale bar = 500 µm. **D** Quantification of organoid growth, using Feret diameter as size metric (data presented as mean ± standard deviation; day 4-6, *n* = 5 organoids; day 10-70, *n* = 8 organoids; **p < 0.01, ***p < 0.001 by two-way ANOVA with Tukey post hoc comparisons). Organoids were generated with TD22 cells.

3.4.3 Effects of matrix stiffness on organoid cellular composition

IPN-embedded brain organoids were fixed after 1 month, sectioned, and immunostained to examine internal organoid structure (**Fig. 3.4A**). As organoids are presumably experiencing growth-induced compression that restricts their size, we first asked whether the internal cellular density was affected by growth in the IPN matrices. Interestingly, there were no significant differences in the number of cells per unit volume (assessed based on nuclear counts) between conditions (Fig. 3.4B), indicating that cells are not differently compacted in different IPNs. Hence, there are fewer total cells in the stiffer matrix, and we therefore reasoned that proliferative or apoptotic differences might underly the observed gross size differences. However, we found no differences in either proliferation (based on an analysis of Ki67 staining; Fig. 3.4C), or apoptosis (based on cleaved caspase-3 staining; Fig. 3.4D; representative images in **Fig. 3.5A**).

Taken together, these findings suggest that apoptosis and/or proliferation may be affected at earlier time points in organoid development than those studied here. We hypothesized that this may be the result of an early shift in stem cell differentiation distributions – i.e. if stem/progenitor cells began differentiating earlier than usual, this shift from proliferation to differentiation would generate fewer cells overall and potentially a different distribution of differentiated cells. Thus, we next analyzed differentiation profiles of expected midbrain organoid constituent cells by staining for and quantifying dopaminergic neurons (expression of TH) and mature neurons (expression of MAP2) in each matrix composition. No significant differences were found in the proportion of dopaminergic neurons (TH+; Fig. 3.4E), but there was a significant increase in the proportion of MAP2-expressing mature neurons (Fig. 3.4F) in the stiffest matrix formulation tested. These findings suggest that either a greater relative number of mature neurons had developed, or that mature neurons had grown longer and larger in this condition. In either case, mature neurons accounted for more of the cells within organoids grown

in this stiffer condition, indicating that external mechanical rigidities contribute towards a difference in the development and maturation of neurons within the encapsulated midbrain organoids.

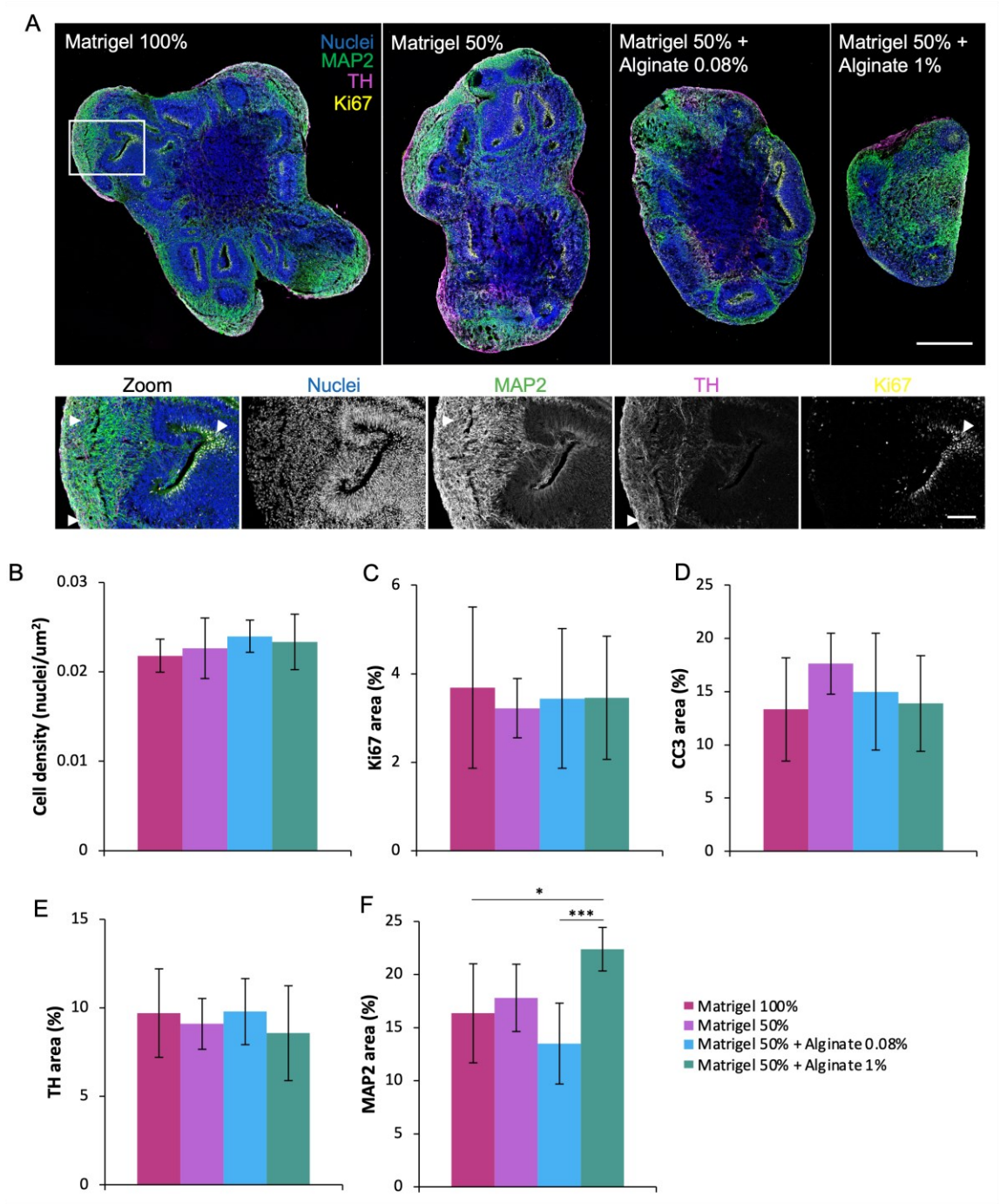

Figure 3.4. Organoid development is affected by stiffness. **A** Representative stained cryosections at 1 month old. White box outlines zoomed region shown in lower panels, with arrowheads marking stained regions. Main scale bar = 500 µm, zoom scale bar = 100 µm.

Quantification of **B** cell density (nuclei per μm^2), **C** Ki67, **D** cleaved caspase-3 (CC3), **E** tyrosine hydroxylase (TH), and **F** microtubule-associated protein 2 (MAP2) staining (% area of section) (data presented as mean ± standard deviation, n = 6-8 individual organoid sections; *p < 0.05, ***p < 0.001 by one-way ANOVA with Tukey post hoc comparisons). Representative images corresponding to **B**, **D** in Fig. 3.5A.

3.4.4 Effects of matrix stiffness on organoid internal architecture

Given the distinctive cellular compositions arising from growth in matrices of different mechanical properties, we explored structures that might give rise to these developmental differences. Neural rosettes are characteristic lumenized structures that appear within brain organoids; they recapitulate features of the neuroepithelium during embryonic brain development, with stem cells centred around the lumens and more mature neurons located farther away from the rosette[2–5,11,15,19]. We observed these structures in all hydrogel conditions, and noted that cells expressing the proliferative marker Ki67 were positioned at rosette centres, indicating the presence of neural progenitor/stem cells immediately adjacent to the rosette lumen; the more mature neurons (MAP2, TH) were located further away from the rosettes (Fig. 3.4A, more visible in **Fig. S3.4**). These observations, across all the matrix conditions tested, are consistent with expectations for midbrain organoids[4,19]. To compare characteristics of these developmentally-important internal structures, we used F-actin to identify them in tissue sections (Fig. 3.5A,B, more visible in **Fig. S3.5**), and quantified rosette number and size. Although rosettes were present in all conditions, significantly fewer were observed in the stiffest IPN (Fig 3.5C). In addition, rosettes exhibited a broad range of sizes in all conditions except in the stiffest IPN, in which the few rosettes present were also extremely small (Fig. 3.5D). As rosettes are the hubs for progenitor cells within the organoid[2–5,11,15,19], these findings are consistent with enhanced maturation of neurons in the stiffest IPNs, and lend further support to our general findings that external hydrogel mechanics influence organoid development and self-organizing capacity, and thus their internal architecture.

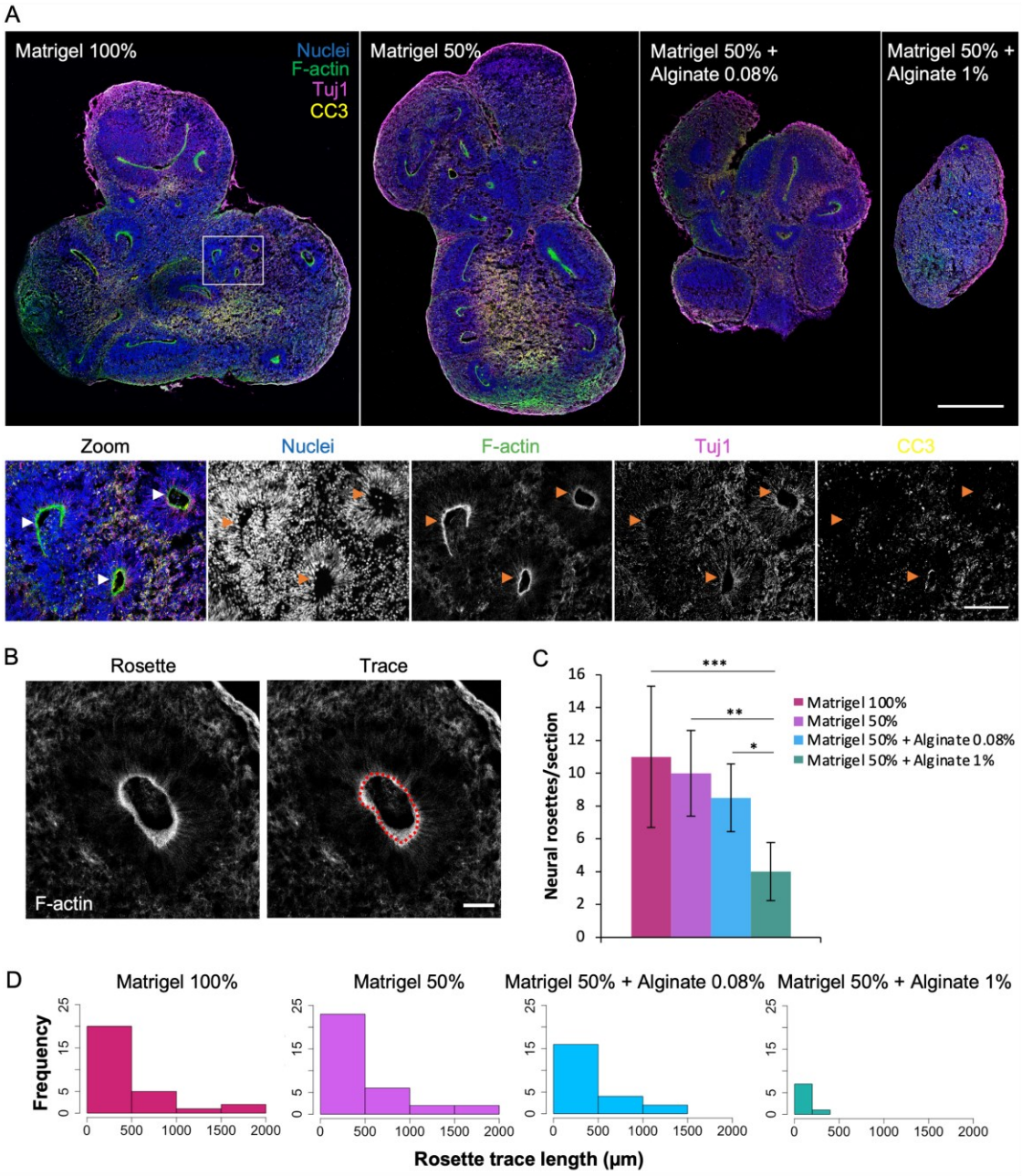

Figure 3.5. Neural rosette number and size are affected by stiffness. **A** Representative stained cryosections at 1 month old. β-tubulin III (Tuj1), a pan-neuronal marker, illustrates presence of neurons, and F-actin highlights neural rosettes. Cleaved caspase-3 (CC3) is quantified in Fig. 3.4. White box outlines zoomed region shown in lower panels, with arrowheads marking rosettes. Main scale bar = 500 µm, zoom scale bar = 100 µm. **B** A neural rosette visualized with F-actin staining (top) and its length traced in ImageJ (bottom). Scale bar = 50 µm. **C** Quantification of neural rosettes per section (data presented as mean ± standard deviation, *n* = 8 individual organoid sections; *p < 0.05, **p < 0.01, ***p < 0.001 by one-way ANOVA with Tukey post hoc comparisons). **D** Quantification of neural rosette length (trace of apical surface) (data presented as frequency distribution, *n* = 3 individual organoid sections).

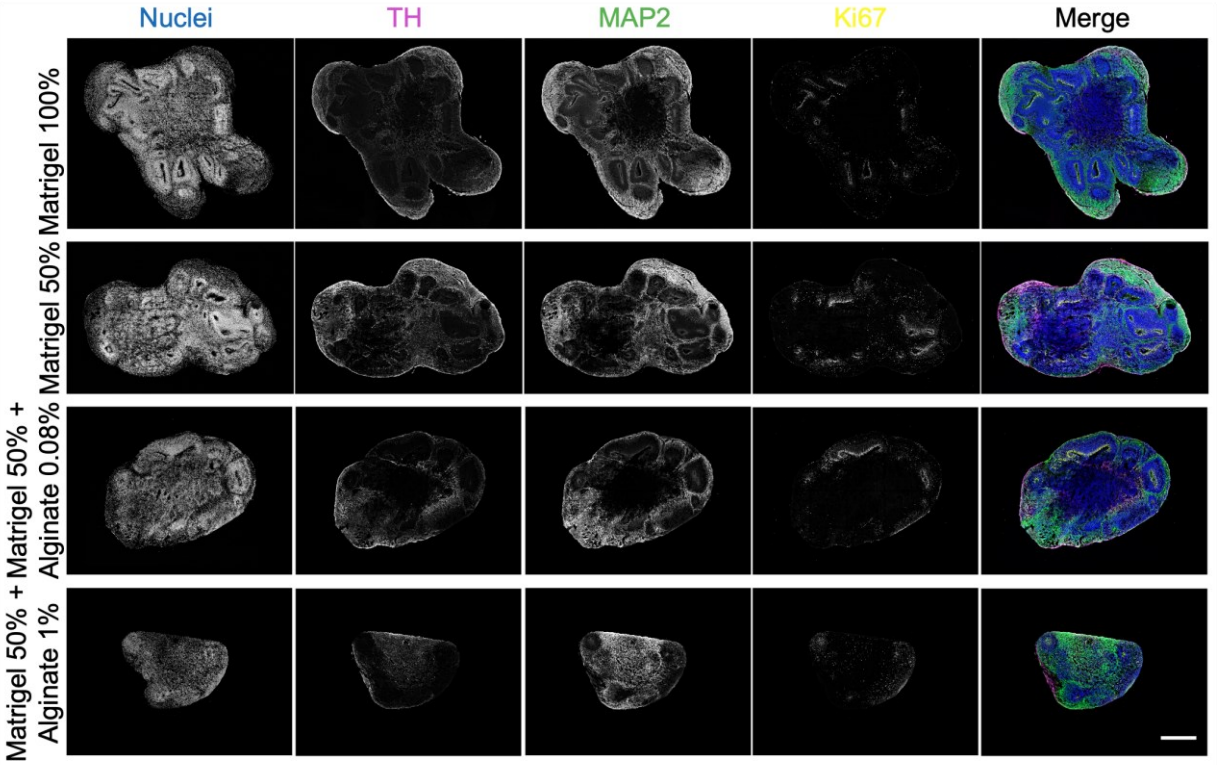

Figure S3.4. Representative stained cryosections at 1 month old. Tyrosine hydroxylase (TH) is a marker of dopaminergic neurons, microtubule-associated protein 2 (MAP2) is a marker for mature neurons, and Ki67 is a marker of cell proliferation. Scale bar = 500 µm.

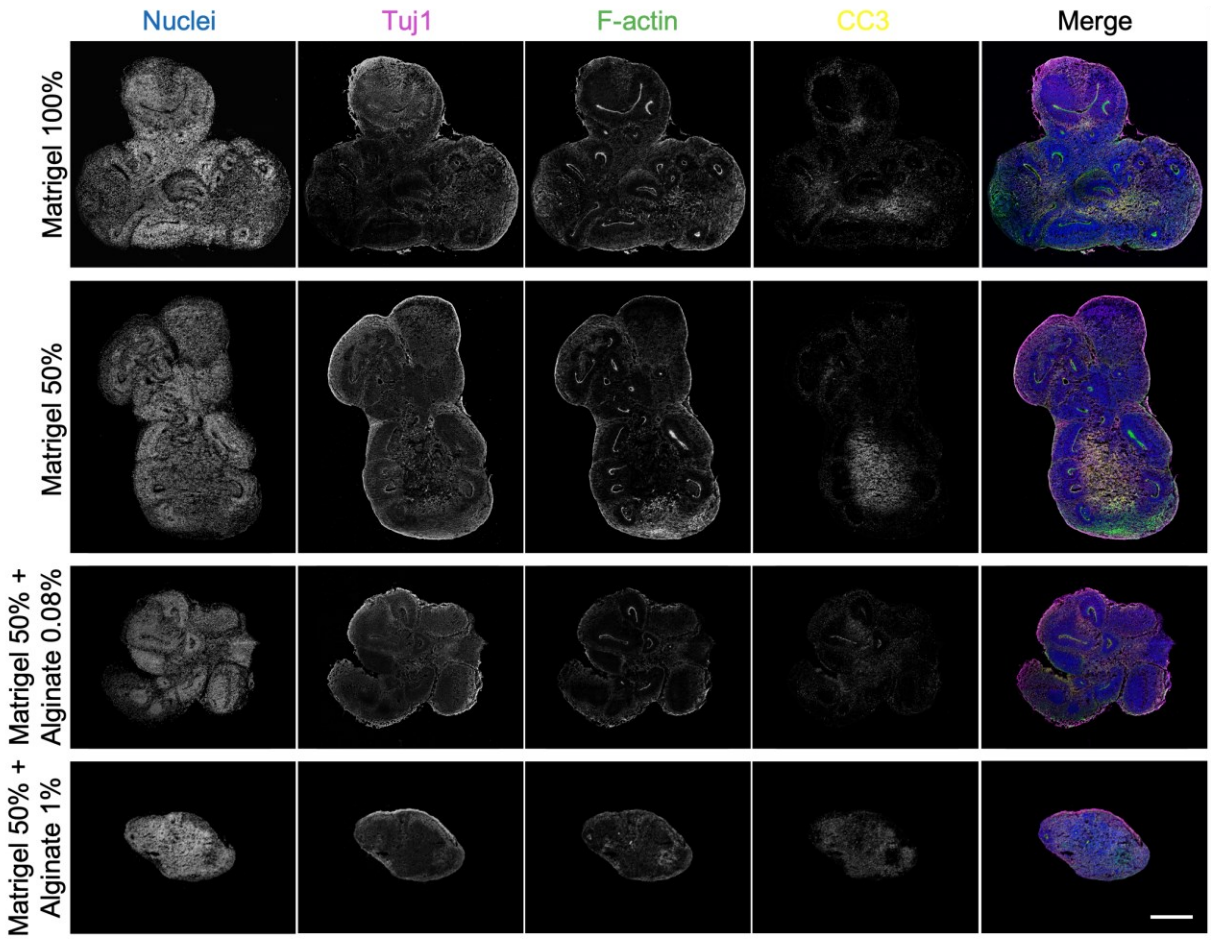

Figure S3.5. Representative stained cryosections at 1 month old. Actin highlights neural rosettes. β-tubulin III (Tuj1) is a pan-neuronal marker and cleaved caspase-3 (CC3) is an apoptotic marker. Scale bar = 500 µm.

3.5 Discussion

As matrix mechanics have been implicated in a wide variety of stem-cell differentiation processes[80–83,85], here we sought to evaluate the impact of this biophysical parameter on brain organoid development. Using alginate-Matrigel IPNs, we independently tuned mechanical properties of the encapsulating brain organoid matrix while controlling for cell binding sites in Matrigel and pore size. We demonstrate that organoids grown within these IPNs maintain normal cell viability, and present with cellular differentiation profiles characteristic of midbrain organoids as well as expected tissue organization. Organoids in the stiffest IPN tested were growth-restricted, but these changes did not appear to correlate with increased cell density,

decreased proliferation, or increased apoptosis at the time-point assessed. However, cell populations skewed towards a more mature and terminally differentiated neuronal phenotype. Consistent with this finding, the mechanics of the encapsulating matrix were also found to impact the number and size of neural rosettes within the organoid, structures associated with maintained stemness and proliferative potential. We propose that the reduced size and number of rosettes in the stiffest IPN are due to growth-induced compression, resulting in forces on the organoid that prevent budding and expansion (Fig. 3-1). Together, these findings demonstrate that external matrix mechanics can dictate the internal self-organization and structure of brain organoids, suggesting new methods with which to predictively control organoid architecture. This further lends support to recent studies that implicate an important role for external mechanics in the growth and development of the neonatal brain[82].

An organoid's ability to self-organize and form physiologically representative structures is one of the primary reasons for their value in studying various neurodevelopmental processes. Our observations that neural rosette formation depends on external cues is particularly interesting, as these structures play an important role in the development of brain organoids and their constituent cells[2,3,5,11,15], but little is known about the factors that influence their organization and emergence. Our observations of the cytoskeletal F-actin architecture surrounding the lumen suggests that these culture models recapitulate the involvement of apical constriction[115,118] in forming these apicobasally-polarized structures[2,3,5,11,15] – and that this process can be significantly affected by the mechanics of the growth microenvironment through mechanotransductive mechanisms associated with growth-induced mechanical compression. Consistent with previous findings that hydrogel stiffness can impact the formation of polarized neuroepithelial cysts from mouse stem cells[115], our work extends this finding towards longer-term developmental processes in human midbrain organoids. Furthermore, a recent paper discovered that stretching neural tube (the developmental precursor to the brain) organoids during growth resulted in increased proliferation and larger organoids, as well as enhanced developmental patterning (of the floor plate region, in particular)[145]. Their simulations suggested that stretching acted to relieve growth-induced compression, whereas our methods increased such compression and demonstrated the reverse phenomena.

We also observed effects on the area covered by mature neurons, suggesting that mechanics affect organoid development and neuronal developmental trajectory as well. We observed higher mature neuronal coverage in our stiffest composite, which could be due either to the number or size of mature neurons. Previous work finding that stiffness affects neuronal differentiation, in both 2D[106] and 3D[115], and at the developmental stage[174], supports this idea. While the effects observed in this work may be more specific to maturation than differentiation (suggested by similar TH staining), perhaps more favorable neuronal differentiation at earlier time points could explain our findings, resulting in more mature neurons at the time point we assessed. If differentiation towards a neuronal (i.e. non-proliferative) phenotype was favored in this way, this could also explain the difference in cell number that we observed, as earlier differentiation would result in fewer cells overall. Additional quantitative methods may be useful in identifying further or more subtle differences between cell populations in future work.

We note several limitations to our study. First, Matrigel itself is highly variable in composition[168–170], and while we ensured batch consistency within our study, whether batch-to-batch variability might affect IPN consistency remains unclear. Furthermore, Matrigel is highly temperature sensitive and heterogenous, making control over its gelation kinetics and the resulting mechanical properties difficult, and ultimately resulting in variable mechanical properties[198,199]. In addition, we have not characterized the mechanics of our hydrogels at the cellular length scale, which may be distinct from bulk measurements[200] with heterogeneity within samples[36,198,201], and could be differentially remodelled as the organoids develop through Matrigel degradation or ECM secretion. Hence it is important to note that all findings are described in terms of the initial mechanical properties, rather than at various stages in organoid growth. Regarding pore size of the hydrogels, the precise values may be different in wet conditions from our measurements on dried samples, but the pores are sufficiently large so as not to significantly hinder transport. We note that there are concerns in the literature about the effects of the freezing process on hydrogel microstructural morphology, however, a study that directly compared pore size measurement techniques found good agreement in measured values in spite of morphological differences[202]. We have not explored how cellular interactions with our materials were affected based on their chemical nature, such as charges of surface functional

groups. Finally, while this work focuses on changes in mechanical rigidity and a fairly consistent phase angle ratio between storage and loss moduli, the effects of matrix viscoelasticity on tissue growth are now emerging as key parameters driving cell function[80,178]. In future work, synthetic materials with independently tunable storage and loss moduli may be of value in better understanding these mechanotransductive processes.

3.6 Conclusion

Our findings that microenvironmental mechanics influence organoid self-organizing capacity demonstrate that mechanical properties are crucial factors in the development of brain organoids. Mechanical tunability thus presents a novel strategy to modulate the internal structure of organoids and elucidate the resulting effects on development. There is increasing evidence that mechanics play a role in disease initiation and progression, in neurodegenerative diseases as well as brain cancer, and thus this is relevant to developmental processes in the brain in both health and disease[82]. In addition, there is significant interest in developing alternative synthetic materials to support organoid growth with the idea that a fully defined, controllable and reproducible material would reduce organoid variability and increase experimental reproducibility[23,80,111]; our findings can inform design of such materials in terms of desirable mechanical properties for brain organoids.

3.7 Acknowledgments

We thank Professors Richard Leask, Matthew Harrington, and Milan Maric (McGill University) for rheometer access and expertise; Carol X-Q Chen for training and expertise in iPSC culture; Chanshuai Han and Meghna Mathur for teaching and assistance with organoid growth; Ronan da Silva and Paula Lépine for training on cryosectioning; and the Neuro Microscopy Imaging Centre. This work was supported by funding received from the CQDM Quantum Leaps program and the Canada First Research Excellence Fund, awarded through the Healthy Brains, Healthy Lives initiative at McGill University to TMD and CM, Canadian Cancer Society (Grant 706002), and NSERC Discovery (RGPIN-2015-05512) to CM. TMD is supported by a project grant from the CIHR (PJT – 169095) and received additional funding support for this project through The Sebastian and Ghislaine Van Berkom Foundation, the Alain and Sandra Bouchard Foundation, the Chamandy Foundation and the Mowafaghian Foundation. MNV is supported by FRSQ and a

Parkinson Canada postdoctoral fellowship. We gratefully acknowledge support from Healthy Brains, Healthy Lives and NSERC Postgraduate Scholarship-Doctoral to CCC, and the Canada Research Chairs in Advanced Cellular Microenvironments to CM.

3.8 Conflicts of interest

The authors declare no conflict of interest.

Chapter 4

The form, i.e. shape, of organs is incredibly important in their function. In several *in vitro* systems, the biophysical cue of geometry has been shown to influence cell and tissue behaviours, such as proliferation and invasion. Previous studies have manipulated the morphology of brain organoids through confinement or genetic manipulation, including my own work in Chapter 3, which showed that the biophysical cue of microenvironmental stiffness affected brain organoid size and shape by restricting growth. Based on this prior work, I selected geometry as the next biophysical cue to explore in the context of brain organoids, examining a more macro level than Chapter 3. In particular, we wanted to mold organoids into defined shapes, controlling geometry at a global tissue scale subsequent to organoid formation.

In this work, we develop a temperature-actuated hydrogel platform to enable application of molding forces in 3D to engineered tissues in culture. This strategy allows much more control over the final organoid shape than the incidental effect we observed on shape in Chapter 3. We first characterize this platform using simple shapes to mold breast cancer spheroids, a well-established model in our lab, and then we use more complex shapes to mold brain organoids into rings, driving them to fuse into continuous units around a post. We find that this molding does not affect organoid development and differentiation at the level we examined, suggesting our platform supports intrinsic developmental programming usually observed in organoid cultures. We therefore propose that this can be used as a tool to mold pre-formed tissues into building blocks with a variety of geometries for bioassembly. This work was published in *Lab on a Chip* by the Royal Society of Chemistry in March 2023.

Although these findings provide evidence that form is not required to drive certain developmental processes in standard organoid protocols, these protocols have been developed without such force application tools. There is growing evidence for the importance of forces in the morphogenesis of organs and organisms, and the contribution of forces to functional development. This platform is a tool that could be used to enable *in vitro* mimicry and application of these forces to tissue cultures, potentially producing improved experimental models and deepening understanding of how morphogenetic transformations take place by exploiting the biophysical cues of force and geometry.

4 Compressive molding of engineered tissues via thermoresponsive hydrogel devices

Camille Cassel de Camps[1#], Stephanie Mok[2#], Emily Ashby[2], Chen Li[2], Paula Lépine[3], Thomas M. Durcan[3], Christopher Moraes[1,2,4,5*]

1. Department of Biomedical Engineering, McGill University, Montréal, H3A 2B4 QC Canada
2. Department of Chemical Engineering, McGill University, Montréal, H3A 0C5 QC Canada
3. Early Drug Discovery Unit (EDDU), Montreal Neurological Institute and Hospital, McGill University, 3801 University Street, Montréal, H3A 2B4 QC Canada
4. Rosalind and Morris Goodman Cancer Institute, McGill University, Montréal, H3A 1A3 QC Canada
5. Division of Experimental Medicine, McGill University, Montréal, H4A 3J1, QC Canada

# These authors contributed equally
* Corresponding author: chris.moraes@mcgill.ca

4.1 Abstract

Biofabrication of tissues requires sourcing appropriate combinations of cells, and then arranging those cells into a functionally-useful construct. Recently, organoids with diverse cell populations have shown great promise as building blocks from which to assemble more complex structures. However, organoids typically adopt spherical or uncontrolled morphologies, which intrinsically limit the tissue structures that can be produced using this bioassembly technique. Here, we develop microfabricated smart hydrogel platforms in thermoresponsive poly(N-isopropylacrylamide) to compressively mold microtissues such as spheroids or organoids into customized forms, on demand. These Compressive Hydrogel Molders (CHyMs) compact at cell culture temperatures to force loaded tissues into a new shape; and then expand to release the tissues for downstream applications. As a first demonstration, breast cancer spheroids were biaxially compacted in cylindrically cavities, and uniaxially compacted in rectangular ones. Spheroid shape changes persisted after the tissues were released from the CHyMs. We then demonstrate long-term molding of spherical brain organoids in ring-shaped CHyMs over one week. Fused bridges formed only when brain organoids were encased in Matrigel, and the resulting ring-shaped organoids expressed tissue markers that correspond with expected differentiation profiles. These results demonstrate that tissues differentiate appropriately even

after long-term molding in a CHyM. This platform hence provides a new tool to shape pre-made tissues as desired, via temporary compression and release, allowing an exploration of alternative organoid geometries as building blocks for bioassembly applications.

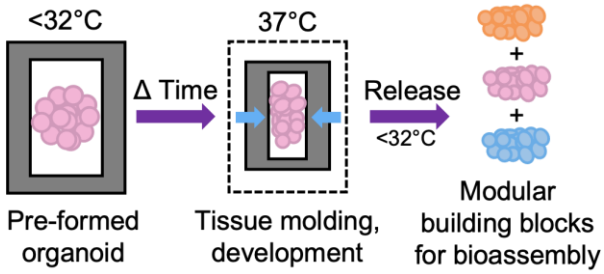

Figure 4.0. Graphical abstract.

4.2 Introduction

Biofabrication aims to create 3D tissue constructs with living cells, for a variety of applications[203,204], and generally requires microscale strategies to organize and position multiple cell types with respect to each other, as well as macroscale approaches to shape the overall tissue. Traditional biofabrication techniques first form a biomaterial scaffold, and then populate the scaffold by seeding with cells[203,205]. Bioprinting has recently gained traction in constructing engineered tissues[203,205], in which cells and matrix material are simultaneously positioned in a layer-by-layer fashion to produce a complex 3D structure[206,207]. However, real tissues and organs are typically much more dense, functionally-diverse, and finely-organized at the microscale[206,208,209] than can be achieved with conventional bioprinting approaches[206,209]. Furthermore, appropriate sources for the wide variety of cells required in most tissues remains a major limitation.

Organoid cultures, differentiated from pluripotent stem cells in a 3D matrix, have emerged as a potential strategy to obtain multiple finely-organized and functional cell types, but differing culture protocols and media formulation requirements often limit their ability to recreate an entire organ system, particularly those with specialized and distinct components. Assembling disparate organoids into a larger tissue via bioprinting may resolve this issue[206,208], while addressing the limitations of each technique: organoids offer high cell density, realistic cell types, and local architectures[3,209,210], while bioprinting can integrate and assemble functional tissue units to recreate organ function[208]. This approach has recently been used to create a

continuous intestinal tube with various gut cells[211], perfusable tissue aggregates[209], and physiologically realistic mammary[212] and neural structures[22,62]. These successes collectively demonstrate that hybrid multi-scale engineering of organoids and assembly via bioprinting or positioning is a promising strategy to reconstruct and study developmental processes *in vitro*, in more complex models than can be achieved with single-type organoids [213].

A potential limitation in this hybrid approach is that the shape of the building block organoid is largely uncontrolled, which in turn limits the tissue patterns that can be created. While some techniques have been developed to influence organoid shape[154,159,214], these strategies either leave embedded structures within the tissues, or will require modification of existing culture protocols which may unexpectedly affect organoid function. Here, we envision a strategy in which an organoid generated with current protocols can be compressively molded into a desired shape on demand, before being released for downstream processing in bioprinting applications. However, molding an organoid into an arbitrary shape presents significant challenges in mechanical design, as the molding structure must reversibly actuate with multiple spatially patterned degrees of freedom and movement. Furthermore, the molding process must create sufficient force to permanently deform the organoid, allow release of the soft biological tissue from the mold, and maintain viability and cell function during and after operation.

To address these challenges, we turned to smart hydrogels that can be formed in specific geometries, and adopt distinct morphologies[120,215–217] in response to various environmental triggers[216–220]. Poly(N-isopropylacrylamide) (PNIPAM) is a well-established material that contracts at temperatures above ~32°C[221], and can maintain a contracted shape at cell culture temperatures. PNIPAM hydrogels have been demonstrated to have good biocompatibility[222]. Here, we develop a strategy to fabricate Compressive Hydrogel Molders (CHyMs; Fig. 4.1A) in PNIPAM that can apply controlled strains to engineered tissues in culture. Tissues can be released on demand by cooling the cultures to room temperature. We demonstrate the utility of this platform using breast cancer spheroids and brain organoids, and show (1) that applied strains are sufficient to compact spheroids and change their shape; and (2) that a model organoid system can be formed into ring-like structures while maintaining their expected differentiation program in long-term CHyM culture.

4.3 Methods

Unless otherwise stated, all cell culture materials and supplies were purchased from Fisher Scientific (Ottawa, ON), and chemicals were from Sigma-Aldrich (Oakville, ON).

4.3.1 Device fabrication & characterization

Assembled mold chambers consisted of several pieces to allow for complete disassembly after casting to easily remove the hydrogel devices. Mold pieces for the CHyM microcavities were designed in Fusion 360 and printed on an AutoDesk Ember STL 3D printer using PR-57K black resin (Colorado Photopolymer Solutions) with 10 µm layer thickness. Molds were washed in isopropanol, and cured overnight in a UV chamber at 36 W. Mold walls were designed in AutoCAD and printed in PLA filament on a Monoprice Select Mini V2 printer. CHyM mold pieces were glued onto glass slides using Gorilla Super Glue to form the bottom of the mold, and mold walls were fastened to the glass slide (Fig. 4.1A). Separate solutions of 1% (w/v) ammonium persulfate (APS) in phosphate-buffered saline (PBS) and PNIPAM pre-gel (consisting of 1215 µL 20% PNIPAM in PBS, 810 µL 2% bis-acrylamide, 405 µL PBS, and 4 µL TEMED per slide) were prepared in glass test tubes, filtered using a 0.22 µm filter, and purged of oxygen by bubbling nitrogen gas through the liquid for 20 minutes, as described previously[200]. The two solutions were mixed in a 1:9 ratio (APS solution to PNIPAM pre-gel), poured into the assembled mold, and a glass coverslip was placed on top to limit oxygen diffusion into the polymerizing hydrogel for 20 minutes. To facilitate casting of the small central pillars in the ring-shaped CHyMs, 70% ethanol was sprayed onto the mold before filling, and a syringe and needle (25 gauge) were used to fill the pillars. The mold was disassembled to release the PNIPAM CHyMs, which were trimmed using a razor blade, rinsed in water, and then washed 3 times in PBS. CHyMs were allowed to swell overnight in 1% antibiotic-antimycotic in PBS, and stored in this solution at 4°C until use. To reduce cell adhesion to contracted PNIPAM (which is hydrophobic), CHyMs were incubated with a filtered solution of 1% BSA in PBS for 2 hours at 37°C the day before spheroid/organoid loading. They were kept in this solution overnight at 4°C, rinsed with PBS, and soaked in media for 2 hours at room temperature immediately before use.

4.3.2 Spheroid & organoid generation

All cell cultures were maintained at 37°C with 5% CO_2. The human breast cancer cell line T47D (ATCC HTB-133) was maintained in Dulbecco's Modified Eagle Medium with 10% fetal bovine serum and 1% antibiotic-antimycotic (complete media) with media changes every 2-3 days, and passaged using 0.25% trypsin-EDTA when 80% confluent. Spheroids were generated as previously described[223], using a polyacrylamide (PAA) micropocket platform to aggregate T47D cells. Briefly, cell suspensions were prepared at 15 x 10^6 cells/mL, dispensed into PAA devices, and incubated for 2 days to allow spheroid formation before loading into CHyMs. Spheroids were also generated in agarose micropockets, with the same method. The agarose micropockets were fabricated using micropocket mold pieces (3D printed as above) in PNIPAM mold assemblies. A 1% agarose solution was microwaved in 10 second intervals until melted, used to fill the mold assemblies, and then allowed to set for 40 minutes. Agarose devices were prepared for cell culture in the same manner as CHyMs.

iPSCs were cultured in mTeSR (StemCell Technologies) on Matrigel-coated plates with daily media changes, and passaged using Gentle Cell Dissociation Reagent (StemCell Technologies) when 70% confluent. Regions of spontaneous differentiation were cleared manually. The use of iPSCs in this research was approved by the McGill University Health Centre Research Ethics Board (DURCAN_IPSC/2019-5374). Cerebral organoids were generated according to the Lancaster protocol[3] using human control iPSC line AIW002-02 (male), which was obtained through The Neuro's C-BIG repository and had passed multistep quality control[224]. Cells that were at least 70% confluent were washed with DMEM and incubated with Accutase (Gibco) for 3-5 minutes. DMEM (equal volume to Accutase) was added, the liquid pipetted across the surface of the culture vessel to assist with detaching the cells, and collected; this was repeated once more. Cells were centrifuged at 1200 rpm for 3 minutes. The pellet was resuspended in 1 mL of hES media (low bFGF, with ROCK inhibitor; consisting of 400mL DMEM-F12 + Glutamax, 100 mL Knockout Serum Replacement, 15mL hESC-quality FBS (Gibco), 5mL MEM-non-essential amino acids, 3.5 µL 2-mercaptoethanol, bFGF at 4 ng/mL final concentration, and ROCK inhibitor at 50 µM final concentration)[3] using a P1000 tip plus a P200 tip on top[19]. An aliquot was stained with Trypan Blue, and cells were counted using a LUNA-II™ Automated Cell Counter. Cell suspensions

were diluted in hES media to seed 10000 live cells/well in 96-well round-bottom ultralow attachment plates (Corning Costar), and centrifuged at 1200 rpm for 10 minutes. Media was changed on Day 2 to hES media (low bFGF, no ROCK inhibitor), on Day 4 to hES media (no bFGF, no ROCK inhibitor), and on Day 6 to neural induction media (consisting of DMEM-F12 + Glutamax, 1% N2 supplement, 1% MEM-non-essential amino acids, and heparin at 1 μg/mL final concentration)[3] using a multichannel pipette. To remove media, the culture plate was held vertically so organoids would fall to the sides of the wells; pipette tips were inserted into the wells at an upwards angle, away from the organoids, and media was aspirated slowly. To add media, the culture plate was rested on a surface horizontally, and pipette tips were inserted into the wells at an angle so that they pressed against the sides of the wells; media was ejected slowly. Organoids were maintained until Day 10 in neural induction media before loading into CHyMs.

4.3.3 Tissue compression in CHyMs & release

To remove spheroids from the PAA micropockets so they could be loaded into CHyMs, media was pipetted rapidly at the micropocket device to displace the spheroids. In a separate plate, media was aspirated out of wells and CHyM microcavities, and P200 pipette tips (with cut tips to enlarge the opening) were used to transfer spheroids or early-stage organoids into the devices. Tissues were allowed to settle into the microcavities for several minutes before adding media to each well (complete media for T47D spheroids, neural induction media for cerebral organoids). Devices were incubated at 37°C for up to 2 weeks with media changes every 4 days. Matrigel was added to some organoids the day after loading by pipetting a droplet onto the ring microcavity. To release tissues from CHyMs after compressive molding, media was removed from the wells and cold media was added to quickly drop the temperature of the devices to expand them and allow for tissue removal, after which tissues were returned to 37°C.

4.3.4 Live tissue analyses

Spheroids and organoids were imaged using an EVOS^{TM} M700 Imaging System or an Olympus IX73 spinning disc confocal microscope. Live/dead staining was performed using calcein AM and ethidium homodimer-1 (Life Technologies) at 4 μM in media for 40 minutes at 37°C. Device and tissue measurements were performed manually in Fiji software[225], using the Stitching plugin[226] where necessary to stitch image tiles together.

4.3.5 Immunostaining

Tissues were fixed with 4% (w/v) paraformaldehyde, spheroids overnight at 4°C, and organoids for 1 hour at room temperature with CHyMs flipped upside down, and then washed 3 times with PBS. Organoids were stained using a whole-mount staining protocol. They were blocked for 4 hours at room temperature with 0.5% Triton X-100 + 5% goat serum in PBS, and incubated with primary antibodies diluted in blocking buffer overnight at 4°C. Organoids were then washed 3 times for 10 minutes in PBS, incubated with secondary antibodies and Hoescht 33342 diluted in blocking buffer overnight at 4°C, and washed 3 times. Early-stage brain organoids were mounted on glass slides with Fluoromount Aqueous Mounting Media, coverslips were sealed with clear nail polish, and images were collected on a Zeiss laser scanning confocal microscope. Organoids compressed in CHyMs were imaged with a Leica TCS SP8 confocal microscope using an imaging chamber created by a stack of adhesive imaging spacers (Electron Microscopy Sciences, 70327-8S) between a glass slide and coverslip. Antibodies and stains were used as follows: anti-N-cadherin at 1:25 (rat monoclonal, DSHB Hybridoma Product MNCD2; MNCD2 was deposited to the DSHB by Takeichi, M. / Matsunami, H.), anti-E-cadherin at 1:200 (rabbit monoclonal, Abcam ab40772), anti-E-cadherin at 1:50 (mouse monoclonal, Abcam ab1416), goat anti-rat IgG (H+L) Alexa Fluor® 555 at 1:500 (polyclonal, Life Technologies A21434), donkey anti-rabbit IgG H&L (DyLight® 650) at 1:500 (polyclonal, Abcam ab96894), goat anti-mouse IgG H&L (Alexa Fluor® 488) at 1:1000 (polyclonal, Abcam ab150113), phalloidin–tetramethylrhodamine B isothiocyanate at 1:50 (Sigma-Aldrich P1951), and Hoescht 33342 at 1:5000 (Invitrogen H3570).

4.3.6 Statistical analysis

Analyses were performed in R statistical software[187]. If data were normally distributed and variances were equal, one-way ANOVA was performed with Tukey post hoc comparisons; if variances were not equal, Welch's t-test was performed for 2 groups, or Welch's ANOVA for more groups with Games-Howell post hoc tests. If data were non-normally distributed, the Wilcoxon signed-rank test was performed for 2 groups, or the Kruskal-Wallis test was performed for more groups. For paired data, as the differences of the pairs were not normally distributed, the Wilcoxon matched-pairs signed-rank test was used. All analyses for significance were carried out with $\alpha = 0.05$.

4.4 Results & Discussion

4.4.1 CHyM device fabrication

To produce the temperature-actuated CHyMs needed to compress tissues (Fig. 4.1A), PNIPAM hydrogels were cast against and released from stereolithographically-printed 3D molds (Fig. 4.1B-D), which we have previously used to produce complex shapes for tissue engineering in polyacrylamide hydrogels[223]. This approach allowed us to rapidly iterate and design a wide variety of geometries, and to incorporate sloped walls above the microcavity to funnel the cultured tissue into the cavity. Replica molded PNIPAM gels released easily from the disassembled polymerization chamber (Fig. 4.1E), and were confirmed to contract at temperatures above ~32°C. When placed in a 37°C incubator, devices rapidly contracted, but expansion of the contracted hydrogels when returned to room temperature was slower and took up to 2 hours to swell completely, depending on device geometry. Fortunately, the initial expansion was generally sufficient to release compressed tissues within minutes, and expansion can be accelerated by adding chilled media, provided the biological tissue can handle the cold shock without long-term impact.

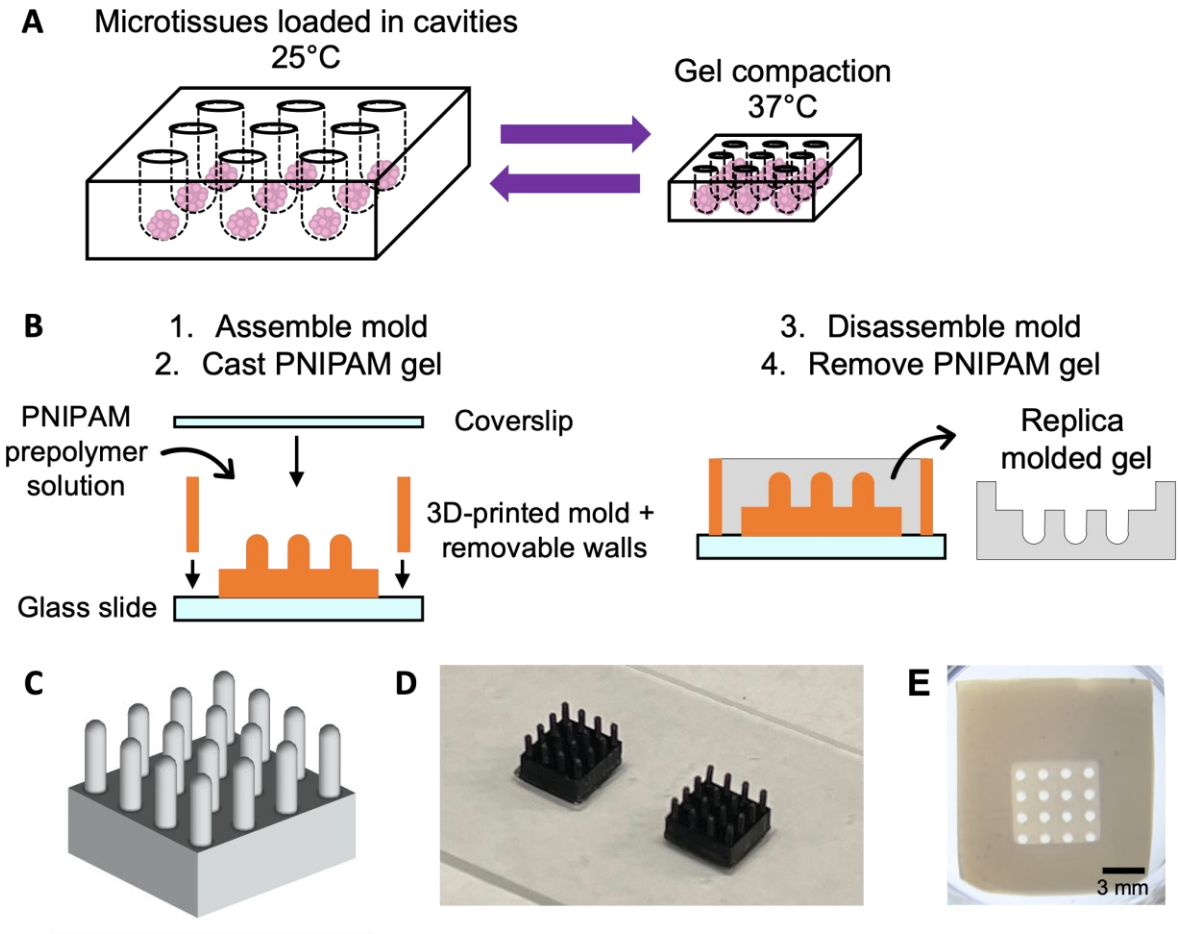

Figure 4.1. Compressive Hydrogel Molder (CHyM) fabrication. A Schematic of microtissue compression in temperature-actuated PNIPAM hydrogel devices. **B** Mold pieces are 3D printed in-house with microcavity geometries as desired, assembled for PNIPAM hydrogel casting, and disassembled to release replica molded gel devices. **C** Mold design, **D** 3D printed microcavity molds glued to glass slide, and **E** replica molded CHyM with circular microcavities.

4.4.2 Directionally-defined compressive molding

To demonstrate the potential for this technology in applying multidirectional strains to tissues of interest, we developed two simple test cases in which tissues can be biaxially compacted in a cylindrical microcavity, or uniaxially compressed between platens in a rectangular microcavity (Fig. 4.2A). With this formulation of PNIPAM, hydrogels reproduced mold features with reasonable fidelity, and cavity shapes were observed to shrink to less than half their original size upon incubation (Fig 4.2B). Although some warping was observed at the CHyM periphery (likely due to manual trimming of the devices during fabrication), the tissue chamber features

themselves shrank evenly with no skew or stretch, and shrinkage was highly consistent and predictable (Fig. 4.2C, D). Since it may be possible to alter the degree of compaction based on gel formulation, we tested other PNIPAM pre-gel formulations with varying concentrations of PNIPAM. Device contraction was found to be significantly impacted, but over a relatively small dynamic range (Fig. S4.1). Alternatively, varying the amount of crosslinker or nanoscale gel architecture may be a useful strategy to achieve more broadly tunable compaction ratios[227,228].

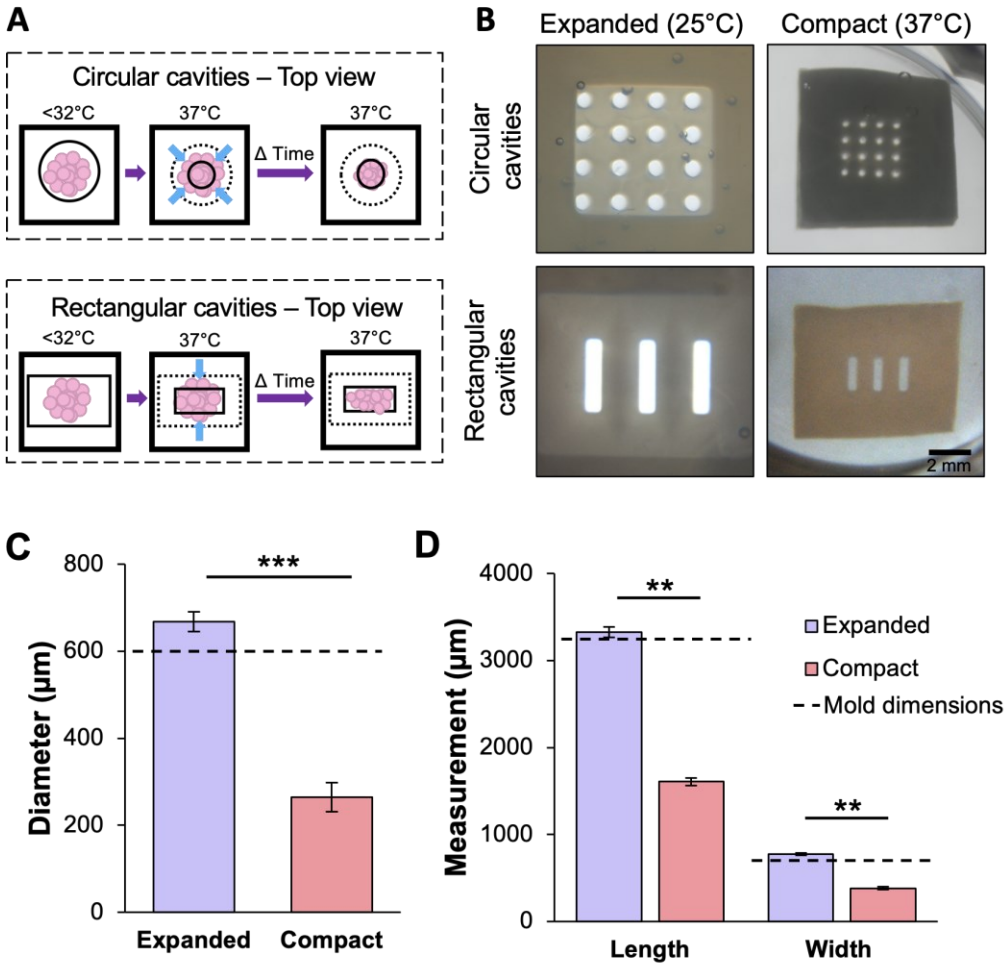

Figure 4.2. Characterization of device operation in biaxial and uniaxial compression designs. A Schematic of PNIPAM hydrogel devices, with circular and rectangular microcavities to hold cultured tissues. **B** Devices and microcavities shrink upon incubation. Measurements of **C** circular and **D** rectangular microcavity dimensions at room temperature (expanded) and after 24h incubation (compact). Dashed lines indicate original mold dimensions. (Data in **C** presented as mean ± standard deviation; n = 38-44 samples; ***$p < 0.001$ by Welch's t-test. Data in **D** presented as mean ± standard deviation; n = 9; **$p < 0.01$ by Wilcoxon matched-pairs signed-rank test.)

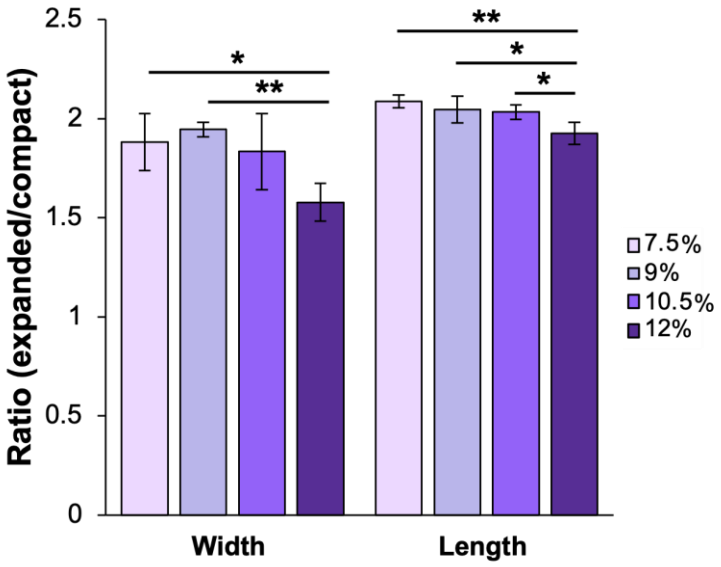

Figure S4.1. Compaction ratios of varied PNIPAM formulations. CHyMs with rectangular cavities were fabricated with varying amounts of PNIPAM, from 7.5-12% in the final gel mixture. Degree of contraction was significantly different for varied formulations, but relatively robust across multiple formulations, with only the highest concentration of PNIPAM compacting slightly less (data presented as mean ± standard deviation; n = 4; *p < 0.05, **p < 0.01 by one-way ANOVA with Tukey post hoc comparisons).

Given the robust shrinkage ratios observed, this approach can hence be applied in principle to generate a wide range of three-dimensional compressive molding fields based on the desired shrunken dimensions of the hydrogel. While the compressive fields generated will be limited by the replica molding cast-and-peel technique which cannot produce fully-enclosed 3D structures, replicating overhanging features[223] can partly ameliorate this concern by enabling fabrication of CHyMs with partially enclosed cavities. We note that while this might permit out-of-plane deformation, microcavities could be designed sufficiently deep to allow this deformation to occur without issue. Feature dimensions however will always be limited by 3D print resolution of molds and the fidelity of the hydrogel replica-molding process. While this may hence require some process optimization, the dimensions demonstrated here are sufficient for a wide variety of spheroid and organoid applications.

4.4.3 Elastic and plastic tissue deformation in CHyM-compacted tissues

As a first demonstration of the tissue molding operation, cancer spheroids were formed in spherical micropocket devices using a previously established protocol[223], loaded into the

cylindrical and rectangular CHyM devices, and compressed for up to 24 hours (Fig. 4.3A, D). Tissue compaction was rapid and plateaued within 4 hours at radial compression levels of ~50% (Fig. 4.3B). Although considerable, these compaction levels are not surprising given our previous findings of significant internal spaces within spheroids formed using this technique[200,229]. Once the CHyMs were expanded and the tissues released, they did slightly increase in size within 30 minutes, but then remained in a compacted state for at least 3 hours (Fig. 4.3C), demonstrating that the spheroid had been both plastically and elastically deformed during compression. Similar results were observed when measuring aspect ratio of spheroids placed under uniaxial compression, where a small amount of elastic recoil was observed after releasing the tissue from compression (Fig. 4.3D, E). In all cases, cell viability remained high after the compaction process (Fig. 4.3D, Fig. S4.2 for comparison to polyacrylamide, agarose).

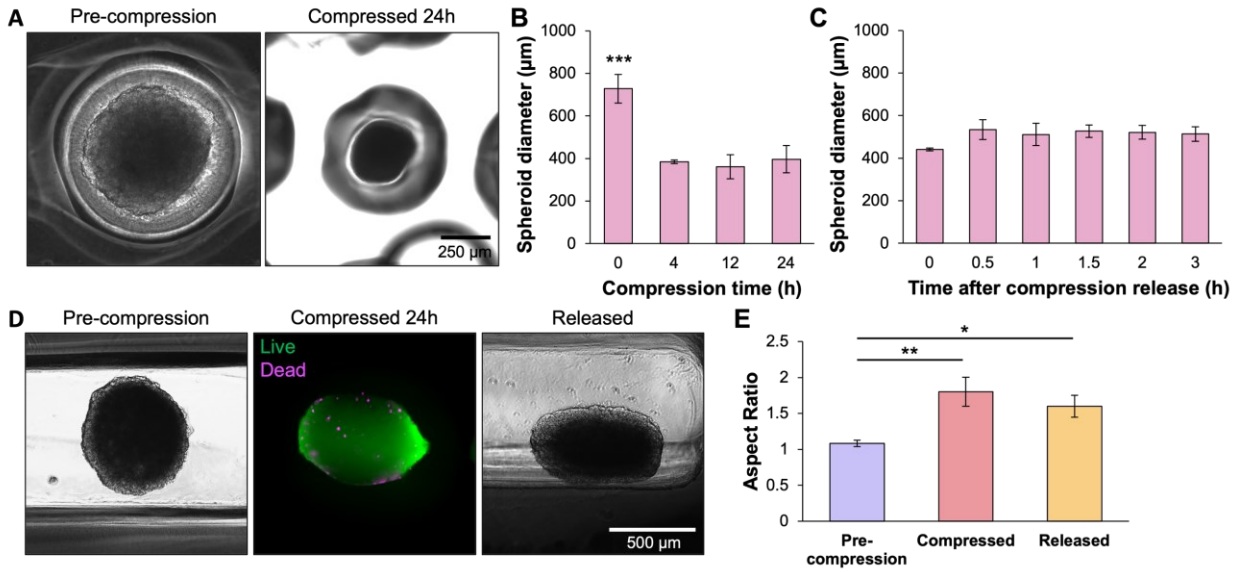

Figure 4.3. Spheroid compression and release with simple shapes. A A T47D spheroid loaded into a room temperature (expanded) circular microcavity, and after 24h of incubation. **B** Spheroid diameter during incubation (data presented as mean ± standard deviation; n = 5-22; ***p < 0.001 by Welch's ANOVA with Games-Howell post hoc test). **C** Spheroid diameter after addition of chilled media to expand devices and release spheroids from compression (data presented as mean ± standard deviation; n = 3; p = 0.1686 by Kruskal-Wallis test). **D** A T47D spheroid loaded into a room temperature (expanded) rectangular microcavity, after 24h of incubation with live/dead staining, and after fixing and release (device is expanded). **E** Measurements of aspect ratio upon loading into rectangular microcavities, after 24h incubation, and after fixing (data presented as mean ± standard deviation; n = 3-6; *p < 0.05, **p < 0.01 by Welch's ANOVA with Games-Howell post hoc test).

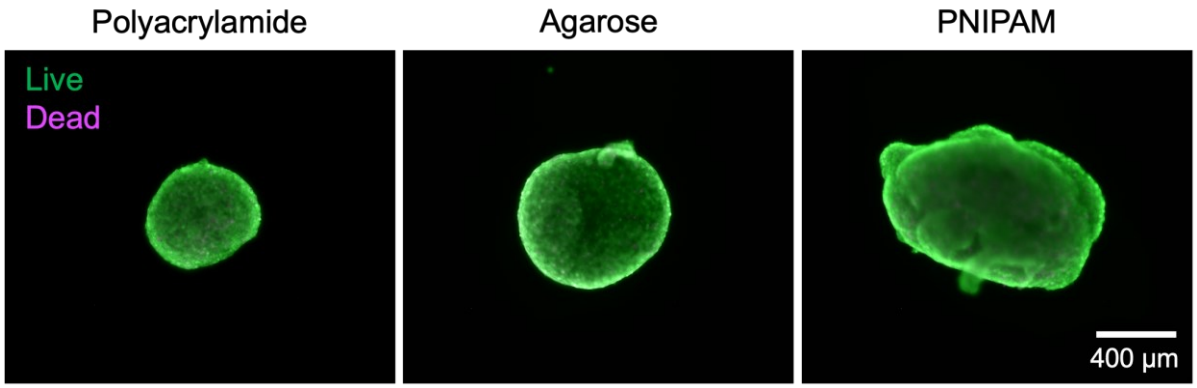

Figure S4.2. Viability of spheroids grown in various hydrogel microwells. T47D spheroids were formed and cultured in hydrogel microwells for 3 days before live/dead staining. Spheroids were then removed from microwells for imaging.

4.4.4 Ring-like brain organoid molding

Since tissues often form tube-like structures such as gut or neural tubes[92,118,230], we next demonstrate the potential utility of this platform by molding organoids into ring-like building blocks, that may ultimately be used to generate tube-like structures via downstream bioprinting[208]. We therefore designed CHyMs with ring-shaped microcavities (**Fig 4.4A**). This more complex shape was reproducible during device fabrication, and demonstrated similar well-controlled and repeatable shrinkage properties as those observed in the uniaxial and biaxial compression devices. Both the cavity space and the central post of the ring shrank upon incubation, and several cavity/post dimension combinations were tested to illustrate the range of possibilities achievable (Fig 4.4B,C). Based on the anticipated size of early-stage brain organoids and their growth rates at the time of molding[231], CHyM devices with 500 µm cavities and 0.75 mm posts were selected and used in all subsequent experiments. These molds produced structures with an expanded diameter of ~1.7 mm, shrinking to ~0.9 mm when compact, which should allow the organoid to wrap around the central pillar over one week in the CHyM.

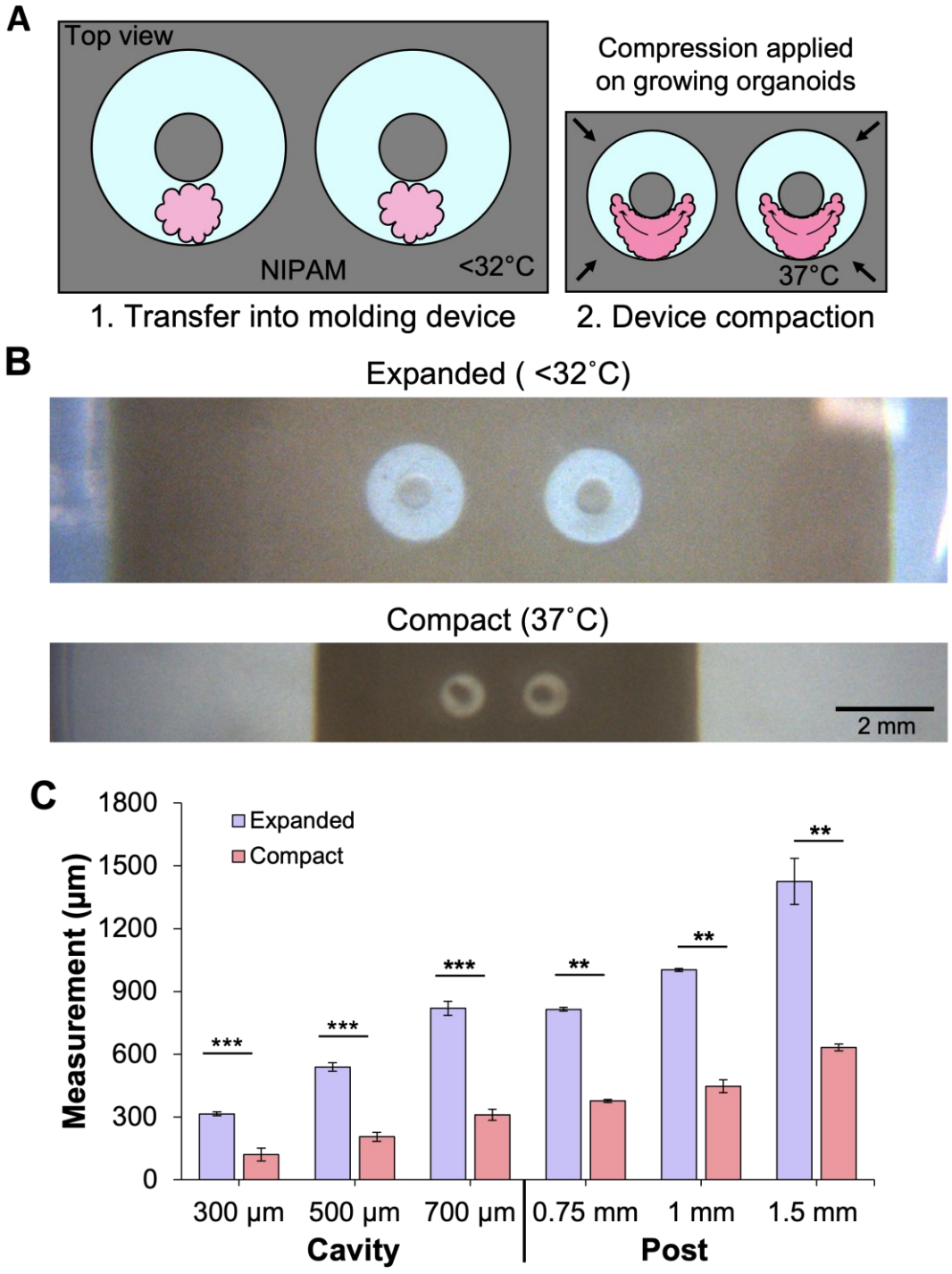

Figure 4.4. Characterization of ring molding devices. A Schematic of PNIPAM hydrogel device with ring-shaped microcavities to guide organoids to adopt ring-like morphologies. **B** Devices and ring microcavities shrink upon incubation. **C** Measurements of various microcavity widths and post diameters at room temperature (expanded) and after 24h incubation (compact) (data presented as mean ± standard deviation; n = 5-10; **p < 0.01, ***p < 0.001 by Wilcoxon signed-rank test).

During brain organoid formation, many protocols suggest encapsulating the organoid in an extracellular matrix approximately 7 days after the initial formation of the embryoid body. We found that the extracellular matrix Matrigel could be readily incorporated into contracted CHyM devices after initial organoid compression (Fig. 4.5A). The initial compression of the mold only slightly deformed the matrigel-embedded brain organoid, which then grew within the compressed cavity to wrap around the central post and reproducibly form a bridge with itself over ~6 days of growth (Fig. 4.5A; schematic in Fig. 4.5C). Interestingly, only those organoids encapsulated in Matrigel fused around the central pillar to form rings (Fig. 4.5B), while organoids that were not encapsulated in Matrigel generally formed a simple elongated organoid adjacent to the central pillar (representative image in Fig. 4.5D). Similar results were observed when organoids were loaded into CHyMs on days 7-11 after organoid seeding; some organoids were cultured for 2 weeks in the devices.

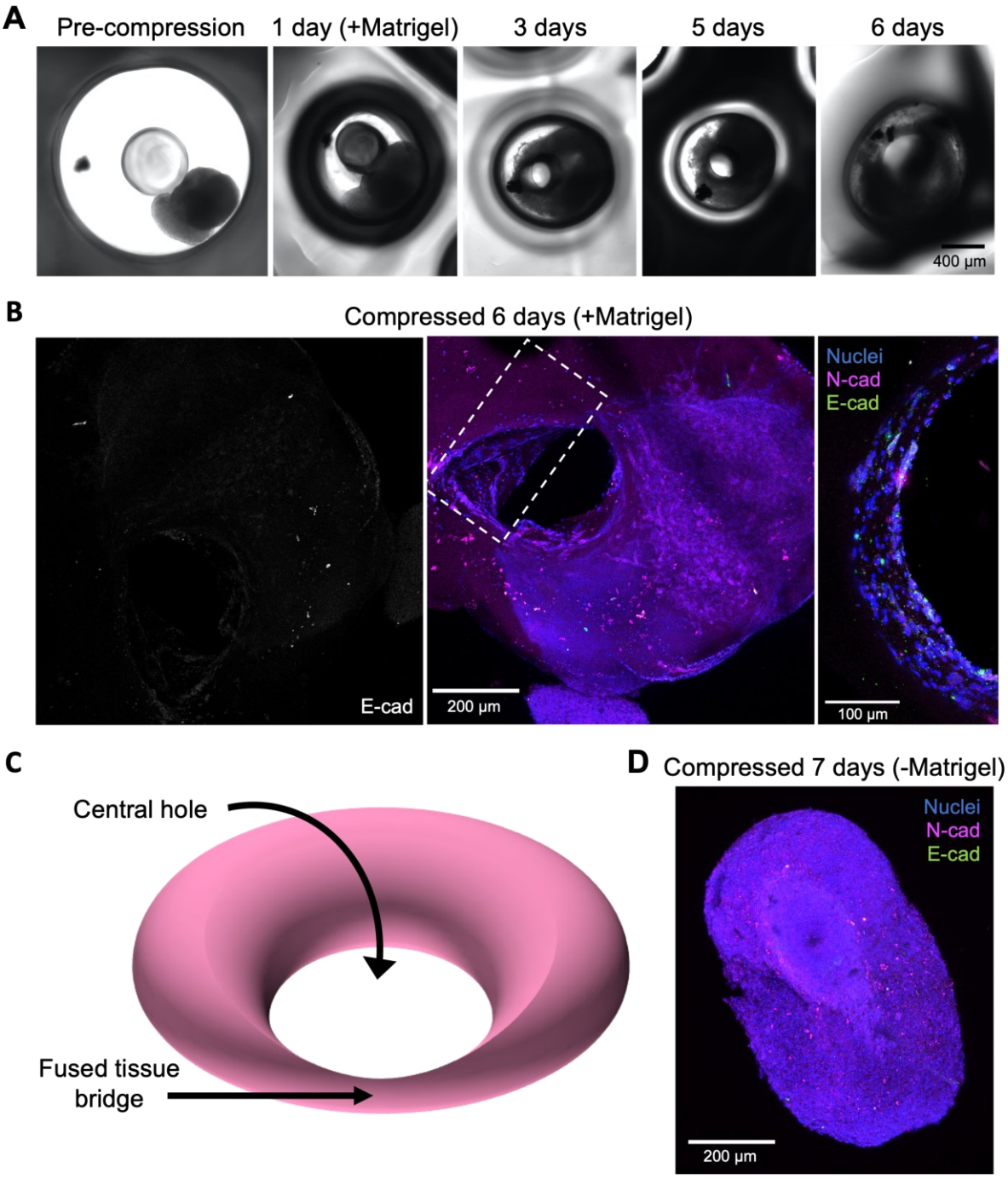

Figure 4.5. Organoid molding in ring CHyMs. **A** A brain organoid loaded into a room temperature (expanded) ring microcavity, and over 6 days of growth in the device. **B** Staining of the ring organoid after 6 days of CHyM compression with closeup of the point of fusion (approximate location outlined in white box) shows dominant N-cadherin (N-cad) and minimal E-cadherin (E-cad) expression. **C** Schematic of an organoid that formed a ring around the central pillar of the CHyM, fusing with itself to form a bridge. **D** Organoids cultured in CHyMs without Matrigel did not form rings.

In contrast with the previous short-term tissue deformation experiments, these molding experiments were longer and required growth of the tissue into the confining mold chamber, after the initial molding stress was applied. Hence, although this is a combination of both compressive and growth-molding processes, dynamically changing the volume of the culture chamber reduced the length of time required to fill the ring-shaped cavity, and also facilitated release after compression for downstream processing and imaging.

Throughout this process, the organoid was maintained within a compacted hydrogel structure which may limit diffusion of nutrients and waste. We therefore wanted to confirm that the CHyM did not affect the biological function of the tissue. We first verified that organoids remained viable after 6 days within the CHyM (Fig. S4.3), suggesting that sufficient nutrient and oxygen exchange was occurring. We then then examined differentiation markers known to characteristically change during this stage of brain organoid culture. At early stages of brain organoid development, tissues strongly express E-cadherin, which is known to be replaced with N-cadherin as differentiation progresses[2,115,163]. We therefore confirmed that organoids showed high levels of E-cadherin expression prior to loading them into the CHyM devices (Fig. S4.4). However, after growth and removal from the CHyM device, E-cadherin expression was minimal, while substantial N-cadherin was observed (Fig. 4.5B). This switch in cadherin expression is consistent with expected progression of cells in this differentiation process, and strongly indicative of appropriate stem cell differentiation. Hence, extended culture in CHyMs did not affect the differentiation of cells, suggesting that the CHyM system may be useful in both short- and long-term compressive molding applications.

Figure S4.3. Brain organoid viability in long-term culture. A brain organoid grown for 6 days a CHyM, with live staining on the final day of culture. (Compacted PNIPAM presents some light-scattering difficulties.)

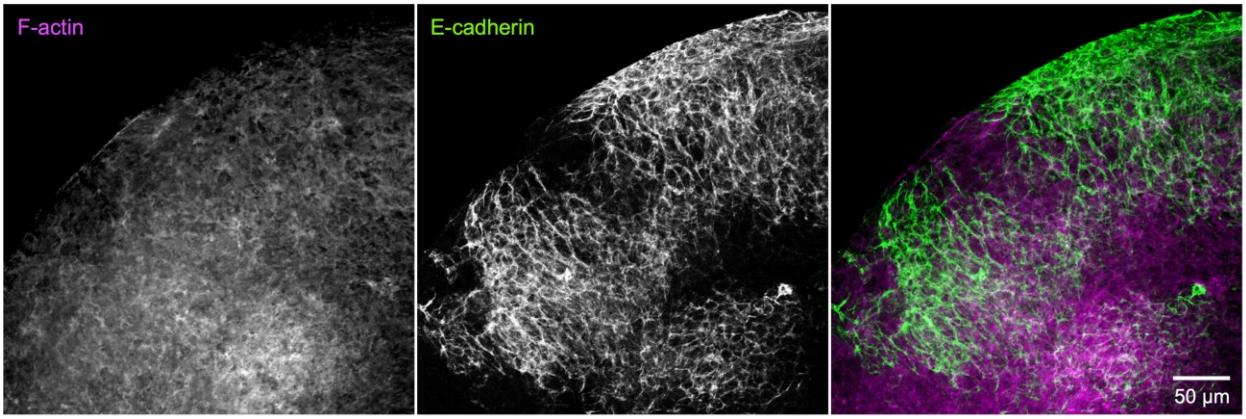

Figure S4.4. Early-stage brain organoids express E-cadherin before compression in CHyMs. 10-day old brain organoid stained for E-cadherin and filamentous actin (F-actin), shown at the organoid periphery.

While the applications demonstrated in this paper are in shaping microtissues via compressive molding, we believe this platform might be of future importance in investigating fundamental and applied questions in tissue biomechanics and mechanobiology. For example, this platform provides the basis with which to apply spatially-directed compressive forces on developing tissues, which could be used to understand the biophysical cues that drive tumour metastasis, and other mechanically-related diseases[98,232–235]. Controlled tissue deformation could be used to measure both mechanical plasticity and recovery, and this information can be used to characterize complex tissue mechanics[234–237]. Such platforms could also be used to recreate the various external stresses present during 3D tissue morphogenesis, the process by

which tissues, organs, and whole organisms are shaped[95,117,234,238]. Given several recent studies demonstrating the clear importance of shape-driven mechanical forces on tissue development in tissues as diverse as the pancreas[151], placenta[239], lung[240,241], kidney[242], mammary gland[155,157], heart[92,93], embryonic germ layers[150,234], and neural tissues[152,153,163,243,244], we believe that the ability to apply 3D deformations to tissues on demand could serve as both a fundamental discovery tool to understand the immediate impact of forces on biological function, as well as an applied strategy to produce shaped tissues of interest.

4.5 Conclusions

We have developed a novel platform utilizing the smart hydrogel PNIPAM to compressively mold microscale tissues such as spheroids and organoids in a standard cell culture incubator. The geometry of the replica-molded microcavities can be designed in a variety of simple or complex shapes, and can be used to apply selected compressive profiles to tissues in culture. The CHyM platform makes it possible to start with uncontrolled and randomly shaped spheroids and organoids, thus enabling integration with existing spheroid/organoid generation methods, and via compressive molding to produce tissues with morphologies as desired. This technology could be applied to shape building blocks for bioassembly to create larger and more complex tissue constructs containing multiple tissue types, combining advantages of organoid cultures and bioprinting. This would yield more realistic and functional synthetic organs, and could also facilitate developmental studies in systems with various interacting components.

4.6 Acknowledgements

We thank Professor Timothy E Kennedy and Melissa Pestemalciyan for generous assistance with antibodies and staining; Meghna Mathur for support with iPSC culture; María Lacalle-Aurioles for use of her imaging chamber; Benjamin E Campbell for his spheroid devices; Christina-Marie Boghdady for use of her device molds; and the Neuro Microscopy Imaging Centre. This work was supported by funding received from the CQDM Quantum Leaps program and the Canada First Research Excellence Fund, awarded through the Healthy Brains, Healthy Lives initiative at McGill University to TMD and CM, the NSERC Discovery (RGPIN-2022-05165) to CM. We gratefully acknowledge personnel support from Healthy Brains, Healthy Lives program, and the NSERC

Postgraduate Scholarship-Doctoral to CCC and SM, and the Canada Research Chairs in Advanced Cellular Microenvironments to CM.

4.7 Conflicts of interest

There are no conflicts of interest to declare.

Chapter 5

Although in Chapter 4 I found that global geometry did not affect brain organoid development at the level we investigated, geometry has been shown to impact cellular processes such as branching and invasion in other systems. As the brain develops *in vivo*, neurons migrate and send projections from one region to another to form neural circuits, which may bear relevance to branching and invasion. Therefore, I chose to continue exploring the biophysical cue of geometry but at a finer scale than in Chapter 4 to explore how it may impact other aspects of neural tissue growth and neuronal behaviour. To do this, I developed another platform for molding organoids via confinement as they grow; this is a more passive method than in Chapter 4, and specifically shapes the organoid periphery. I produced several different geometries, but a wide range are possible. To enable study of neuronal migration and projection, this platform is able to support simultaneous culture and shaping of two different types of organoids, precisely positioning them in relation to each other to observe how they interact, once they are allowed to do so. We use this platform to investigate the impact of peripheral geometry on cocultures of midbrain and cerebral organoids, and observe that cell migration out of cerebral organoids is affected. Our system also enables the growth of axonal projections out of midbrain organoids, providing a platform for easy observation and measurement of these processes, which showed that they exhibit directed growth towards nearby organoids. After continued culture, midbrain and cerebral organoids expand to make contact and fuse, forming assembloids. These results demonstrate that geometrical shaping can influence certain organoid cell behaviours, and, comparing to Chapter 4, the scale of manipulation of this biophysical cue is important.

Taken together, this platform could be used to study how organoids representative of two distinct regions in the brain interact during development and help us further our understanding of the steps and process. Current methods to achieve this create “assembloids” by placing separate organoids side by side so they can fuse together. This extension of organoid technology expands their potential as a modeling system, and our platform offers the advantages of precise positioning, geometric shaping, and easy observation that could facilitate valuable insights into neural circuit formation. In addition, with certain organoid protocols, this platform

could be used to generate assembloids in a much more facile manner than current methods, expanding the tools available to maximize organoid value.

5 Microfabricated dynamic brain organoid cocultures to assess the effects of surface geometry on assembloid formation

Camille Cassel de Camps[1], Sabra Rostami[2], Vanessa Xu[2], Chen Li[2], Paula Lépine[3], Thomas M. Durcan[3], Christopher Moraes[1,2,4,5*]

1. Department of Biomedical Engineering, McGill University, Montréal, H3A 2B4 QC Canada
2. Department of Chemical Engineering, McGill University, Montréal, H3A 0C5 QC Canada
3. Early Drug Discovery Unit (EDDU), Montreal Neurological Institute and Hospital, McGill University, 3801 University Street, Montréal, H3A 2B4 QC Canada
4. Rosalind and Morris Goodman Cancer Institute, McGill University, Montréal, H3A 1A3 QC Canada
5. Division of Experimental Medicine, McGill University, Montréal, H4A 3J1, QC Canada

* Corresponding author: chris.moraes@mcgill.ca

5.1 Abstract

Organoids have emerged as valuable tools for the study of organ development and disease. Assembloids, an extension of organoid cultures, are formed by assembling multiple organoid types together, such as different brain region-specific organoids, to create more complex models. Work in other systems inspired us to develop devices to enable the co-culture of distinct brain organoid types that allowed manipulation of geometry at the organoid surfaces, with timing of their interaction controlled by removal of the barrier between the two organoid types. We designed poly(dimethylsiloxane) (PDMS) devices with separate channels and media reservoirs, and optimized a dual-sided molding method for their fabrication. Cultures of single cells and pre-formed brain organoids were successfully established in the devices, demonstrating their suitability for both culture types. With cocultures of midbrain and cerebral organoids, we were able to form assembloids and easily observe their interactions during the process. We observed and measured axonal projection from midbrain organoids and cell migration out of cerebral organoids as the two types of organoids were allowed to interact. Many axonal projections were directed towards nearby organoids, suggesting directed axonal growth. We investigated the impact of geometry on cell migration by varying the shape of the separating wall between the organoids, molding the cerebral organoids into points or flat peripheries, finding that cells migrated slightly farther from a flat periphery than from the flat midpoint of a triangle edge. This

platform provides a tool to easily observe cellular interactions between organoids in a controlled manner, with the ability to manipulate organoid surface geometry, and could be used to explore neuronal migration and axon target-seeking between brain regions or with other organs.

5.2 Introduction

Organoids have gained popularity as experimental models for developmental and disease studies. Grown from stem cells, these 3D tissue engineered cultures can differentiate towards diverse lineages that capture the complexity of *in vivo* tissues[11,16,24–26,28,30,31,63]. Multiple organoid types can also be assembled to interact, fuse and mature[62,64], and these 'assembloids' can model realistic development and function of multi-component organs and organ systems, with far greater fidelity and relevance than single-type organoids[62,64–66]. In the developing brain for example, complex circuits are established by neuronal projection and migration to create both local and long-distance connections[62,245–247]. Region-specific organoids can hence be assembled to create *in vitro* models of the circuits that run throughout the brain. For example, functional synaptic connections can form between cortical and striatal organoids, specific neurons can migrate from ventral to dorsal forebrain organoids[21,22], and muscle contraction can be stimulated by brain organoid activity[20]. Assembloids can hence be powerful in vitro models for a wide variety of neurodevelopmental disease processes[21,22].

Tissue geometry is now well-established to influence fundamental cellular processes, such as proliferation, differentiation, branching, and invasion[151,155–157,239,248–250]. Driven by endogenous cellular stresses that spontaneously arise in three-dimensional tissues[156,157,229], these cellular phenotypes drive feedback loops that govern tissue organization, specification and maturation[155,248,251]. While previous studies have demonstrated that geometric confinement and associated mechanical stresses drive organization of developing neural structures[152,153], whether these geometric features play a role in neural organoid development and assembloid formation remains an open question. Such experiments would require the technical capacity to simultaneously impose a specific geometry on independently-cultured organoids, and control their relative positions before allowing them to interact. Moreover, such experiments would require long-term culture in biologically permissive and optically addressable formats. Given the

intrinsic challenges associated with precisely manipulating soft living matter, technical innovations are required to better understand assembloid formation.

Recent developments in organoid culture models suggest a path to achieve these goals. Park et al. recently developed a microfabricated culture approach in which oxygen-permeable silicone inserts are used to restrict the size and shape of organoids as they grow into a hydrogel matrix. This approach was successfully used to allow stem cell proliferation and maturation, while controlling the global geometry of mature intestinal organoids, such that diffusive transport of oxygen, nutrients, and waste was sufficient to prevent the formation of a necrotic core that commonly arises in large, dense tissues[214]. Inspired by this approach, here we develop a strategy to separately culture distinct brain organoid types in adjacent compartments, while shaping the surface geometry of the tissues. After establishing mature organoids, an insert separating the organoid compartments can be manually removed and replaced with a thin layer of extracellular matrix, allowing the precisely-positioned organoids to begin forming an assembloid (**Fig. 5.1**). To prove this concept, here we use various channel geometries to shape cerebral and midbrain organoids. We demonstrate simultaneous axonal projections emanating from the midbrain organoids, and surface geometry-specific cell migration from cerebral organoids. We hence propose that this technical innovation allows systematic investigation of the role of interacting surface geometries in assembloid formation.

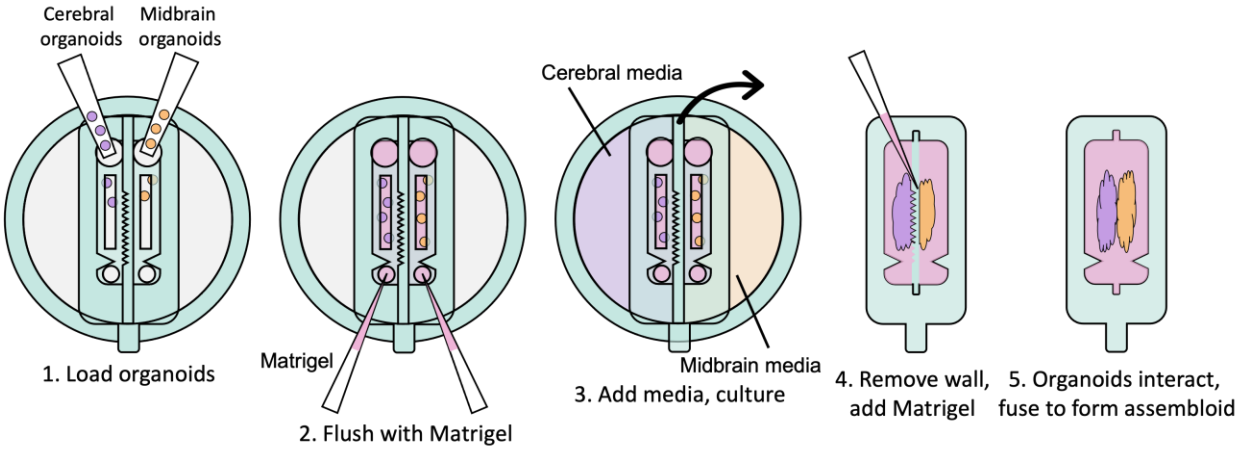

Figure 5.1. Schematic of device for coculture and assembloid formation. Two different types of organoids are loaded into separate channels and fed by separate media reservoirs. The geometry of the wall separating the channels shapes the organoids as they grow. When mature, the separating wall can be physically removed, allowing the organoids to interact and eventually fuse, while observing their interactions throughout culture.

5.3 Methods

Unless otherwise stated, all cell culture materials and supplies were purchased from Fisher Scientific (Ottawa, ON), and chemicals were from Sigma-Aldrich (Oakville, ON). The use of induced pluripotent stem cells (iPSCs) in this research was approved by the McGill University Health Centre Research Ethics Board (DURCAN_IPSC/2019-5374).

5.3.1 Device fabrication process

Molds were designed in Fusion 360 (AutoDesk), and printed on a ProFluidics 285D 3D resin printer using Master Mold Resin (CADworks3D) with a layer thickness of 50 µm. After washing with isopropanol, mold pieces were cured in a 36W ultraviolet (UV) chamber overnight. Molds were designed for assembly into chambers with patterned features on both the base and lid (**Fig. 5.2A**). Polydimethylsiloxane (PDMS) prepolymer and curing agent were mixed at a ratio of 10:1 (w/w), poured into the chamber, and degassed under vacuum. The molded lid was then lowered slowly from one side to avoid trapping air bubbles in the chamber. The lid was then pressed down to displace excess PDMS. Tongue-and-groove convex/concave features in the chamber base and lid contained the PDMS prepolymer after chamber assembly. PDMS was cured overnight in an oven at 40°C to minimize shrinkage[252], and demolded using 70% ethanol to help release the devices from the 3D printed resin.

5.3.2 Device preparation for organoid culture

Base devices were coated with dopamine to improve adhesion to Matrigel[253]. Briefly, dopamine hydrochloride was dissolved in 10mM Tris buffer (pH 8.5; 2 mg/mL), pipetted into the devices, and incubated overnight at room temperature. After treatment, devices were rinsed in reverse osmosis water, and dried with a stream of dry compressed air. To facilitate release from the devices and reduce adhesion to tissue cultures, the removable inserts were passivated with Pluronic® F-68 (5% in water, overnight at room temperature)[254,255]. Treated devices were rinsed in water, and dried with compressed air. All components were sterilized for 20 minutes in a 36W UV chamber before assembly. Devices were assembled on a coverslip, which formed the bottom of the media reservoirs and allowed the device to be easily manipulated as a unit. For

experiments without a removable insert, glass coverslips were used as the base surface, after functionalization with dopamine. Assembled devices were sterilized by UV for 45 minutes.

5.3.3 Cell and organoid culture

T47D human breast cancer cells (ATCC HTB-133) were cultured in Dulbecco's Modified Eagle Medium with 10% fetal bovine serum and 1% antibiotic–antimycotic (complete DMEM). Media was changed every 3-4 days, and cells were passaged using 0.25% trypsin–EDTA at 80% confluence. The iPSC lines TD22 (male) and AIW002-02 (male) were maintained on Matrigel-coated plates in mTeSR (StemCell Technologies) with media changed daily, and passaged with Gentle Cell Dissociation Reagent (StemCell Technologies) at 70% confluence. Both human control lines were obtained from The Neuro's C-BIG repository and had undergone multistep quality control[224]. All cultures were maintained at 37 °C with 5% CO2.

Midbrain organoids[19] and cerebral organoids[3] were generated using published protocols, with previously described modifications[256]. Briefly, iPSCs at 70% confluency were detached with Accutase (Gibco), resuspended in the appropriate media, seeded at 10 000 cells/well in 96-well round-bottom ultralow attachment plates (Corning Costar), and centrifuged for 10 minutes at 1200 rpm to aggregate the cells. Organoids were seeded so that they would be ready for Matrigel embedding on the same day (Day 7 for midbrain, and Day 12 for cerebral).

Media was changed every other day according to published protocols[3,19]. For cerebral organoids: hES media (low bFGF, with ROCK inhibitor) was used on Day 0 (consisting of 400 mL DMEM-F12 + Glutamax, 100 mL Knockout Serum Replacement, 15 mL hESC-quality FBS (Gibco), 5 mL MEM- non-essential amino acids, 3.5 µL 2-mercaptoethanol, bFGF at 4 ng/mL final concentration, and ROCK inhibitor at 50 µM final concentration); hES media (low bFGF, no ROCK inhibitor) on Day 2; hES media (no bFGF, no ROCK inhibitor) on Day 4; neural induction media on Day 7 and 9 (consisting of DMEM-F12 + Glutamax, 1% N2 supplement, 1% MEM-non-essential amino acids (MEM-NEAA), and heparin at 1 µg/mL final concentration); cerebral organoid differentiation media without vitamin A on Day 12 and 14 (consisting of 125 mL DMEM-F12 + Glutamax, 125 mL Neurobasal, 1.25 mL N2 supplement, 62.5 µL insulin, 1.25 mL MEM-NEAA, 2.5 mL penicillin-streptomycin, 1.75 µL of 1/10 2-mercaptoethanol dilution in neurobasal, and 2.5

mL B27 supplement without vitamin A); cerebral organoid differentiation media with vitamin A on Day 16 onwards (made using B27 supplement with vitamin A).

For midbrain organoids: neuronal induction media was used on Day 0 (consisting of 25 mL DMEM-F12 + Glutamax + 1% antibiotic-antimycotic, 25 mL neurobasal, 500 µL N2 supplement, 1 mL B27 without vitamin A, 500 mL MEM-NEAA, 1.75 µL of 1/10 2-mercaptoethanol dilution in neurobasal, heparin at 1 µg/mL final concentration, SB431542 at 10 µM final concentration, noggin at 200 ng/mL final concentration, CHIR99021 at 0.8 µM final concentration, and ROCK inhibitor at 10 µM final concentration); neuronal induction media without ROCK inhibitor was used on Day 2; midbrain patterning media was used on Day 4 (consisting of neuronal induction media without ROCK inhibitor with the addition of Sonic Hedgehog (SHH) at 100 ng/mL final concentration, and Fibroblast Growth Factor 8 (FGF8) at 100 ng/mL final concentration); tissue induction media was used on Day 7 (consisting of 50 mL neurobasal, 500 µL N2 supplement, 1 mL B27 without vitamin A, 500 mL MEM-NEAA, 1.75 µL of 1/10 2-mercaptoethanol dilution in neurobasal, 12.5 µL insulin, laminin at 200 ng/mL final concentration, SHH at 100 ng/mL final concentration, FGF8 at 100 ng/mL final concentration, and 50 µL penicillin-streptomycin); final differentiation media was used on Day 8 onwards (consisting of 50 mL neurobasal, 500 µL N2 supplement, 1 mL B27 without vitamin A, 500 mL MEM-NEAA, 1.75 µL of 1/10 2-mercaptoethanol dilution in neurobasal, BDNF at 10 ng/mL final concentration, GDNF at 10 ng/mL final concentration, ascorbic acid at 100 µM final concentration, db-cAMP at 125 µM final concentration, and 50 µL penicillin-streptomycin).

5.3.4 Live tissue analyses

Device cultures were imaged using an EVOS™ transmitted light microscope (XL Core) or an EVOS M700 Imaging System. Live/dead staining for viability was performed with calcein AM and ethidium homodimer-1 (Life Technologies) diluted in media at 4 µM each for 30 minutes at 37 °C. Staining with CellTracker™ Green was performed at 20 µM diluted in media overnight at 37 °C.

5.3.5 Device loading

Cell cultures were either loaded as single cells or as pre-formed organoids into the devices. Single cell cultures were obtained by trypsinization (T-47D) or detachment (iPSCs, using Accutase as

previously described[256]) and resuspended in Matrigel (Corning 356230) at concentrations of 8 × 10^6 cells/mL for T-47D, or 1×10^6, 3×10^6, or 1×10^7 cells/mL for iPSCs. All pipetting steps were performed with chilled pipette tips to prevent premature polymerization of the Matrigel. To load the organoids into the devices, they were pipetted directly into the loading ports in media with cut P200 pipette tips. Once in the chamber, they were too big to pass through the channel restriction. Media was aspirated, leaving the organoids in the device, and replaced with Matrigel. All devices were incubated for 20 minutes at 37 °C to polymerize the Matrigel. The appropriate media was added after polymerization, and replaced every 2 days[19].

5.3.6 Insert removal

Once the organoids had grown and adopted the shapes defined by the compartment dimensions, the inserts separating the compartments were removed. One pair of tweezers was used to hold the base device down, while another was used to slowly pull the insert away. Media was gently aspirated from between the organoids, and replaced with Matrigel to fill in the space. Devices were left at room temperature for 5 minutes to allow the newly added liquid Matrigel to seep into the existing Matrigel, and then incubated for 20 minutes at 37 °C. Final differentiation medium from the midbrain protocol[19], with the addition of insulin at a concentration of 0.25 µL/mL, was added to the well for this stage of combined culture. This media formulation was selected based on consultation and comparison of existing organoid and assembloid protocols and the function of each component[3,22,257], and would need to be adjusted if other types of organoids were grown in the coculture device.

5.3.7 Tissue staining

Live CellTracker™ Green or Red were loaded into cells at 20 µM in media overnight at 37 °C. Live/dead viability assays were performed with calcein AM and ethidium homodimer-1 (Life Technologies), diluted in media to 4 µM each and incubated with devices for 30 minutes at 37 °C.

For immunostaining, Matrigel was first dissolved using Cell Recovery Solution (Corning; at 4 °C for 20 minutes, twice). Devices were washed twice with phosphate buffered saline (PBS), fixed in 4% paraformaldehyde for 1 hour at room temperature, and washed three times for 15 minutes each with PBS before storage at 4 °C until staining. Whole mount staining was performed on organoids directly in the devices, using standard protocols[256]. Antibodies and

stains were used as follows: anti-tyrosine hydroxylase (TH) at 1:200 (rabbit polyclonal, Pel Freez P40101-150), anti-β-tubulin III (Tuj1) at 1:300 (chicken polyclonal, Millipore Sigma AB9354), anti-tau-1 clone PC1C6 at 1:200 (mouse monoclonal, Millipore Sigma MAB3420), anti-glial fibrillary acidic protein (GFAP) at 1:250 (rabbit polyclonal, Millipore Sigma AB5804), anti-microtubule-associated protein 2 (MAP2) at 1:400 (chicken polyclonal, EnCor Biotechnology CPCA-MAP2), goat anti-chicken IgY H&L (DyLight® 488) at 1:500 (Abcam ab96947), donkey anti-rabbit IgG H&L (DyLight® 488) at 1:500 (Abcam ab96891), donkey anti-mouse IgG H&L (DyLight® 594) at 1:500 (Abcam ab96877), donkey anti-Rabbit IgG (H+L) Alexa Fluor™ 594 at 1:500 (Invitrogen A-21207), and Hoescht 33342 at 1:5000 (Invitrogen H3570).

5.3.8 Microscopy and image analysis

Devices were imaged using an EVOS™ transmitted light microscope (XL Core) or an EVOS M700 fluorescent imaging System. Images were processed and analyzed in Fiji (NIH)[225]. Pairwise stitching was performed using the Stitching plugin[226] when needed. Axonal projections were measured from the organoid surface to projection tip to obtain their length and angle. Cell migration distances were measured from the organoid surface to the edge of the migrating cell front, 2-3 days after removal of the separating wall.

5.3.9 Statistical analysis

Analyses were performed in R statistical software[187]. The measurements of axonal projection lengths towards nearby organoids were normalized by lengths not directed towards a nearby organoid within samples, and then a two-sample t-test was used to compare between axons directed towards midbrain versus cerebral organoids. The measurements of axonal projection angle for each organoid were used to calculate kurtosis, after centring distributions around the angle defined as towards the nearby organoid; one-sample t-tests were used to compare against random chance (i.e., uniform distribution, kurtosis of 1.8), and a two-sample t-test was used to compare between groups. One-way ANOVA was performed with Tukey post hoc comparisons for measurements of cell migration distance. All analyses for significance were carried out with $\alpha = 0.05$.

5.4 Results

5.4.1 Device design for separated adjacent co-cultures

Double-sided 3D-printed molding chambers (**Fig. 5.2A**) were essential for the successful operation of these devices, as complex 3D geometries and multiple overhanging and double-sided layer features were required, which could only be achieved by designing interlocking surfaces for double-sided PDMS molding. The PDMS devices themselves were designed to facilitate pipetting of Matrigel and cell/organoid solutions into the channels via inlet ports, while leaving the tops of the channels open for nutrient exchange. This was achieved using an overhanging phase guide that allows surface tension to hold injected liquid (prepolymerized Matrigel) in a confined space, while leaving a slit in the top of the channels open for media exchange (slit was 600 μm across). We adapted this design to create two adjacent channels, each fed by an integrated and independent media reservoir to support growth of organoids with separate media requirements (Fig. 5.2B; shown with red and blue liquids to represent different media formulations).

We first verified that our devices were operational, suitable for cell culture, and that the media reservoirs were functionally isolated from each other by loading an available cell line (T47D breast cancer cells, used as a model cell line for preliminary experiments). We verified that the devices successfully separated cell compartments by dying the T47D breast cancer cells with either CellTracker Red or Green, and loading them in Matrigel into adjacent channels (each 1 mm wide, separated by ~500 μm; Fig. 5.2C). Devices were cultured for three days, and no colour exchange was observed between compartments. Next, we sought to validate media reservoir function. T47D cells were suspended in Matrigel and loaded into channels. One reservoir was filled with regular media, and the other was filled with media containing CellTracker Green. Over several days in culture, only the cells in the channel fed by that reservoir were dyed green, demonstrating functional separation of the reservoirs produced by this fabrication technique (Fig. 5.2D).

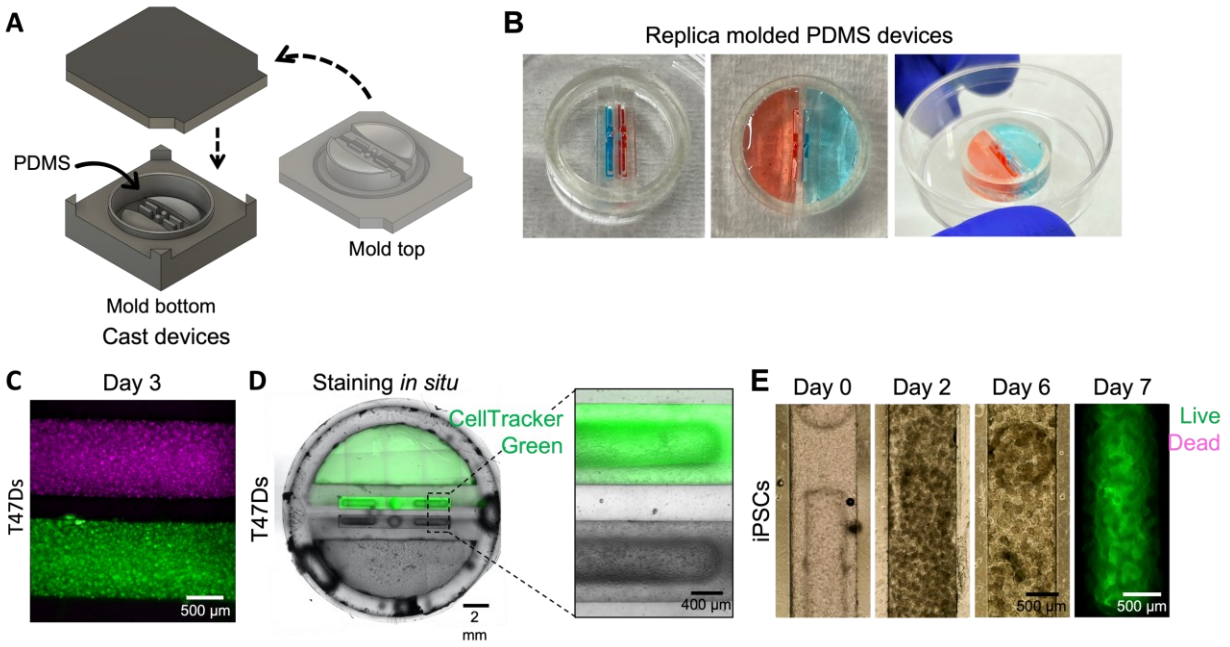

Figure 5.2. Functional, separate channels and reservoirs. A Base and insert parts of displacement mold for casting devices for single cell culture. **B** Replica molded PDMS devices, shown with channels filled with dye, left, and reservoirs filled, middle and right. **C** T47D cells were stained with CellTracker Red or Green, and then loaded into channels with Matrigel. After 3 days of culture, cells remain separated in their respective channels. **D** T47D cells were loaded with Matrigel into both channels of a device, with cells in one channel dyed once inside the channel by adding CellTracker Green to that media reservoir. **E** iPSCs were loaded into channels with Matrigel, and cultured with midbrain organoid media. Live/dead staining shows high viability after 7 days in culture.

5.4.2 Devices support iPSC culture

Once device design was validated, we next sought to verify that the devices could support iPSC culture, which is typically much more stringent, and would be required to grow developing organoids within the compartments. iPSCs were suspended in Matrigel at several different densities, loaded into the device channels as described, and cultured with midbrain organoid media[19]. Initially loaded at 10 million cells/mL, the density of cells in the channels increased over days in culture, and multiple cells aggregated together to form numerous small clusters within the channels (Fig. 5.2E). At 1 and 3 million cells/mL, cells also aggregated to form extremely small clusters that grew over time (data not shown). We also confirmed that iPSCs were viable for at least one week in culture (Fig. 5.2E) before proceeding with organoid culture experiments.

5.4.3 Removable inserts for dynamic organoid culture

Devices for dynamic organoid co-culture were fabricated as two separate pieces, the lower of which acts as a base to hold the organoids, while the upper piece includes the separating wall and media reservoirs. The separating wall can be designed with a variety of geometries to shape the growing organoids. The organoid loading ports were designed to be sufficiently large to load pre-formed organoids, as required in standard brain organoid culture protocols (**Fig. 5.3A-C**), while a small outlet port was designed to allow Matrigel loading, while keeping the organoids in the channels. We then confirmed that midbrain organoids remained viable for at least one week in culture after loading (Fig. 5.3D).

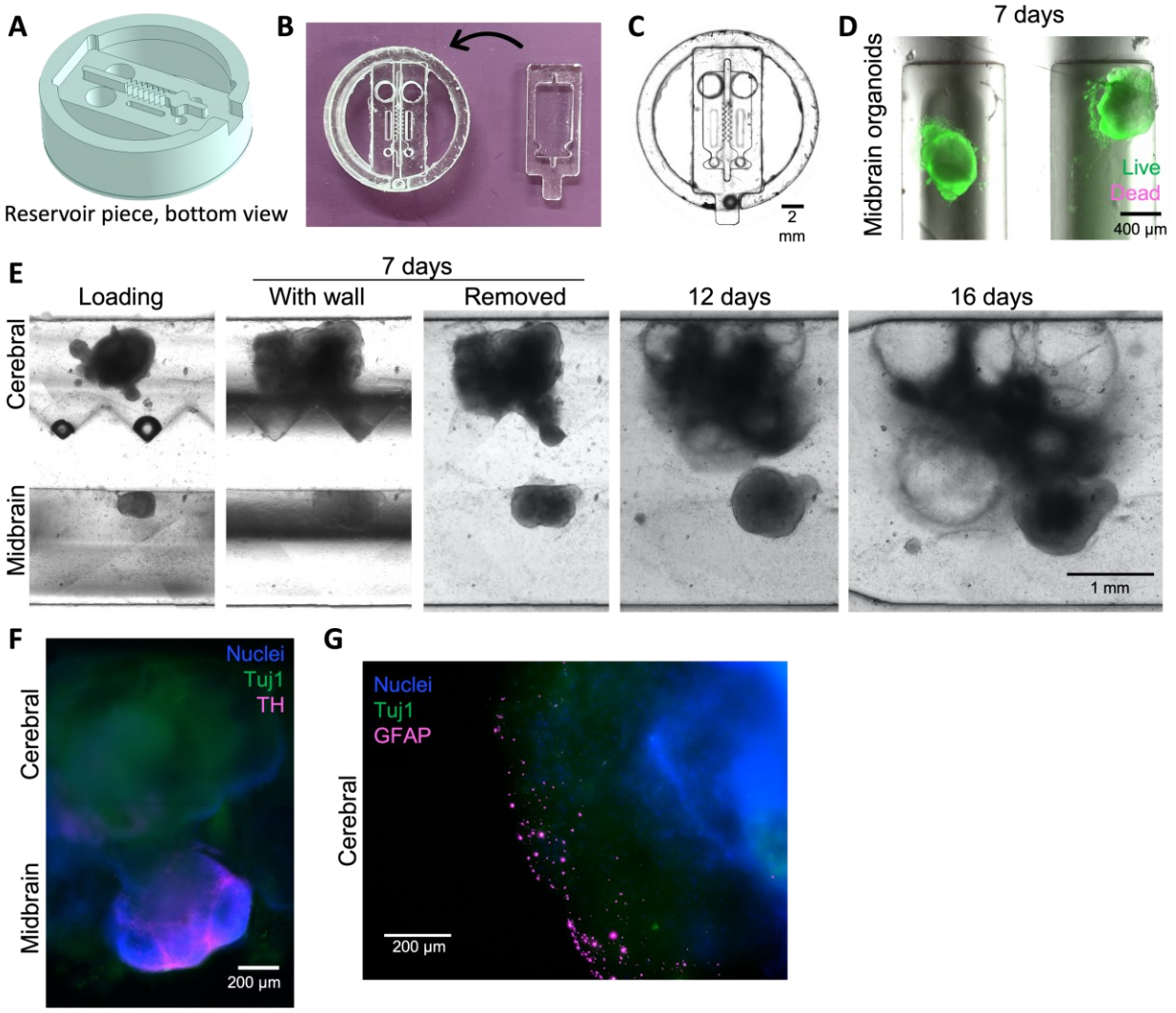

Figure 5.3. Assembloid formation in two-piece devices for dynamic culture of organoids. A 3D schematic of removable insert mold; shown here with a triangular wall geometry. **B** Replica

molded two-piece PDMS devices, with base mold and insert pieces shown. **C** Assembled two-piece device, imaged from below. **D** Midbrain organoids were loaded into channels with Matrigel, and maintained viability for 7 days in culture. **E** Cerebral and midbrain organoids were loaded into channels with Matrigel and cultured for 7 days before removing the separating wall. Organoids then grew and fused together to form an assembloid. **F** Cerebral organoids uniquely express of neural marker β-tubulin III (Tuj1), while midbrain organoids uniquely express of dopaminergic neuron marker tyrosine hydroxylase (TH). **G** Astrocytes identified with glial fibrillary acidic protein (GFAP) are observed on the edges of cerebral organoids only.

5.4.4 Devices support assembloid formation

As a first proof-of-concept, midbrain and cerebral organoids were loaded in Matrigel in adjacent channels to form assembloids with two distinct tissues representative of distinct brain regions. After 5-28 days, when the organoids had grown to fill the channels, the inserts were removed from the bases, leaving the organoids and surrounding Matrigel separated by the width of the separating wall (600 μm, but could be varied by mold design). This gap was back-filled with Matrigel, and the assembloids were then monitored during growth. We first confirmed that using this system, the organoids expanded into the inter-organoidal space and fused together (Fig. 5.3E). Staining for Tuj1 confirmed both organoids in the assembloid were composed of neural tissue, and staining for tyrosine hydroxylase (TH) confirmed the presence of dopaminergic neurons in the midbrain organoids only (Fig. 5.3F), as expected for this type of organoid[19]. Staining for glial fibrillary acidic protein (GFAP) also demonstrated development of astrocytes in cerebral organoids (Fig. 5.3G). These results confirm (1) appropriate and expected differentiation of these neural organoids within our devices, including differentiation towards the non-neuronal lineages expected in brain organoids[25]; (2) that our separated device supports distinct differentiation patterns in adjacent compartments; and (3) that assembloids can form after removal of the separating wall.

5.4.5 Axonal projections arise from midbrain organoids during assembloid formation

The device architecture enables us to reliably examine a reproducible interface between organoids during assembloid formation. We noted long and thin cellular processes arising from midbrain organoids, that began to appear after ~7-9 days of co-culture in our devices (~15-16 days after organoid seeding; **Fig. 5.4A**). We confirmed that these were axonal projections by

immunostaining for tau-1 which localizes to axons only[258,259], as well as for TH, which can also be found in axons[260] (Fig. 5.4B).

Based on mechanisms of axon guidance[245–247], it is reasonable to suppose that factors secreted during co-culture may direct axonal outgrowth. Given the reproducible positioning possible in these devices, we asked whether quantitative analysis would allow us to better understand the factors that might affect axon targeting behaviours. Axonal projections grew from all sides of the midbrain organoid (Fig. 5.4C), but we also measured the angle of all projections from the organoid of origin, and found that the majority of axons were directed towards a nearby organoid. By comparing the frequency distributions of axons (Fig. 5.4D) projecting towards either cerebral or adjacent midbrain organoids against random chance, we found that axonal projections from midbrain organoids were only significantly biased towards other midbrain organoids (n = 50-159 axons from 3-4 organoids; * $p < 0.05$ by one-sample t-test towards another midbrain organoid), while projections towards cerebral organoids only approached significance ($p < 0.1$). In contrast, axon lengths were not significantly different whether they were directed towards either midbrain or cerebral organoids (Fig. 5.4E). This quantitative analysis would therefore suggest that when allowed to form in co-culture, the distribution of directed axon targeting may be biased towards self-similar regions of the brain.

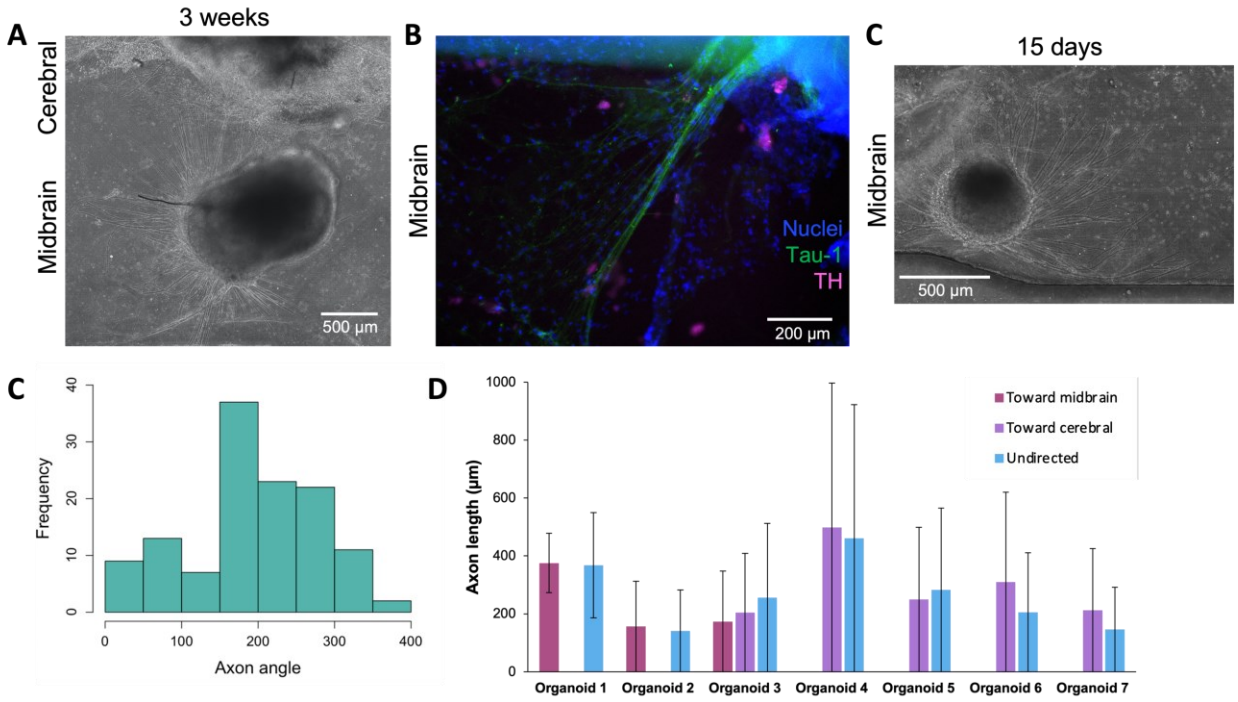

Figure 5.4. Axonal projection from midbrain organoids. A Axonal projections extending from midbrain organoid, and **B** staining positive for axonal marker tau-1. **C** Axonal projections arise from all sides of the midbrain organoid. **D** Representative frequency distribution of angles of axonal projections from a midbrain organoid, showing majority of axons angled towards nearby cerebral organoid (distribution is centred around angle towards nearby cerebral organoid, 180°). **E** No significant differences in axon lengths directed towards a cerebral or another midbrain organoid were observed (data presented as mean ± standard deviation; n = 3-57 axons from 7 organoids; $p > 0.1$ by two-sample t-test).

5.4.6 Organoid surface geometry influences cell migration

We also observed invasive migration of cells from the cerebral organoids into the intra-organoidal space, and given the known impact of tissue geometry on cellular invasion and migration[155–157], we asked whether organoid surface geometry might influence this invasive behaviour during assembloid formation. We therefore tested flat versus triangular geometric shapes of the separating wall (**Fig. 5.5A**), and the organoids grew to fill the shapes provided (Fig. 5.5B, C). Once the organoids had reached this stage, the separating inserts were removed. Interestingly, cells migrated out from the cerebral organoids into the Matrigel towards the midbrain organoids regardless of organoid peripheral geometry (Fig. 5.5C), and immunostaining indicated that some of these migrating cells were astrocytes, positive for GFAP (Fig. 5.5D).

However, migration distance was significantly different based on the global originating tissue shape (Fig. 5.5E, F). Cells migrating from a flat organoid periphery travelled significantly farther than cells migrating from the flat midpoint of a triangle edge. Given that flat surfaces are predicted to have lower mechanical tension than surfaces of high curvature, it seems likely that differential mechanical priming arising from shape could lead to different migration distances.

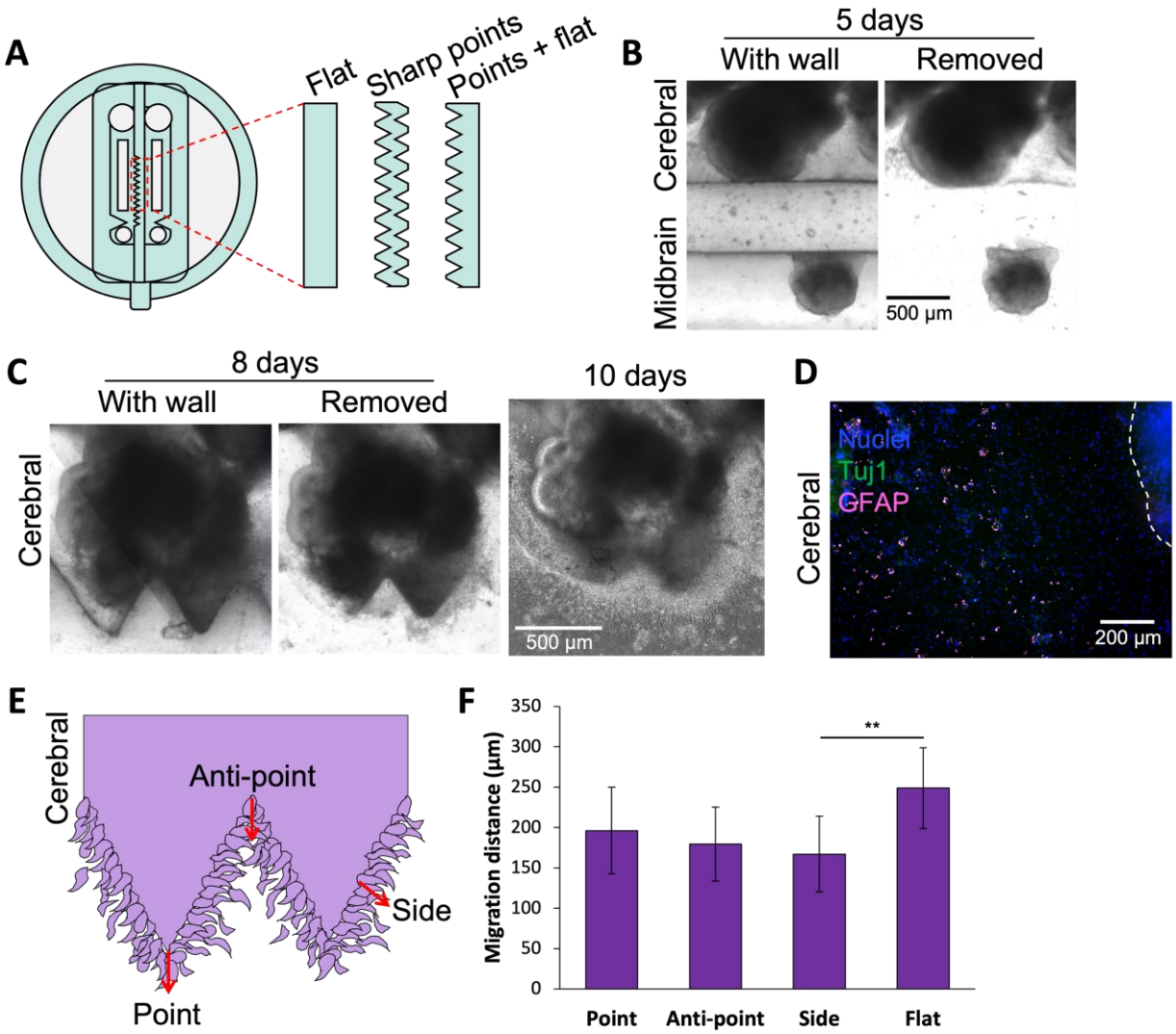

Figure 5.5. Geometrical shaping of organoids and cell migration. A Schematic showing channel-separating walls with different geometries. **B** Cerebral and midbrain organoids with flat peripheries, shaped by flat separating wall. **C** Cerebral organoid shaped into triangles by separating wall with points, and maintaining shape after wall removal. Cells migrate out of organoid at periphery, regardless of geometry. **D** Stained cerebral organoid shows expression of astrocyte marker glial fibrillary acidic protein (GFAP), with astrocytes having migrated out of organoid. The dashed line indicates edge of cerebral organoid. **E** Schematic showing locations of

measurements of cell migration front from cerebral organoid. **F** Measurements of migration distance of cells leaving cerebral organoids from locations with different geometries 2-3 days after wall removal (side refers to location at midpoint of triangle edge) (data presented as mean ± standard deviation; n = 5-8 locations; **p < 0.01 by one-way ANOVA with Tukey post hoc comparisons).

5.5 Discussion

In this work, we build on recent advances by Park et al. in culturing shaped organoids[214], and develop a platform and methodology to individually culture multiple organoids of distinct types and control their global shapes, before allowing them to interact and form an assembloid on demand. The use of microfluidic culture technologies to achieve this allows robust, reliable, and repeatable creation of assembloid formation conditions, as the distance between shaped organoids can be precisely defined, and the process of assembly can be closely observed *in situ*, within the device itself. Constructing devices capable of supporting long-term growth of organoids into predefined shapes, while affording the ability to (1) allow simultaneous but separate culture protocols for each of the organoid types, (2) support distinct surface modification strategies to enhance or prevent adhesion, and (3) to gently remove a separating barrier on demand required complex device geometries. To meet these fabrication demands, we developed a 3D printer-supported double-sided molding technique, which we successfully demonstrated to create barriers as thin as ~200µm. This fabrication method has the advantage of being extremely rapid and versatile, allowing design-to-device turnaround times of less than 8 hours, while creating novel structures that would be extremely difficult to produce using conventional single-side replica molding approaches.

As a first application, we investigated assembloid formation processes between midbrain and cerebral organoids, and observed axonal projections from the midbrain organoids, and invasion of individual cells from the cerebral organoids. Together, these processes should capture key features of the assembloid formation process as two organoids merge with each other, which would be quite challenging to observe and quantitatively evaluate when simply placing optically-dense organoids against each other. Using the capacity for microfluidics to position and support these interactions, we were able to demonstrate that that axonal projections from the midbrain organoids display differential targeted outgrowth. Since dopaminergic neurons project to a

variety of brain regions *in vivo*[261], these findings may ultimately be relevant in understanding how and why neural connections form differently in different regions of the brain. We were also able to observe that cell invasion from the cerebral organoids was affected by global surface geometries. Unexpectedly, cells leaving flat organoids displayed higher invasive potential than cells leaving the flat regions of triangular shapes. This was unexpected because higher endogenous stress levels at tissue stress points such as triangular apexes have previously been thought of as 'launching sites' for invasive cells in cancer models[155–157], but the opposite was observed in our neural cultures. Taken together, these results suggest that the process of assembloid formation can be dissected using microfluidic systems, and that this general approach might be leveraged to improve our understanding of the development of neural circuitry, in healthy and diseased states, both within the brain and targeting of other organs such as muscle or gut. More generally, our observations that assembloid-formation behaviours can be directed through physical cues in the local microenvironment suggests that such approaches may ultimately be useful in establishing predictive control over complex assembloid formation processes.

Several limitations should be considered in the utility of these devices. First, although the experiments here were designed primarily to prove the concept of these devices using brain organoid components, applying this strategy to other organoids may present unexpected complications. For example, the device architecture was sufficient to support the metabolic needs for brain organoid maturation, but other more energy-intensive processes may require alternative designs or other strategies to enhance metabolic transport and availability. Second, the capacity to observe assembloid-associated processes between organoids is enhanced through our microfluidic system, but is ultimately limited by difficulties in imaging through optically-dense organoids. Strategies such as brain organoid tissue clearing for end-point analysis[59] and genetically-encoded live stains to monitor processes in real time may be useful here, but cannot be used in parallel to allow for live, high-resolution imaging of such structures. Alternative imaging modalities such as MicroCT or ultrasound imaging may also have significant value in addressing this specific issue. Finally, the true capacity for assembloid formation to accurately capture *in vivo* processes and final structures remains unclear. While we hope that the

devices presented here will provide important tools in answering such questions, much remains to be done in establishing the fundamental utility of assembloids as *in vitro* models of development and disease.

5.6 Acknowledgements

We thank Ayesha Basu for her assistance with analysis of axon length. This work was supported by funding received from the CQDM Quantum Leaps program and the Canada First Research Excellence Fund, awarded through the Healthy Brains, Healthy Lives initiative at McGill University to TMD and CM, the Chamandy foundation and the Alain and Sandra Bouchard foundation for support to TMD, and the NSERC Discovery (RGPIN-2022-05165) to CM. We gratefully acknowledge personnel support from the NSERC Postgraduate Scholarship-Doctoral to CCC, and the Canada Research Chairs in Advanced Cellular Microenvironments to CM.

5.7 Conflicts of interest

There are no conflicts of interest to declare.

Chapter 6

6 Final remarks

6.1 Comprehensive discussion

The original motivation of this work was to explore the impact of biophysical cues on brain organoid growth and development. However, at the time, tools to conduct such studies on certain biophysical factors were limited, so this work also aimed to develop the necessary platforms. In Chapter 2, I presented an overview of brain organoids as a model system, highlighting their remarkable potential for modeling human brain development and disease[2,3,40–46,5,10–15,28]. I reviewed a variety of mechanical and biophysical factors that play important roles in development and morphogenesis *in vivo*[81,86–89,92], and have also been shown to affect cellular differentiation and function in cell and tissue experiments *in vitro*[102,110–114,128,150]. Despite increasing recognition of the significance of these factors, how these different biophysical cues affect neural tissue and brain organoids was not well studied. Recognizing this gap in the field, I: 1) examined the impact of matrix stiffness on brain organoids, and developed platforms to 2) mold pre-formed brain organoids into fused rings, altering their geometry, and 3) explore how peripheral geometry affects cell migration and axonal projection between brain organoids. This body of work aims to broaden knowledge of the influence of biophysical cues, which may ultimately improve brain organoids as experimental models by informing approaches to leverage these cues.

First, focusing on the mechanical properties of the microenvironment, in Chapter 3, I tailored the stiffness of the encapsulating hydrogel matrix by combining alginate with Matrigel. I found that brain organoids grown in stiffer hydrogels were smaller and exhibited differences in gross morphology and internal architecture. Namely, the characteristic developmental structures known as neural rosettes were affected, with reduced size and numbers. These findings underscore the influence of mechanics on the self-organizing capacity of brain organoids, which is one of their defining features, thus emphasizing the importance of considering the mechanical aspect of the microenvironment to facilitate self-organizing processes. In addition, mature

neuronal area was increased, suggesting that stiffness also affected processes of differentiation and maturation.

Similar observations have been reported in studies of intestinal organoids, where the mechanical properties of the matrix, such as stiffness and degradability, influenced the organoids' ability to grow and develop[110,111,113,114]. Stiff matrices impeded formation of intestinal organoids, and this correlated with differential mechanotransduction signaling through yes-associated protein 1 (YAP) compared to organoids grown in soft matrices; the authors suggest that confinement by the stiff hydrogel led to growth-induced compression, thereby feeding into YAP signaling and causing the observed interference with organoid self-organization and morphogenesis[111].

My data also aligns with work done on neuroepithelial cysts, 3D single lumen models of the early central nervous system grown from mouse stem cells. The authors found hydrogels of intermediate stiffness promoted neural differentiation and enhanced patterning, as did matrices that were non-degradable[115]. Their intermediate stiffness matches with the stiffest hydrogel we used for brain organoids, supporting our observed effects on differentiation. Our work builds on this study by using more complex brain organoid models, grown with human cells, and analyzed after much longer periods of culture. They also showed that actomyosin activity mediates cytoskeletal rearrangements through Rho signaling pathways to form the polarized cyst structure[115]. This study as well as others[152,262] support the idea that this is likely how neural rosettes are formed in brain organoids, too, so if actomyosin activity was interfered with by our stiffest condition, that may be a mechanism that explains our findings.

The effects I observed on brain organoid size, rosettes, and maturation may be produced via mechanotransduction pathways such as those observed in intestinal organoids. This may occur through integrin-mediated signaling, where increased or decreased clustering is involved in cell responses to ECM mechanical properties by relaying that information to the nucleus[89]. Integrin clustering was found to govern stem cell differentiation in response to stiffness and degradability of the surrounding matrix; although downstream signalling pathways in 3D are not well-known[89], integrins may be involved in the mechanism responsible for the differences I observed in brain organoids grown in the stiffer hydrogel. Another mediator of

mechanotransduction that may work in combination with integrins, mechanosensitive ion channels have been found to be important for cells to sense mechanical confinement and respond by regulating cell volume[89]. Cell volume expansion is limited in non-degradable or elastic hydrogels, such as the alginate component I used, and can trigger downstream signalling affecting differentiation and proliferation[89]. As the organoids grew within the alginate-containing hydrogel, they would have experienced mechanical confinement, which could have led to the observed effects via mechanosensitive ion channels. Although this global compression does not necessarily replicate what occurs in the developing brain *in vivo*, there are local stiffness changes as well as compressive forces from neighbouring tissues that are important in directing shape changes[96,97,121,123–125].

Future work could look to explore these mechanotransduction mechanisms to elucidate the pathways involved in the results we observed in brain organoids, and understand why neural rosettes were fewer and smaller in stiffer hydrogels. The modulus of early embryonic neural tissue, the neural plate, increases as development progresses[122,139,263], so it may be possible that the stiffer matrix somehow signaled a more advanced time point to the organoid cells, simultaneously enhancing neuronal maturation and reducing rosette formation. It would be interesting to investigate how hydrogel stiffness affects actomyosin contractility in these 3D structures, especially as actin and myosin contribute to determining the modulus of the neural plate itself[122,139,263]. Expanding on our work, how the degradability of the matrix influences brain organoids and rosettes could be explored, and how that interacts with stiffness, as work in intestinal organoids has demonstrated interaction[111]. This may help understand how neural rosette formation is triggered, and if mechanical cues contribute to the establishment of apicobasal polarity in this case. Another polarity axis relevant here is planar cell polarity (PCP); the PCP pathway is known to be important for neurulation, and mechanical strain was found to be critical in forming the global axis of planar polarity in developing skin ectoderm[140], so mechanical cues may likewise feed into this pathway in the context of neural tissues. If rosette formation is similar to cavitation in secondary neurulation, the process that forms the posterior region of the neural tube in humans[141,230], this may help us understand the mechanisms involved, and how they can go awry, leading to neural tube defects[133]. Regarding overall organoid size, we

did not observe differences in proliferation or cell death that explained why organoids grown in stiffer hydrogels were smaller. However, maybe early differences in these phenomena, prior to the time point we analyzed, are the underlying reason; future work could look to verify this, and explore how stiffness may trigger pathways that cause these differences.

In Chapters 4 and 5, I focus on the more macroscale biophysical cue of geometry. Specifically, in Chapter 4, I develop a platform to mold cultured tissues into geometries as desired using the thermoresponsive hydrogel NIPAM. I was able to mold pre-formed brain organoids, changing their shape, and forming them into rings such they formed bridges with themselves, fusing into one cohesive unit of tissue. I found that ring formation did not affect differentiation profiles, at least according to the metrics we examined. This implies that this platform could be used as a molding tool on pre-formed organoids, without interfering with their development. This is a novel application of NIPAM, capitalizing on its thermoresponsive properties in a way that has not been done before, and a novel application of hydrogel actuators to apply 3D forces to 3D tissues in culture, providing a new tool to the field.

This is particularly of interest in the context of morphogenesis. Morphogenesis necessarily involves mechanical forces acting in 3D, and there is a significant body of work demonstrating their importance in development[92,94,116–120]. However, tools to apply such forces *in vitro*, in a tissue culture setting, are lacking[264]. In an embryo, there are intrinsic forces that contribute to morphogenesis, i.e. forces generated by the tissue that is undergoing a shape change, and extrinsic forces, i.e. forces that are not generated by the shape-changing tissue itself[118–120]. These forces are generated by neighboring cells or emerge within the overall tissue, and include differential growth in the plane or in different layers of the tissue, and tensile or compressive forces exerted by adjacent tissues[118,119]. The latter, external compressive forces, are especially relevant to the system we developed, as our devices could be used to apply, mimic, and model such forces.

One example from the embryo is neural tube folding and closure, where a flat sheet of cells bends, folds, and fuses to form a tube that becomes the brain and spinal cord[121,141]; multiple studies suggests that forces exerted by the neighbouring tissue (nonneural ectoderm), i.e. extrinsic forces, are involved[123–125], and therefore applying external forces could act to mimic

these driving forces *in vitro*. One study used a minimal approach, with no external force application, to model the process of neural tube folding and closure in tissue culture by geometrically patterning stem cells in such a way that fostered self-organization into embryonic neural and nonneural regions, which underwent shape changes to produce a neural tube-like structure[163]. Based on the evidence demonstrating the importance of external forces in this process *in vivo*, integrating such forces through our platform could potentially improve this or similar models, and allow further understanding of their contribution. Although this thesis focuses on neural tissues, multiple organs in the body begin as tubes, such as the lungs, gut, and heart[92,118,230]. Our demonstration of ring formation thus bears relevance to these tissues as well, and our devices could lend themselves to a potential strategy for modeling tubular tissues *in vitro*.

In addition, work in the cancer field has demonstrated that mechanical cues such as forces contribute to malignant transformation and tumour aggression[98,232,234]. Specifically relevant, compressive stresses have been found to produce numerous effects in tumours, that lead to tumour progression and increased cancer cell migration[234]. Our platform could be used to apply tailored forces to engineered tumour tissues or biopsies, and explore how this may affect cell invasiveness, expression of certain markers, epithelial-to-mesenchymal transition, or even drug responsiveness over time. This could ultimately contribute to understanding of how the biophysical cue of force plays a role in metastasis and influences disease prognosis.

We initially develop and use this platform as a system to mold tissues, as a contribution to bioassembly and biofabrication approaches. Additionally, this platform achieves application of mechanical forces in 3D on cultured tissues, creating new opportunities. This new tool could enable investigation of dynamic changes in tissue culture, as a potential strategy for modeling forces in morphogenetic processes and tumour progression. The platform allows observation of tissue response to user-defined forces, and could facilitate exploration of the contributions of these mechanical forces in morphogenesis to further our understanding of this complex and difficult-to-study process.

Although I found in Chapter 4 that geometry did not impact the outcomes we assessed, work in other systems such as mammary epithelium and cancer has shown that multiple cell

behaviours, including branching, proliferation, or invasion[155–157], can be influenced by geometry. Work in 2D neural cultures has also shown effects of geometry in certain contexts, such as improving organization and reproducibility of developing neural structures by microscale geometric confinement[152,153]. Therefore, we decided to further explore the biophysical cue of geometry at a finer scale than our work in Chapter 4, both in terms of the geometry itself and the outcomes examined.

In Chapter 5, I develop a platform to coculture two different types of brain organoids that shapes their geometry as they grow, to investigate how that geometry affects cell behaviour at the periphery. I found that peripheral geometry impacted cell migration from cerebral organoids, and observed growth of axonal projections from midbrain organoids, which exhibited target-seeking behaviour. I also demonstrated the utility of this platform for functionally separate cultures, and subsequent formation of assembloids. These findings highlight the influence of geometry on brain organoid cell behaviours at this scale.

Although these results agree in general principle with work showing that geometry affects cell motility behaviours, the details appear to be different. Studies in breast cancer found that geometry could either enhance or suppress tumour cell proliferation and invasion; sites of increased stress within the tissue appeared to trigger invasion[156]. Likewise, in normal mammary epithelium, geometry controlled the position of branches, with points of higher stress triggering branching[155,157]. However, in our work with brain organoids, we saw increased migration from regions with flat geometries, not from sites with pointed geometries; point geometries would theoretically be the sites of higher stress[155–157], which seems to suggest the opposite trend. Of course, our work was conducted with an entirely different organ system, and cell migration in neural tissue is likely a fundamentally different process than branching and invasion in mammary epithelium, which might explain the differences.

In addition, we observed several instances where brain organoids appeared to have assumed the imposed pointed shape, but once they were released from that geometric confinement, they immediately relaxed to a rounded shape. This aligns with previous work showing that internal stresses generated in spheroids by cells at the periphery create a tensional 'skin', which may act to maintain a rounded shape[229], potentially causing the organoids to 'spring

back' once their environment allowed. We can suppose that our pointed peripheral geometries may somehow encourage or enhance the development of that tensional stress, or at least maintain it, which thereby resulted in slowing migration compared to flat geometries that might have produced lower stress profiles at the periphery, allowing cells to more easily exit the tissue. Future work could explore this possibility.

These observations also relate to work in Chapter 4. With our compressive hydrogel devices, we successfully molded spheroids and brain organoids into imposed shapes. Our devices in Chapter 5 relied on a more passive approach, where organoids were molded by growing into defined geometries. Although this was successful in most cases, the examples we observed where pointed organoid peripheries sprang back to assume round peripheries upon release of confinement suggests that more active geometric molding like that in Chapter 4 may produce more consistent shaping. In addition, these observations of the influence on cell migration also indicate that processes such as this could have been affected by the geometrical shaping we conducted in Chapter 4. Future work could look farther in depth to examine the periphery of the brain organoids in our compressive hydrogel shaping devices, especially as they grew near each other approaching ring formation.

The coculture platform allowed us to easily observe axonal projections growing from midbrain organoids, which we have not seen before. This kind of long-term observation, allowing continued surveillance and measurement throughout culture, is not possible with standard brain organoid or assembloid protocols. Future work could capitalize on this, using it as a platform to explore axon target seeking and cell migration between organoids of specific brain regions. As in previous work with assembloids[21,22], this could model the formation of neural circuits as happens *in vivo* during fetal brain development, allowing examination of the process, steps, and cell types and signaling involved. This could contribute to our understanding of neural circuit development, and allow for experimental manipulations, such as to study disease states and test responses to drugs or toxin exposure. While we initially set out to explore the effect of geometry of the organoid periphery, we incidentally observed that axonal projections appeared to direct themselves away from nearby barriers, before making contact. This suggests that the geometry of such barriers might be interesting to investigate in future work, to explore how axons could

be directed by this biophysical cue to take predefined paths, including in the absence, or presence, of chemical signalling molecules.

This platform provides a new tool to the growing field of assembloid work, and, if following organoid protocols that begin with single cell suspensions in a hydrogel matrix, our devices could offer an easy method to generate assembloids with specific positions and geometries, in addition to the observation advantages already discussed. This system could be employed for tissues of different types, not limited to brain organoids, for example to study innervation of muscle or gut. To facilitate culture of such distinct tissues, next steps could look to design a modified version of the device, with an additional piece that could be placed onto the culture after removal of the separation barrier, containing separate media reservoirs but still allowing interaction between tissue types.

This thesis explored the impact of several biophysical factors on brain organoids in various contexts. Insights from this work contribute to knowledge of how the biophysical cues of matrix stiffness, and overall and peripheral geometry can shape brain organoid growth and development at micro- and macroscales. Ultimately, strategies incorporating biophysical cues could lead to improved and more realistic models of human brain developmental processes, facilitating exploration of healthy and diseased states. Additionally, these strategies are not limited to the brain, and could be extended to study and model many other organs and multi-organ systems.

6.2 Summary & conclusions

In this thesis, I have explored how different biophysical cues affect brain organoid growth and development at different scales. I examine the impact of matrix stiffness on brain organoid gross morphology, microarchitecture, and cellular differentiation using alginate combined with Matrigel in Chapter 3. I then focus on geometry in Chapters 4 and 5. I develop a platform to mold pre-formed organoids into user-defined geometries with thermoresponsive PNIPAM compressive hydrogel devices, and investigate the impact on brain organoid development in Chapter 4. I engineer a system to passively shape brain organoid peripheries, and observe the influence of peripheral geometry on cell migration as two different types of organoid are allowed to interact in Chapter 5.

Together, these works contribute knowledge about the influence of biophysical cues on brain organoid development, and suggest their importance in certain contexts, as well as supply new tools to conduct further such studies. The finding that material properties influence brain organoid self-organization could inform future work to understand and improve the process, potentially yielding better experimental models. The platform developed to mold tissues could be extended as a tool to further understanding of how forces contribute to morphogenetic events, and to integrate such forces into *in vitro* tissue development to produce more accurate models. The system engineered to shape peripheral geometries and observe cellular behaviours over long-term coculture could expand assembloid capabilities to study and model neural circuit formation, within the brain and with other organs.

Further work and development of these platforms could contribute to understanding the influence of biophysical cues in many processes of human brain development, and to producing improved experimental models for studies of development and disease. Although this thesis focuses on brain organoids, the tools developed here are broadly applicable to other tissue types, and create opportunities to study biophysical cues in novel ways. This could ultimately advance regenerative medicine efforts.

Chapter 7

7 Complete references

1. Heide, M., Huttner, W. B. & Mora-Bermúdez, F. Brain organoids as models to study human neocortex development and evolution. *Curr. Opin. Cell Biol.* **55**, 8–16 (2018).
2. Lancaster, M. A. *et al.* Cerebral organoids model human brain development and microcephaly. *Nature* **501**, 373–379 (2013).
3. Lancaster, M. A. & Knoblich, J. A. Generation of cerebral organoids from human pluripotent stem cells. *Nat. Protoc.* **9**, 2329–2340 (2014).
4. Jo, J. *et al.* Midbrain-like Organoids from Human Pluripotent Stem Cells Contain Functional Dopaminergic and Neuromelanin-Producing Neurons. *Cell Stem Cell* **19**, 248–257 (2016).
5. Qian, X. *et al.* Brain-Region-Specific Organoids Using Mini-bioreactors for Modeling ZIKV Exposure. *Cell* **165**, 1238–1254 (2016).
6. Paşca, S. P. The rise of three-dimensional human brain cultures. *Nature* **553**, 437–445 (2018).
7. Arlotta, P. & Paşca, S. P. Cell diversity in the human cerebral cortex: from the embryo to brain organoids. *Curr. Opin. Neurobiol.* **56**, 194–198 (2019).
8. Benito-Kwiecinski, S. & Lancaster, M. A. Brain Organoids: Human Neurodevelopment in a Dish. *Cold Spring Harb. Perspect. Biol.* **12**, a035709 (2020).
9. Quadrato, G., Brown, J. & Arlotta, P. The promises and challenges of human brain organoids as models of neuropsychiatric disease. *Nat. Med.* **22**, 1220–1228 (2016).
10. Velasco, S. *et al.* Individual brain organoids reproducibly form cell diversity of the human cerebral cortex. *Nature* **570**, 523–527 (2019).
11. Otani, T., Marchetto, M. C., Gage, F. H., Simons, B. D. & Livesey, F. J. 2D and 3D Stem Cell Models of Primate Cortical Development Identify Species-Specific Differences in Progenitor Behavior Contributing to Brain Size. *Cell Stem Cell* **18**, 467–480 (2016).
12. Quadrato, G. *et al.* Cell diversity and network dynamics in photosensitive human brain organoids. *Nature* **545**, 48–53 (2017).
13. Bershteyn, M. *et al.* Human iPSC-Derived Cerebral Organoids Model Cellular Features of Lissencephaly and Reveal Prolonged Mitosis of Outer Radial Glia. *Cell Stem Cell* **20**, 435-449.e4 (2017).
14. Rosebrock, D. *et al.* Enhanced cortical neural stem cell identity through short SMAD and WNT inhibition in human cerebral organoids facilitates emergence of outer radial glial cells. *Nat. Cell Biol.* **24**, 981–995 (2022).
15. Kadoshima, T. *et al.* Self-organization of axial polarity, inside-out layer pattern, and species-specific progenitor dynamics in human ES cell–derived neocortex. *Proc. Natl. Acad. Sci.* **110**, 20284– 20289 (2013).
16. Pasca, A. M. *et al.* Functional cortical neurons and astrocytes from human pluripotent stem cells in 3D culture. *Nat. Methods* **12**, 671–678 (2015).
17. Muguruma, K., Nishiyama, A., Kawakami, H., Hashimoto, K. & Sasai, Y. Self-organization of polarized cerebellar tissue in 3D culture of human pluripotent stem cells. *Cell Rep.* **10**, 537–550 (2015).

18. Clevers, H. Modeling Development and Disease with Organoids. *Cell* **165**, 1586–1597 (2016).
19. Mohamed, N.-V. *et al.* Generation of human midbrain organoids from induced pluripotent stem cells. *MNI Open Res.* **3**, 1 (2021).
20. Andersen, J. *et al.* Generation of Functional Human 3D Cortico-Motor Assembloids. *Cell* **183**, 1913-1929.e26 (2020).
21. Birey, F. *et al.* Assembly of functionally integrated human forebrain spheroids. *Nature* **545**, 54–59 (2017).
22. Miura, Y. *et al.* Generation of human striatal organoids and cortico-striatal assembloids from human pluripotent stem cells. *Nat. Biotechnol.* **38**, 1421–1430 (2020).
23. Oksdath, M. *et al.* Review: Synthetic scaffolds to control the biochemical, mechanical, and geometrical environment of stem cell-derived brain organoids. *APL Bioeng.* **2**, 041501 (2018).
24. Di Lullo, E. & Kriegstein, A. R. The use of brain organoids to investigate neural development and disease. *Nat. Rev. Neurosci.* **18**, 573–584 (2017).
25. Sloan, S. A. *et al.* Human Astrocyte Maturation Captured in 3D Cerebral Cortical Spheroids Derived from Pluripotent Stem Cells. *Neuron* **95**, 779-790.e6 (2017).
26. Qian, X., Nguyen, H. N., Jacob, F., Song, H. & Ming, G. Using brain organoids to understand Zika virus-induced microcephaly. *Development* **144**, 952–957 (2017).
27. Gordon, A. *et al.* Long-term maturation of human cortical organoids matches key early postnatal transitions. *Nat. Neurosci.* **24**, 331–342 (2021).
28. Velasco, S., Paulsen, B. & Arlotta, P. 3D Brain Organoids: Studying Brain Development and Disease Outside the Embryo. *Annu. Rev. Neurosci.* **43**, 375–389 (2020).
29. Camp, J. G. *et al.* Human cerebral organoids recapitulate gene expression programs of fetal neocortex development. *Proc. Natl. Acad. Sci. U. S. A.* **112**, 15672–15677 (2015).
30. Hofer, M. & Lutolf, M. P. Engineering organoids. *Nat. Rev. Mater. 2021 65* **6**, 402–420 (2021).
31. Rossi, G., Manfrin, A. & Lutolf, M. P. Progress and potential in organoid research. *Nature Reviews Genetics* **19**, 671–687 (2018).
32. Lancaster, M. A. & Knoblich, J. A. Organogenesis in a dish: Modeling development and disease using organoid technologies. *Science (80-.).* **345**, (2014).
33. Dekkers, J. F. *et al.* A functional CFTR assay using primary cystic fibrosis intestinal organoids. *Nat. Med. 2013 197* **19**, 939–945 (2013).
34. Xu, M. *et al.* Identification of small-molecule inhibitors of Zika virus infection and induced neural cell death via a drug repurposing screen. *Nat. Med.* **22**, 1101–1107 (2016).
35. Schwartz, M. P. *et al.* Human pluripotent stem cell-derived neural constructs for predicting neural toxicity. *Proc. Natl. Acad. Sci. U. S. A.* **112**, 12516–12521 (2015).
36. Kozlowski, M. T., Crook, C. J. & Ku, H. T. Towards organoid culture without Matrigel. *Commun. Biol. 2021 41* **4**, 1–15 (2021).
37. Mora-Bermúdez, F. *et al.* Differences and similarities between human and chimpanzee neural progenitors during cerebral cortex development. *Elife* **5**, (2016).
38. Lancaster, M. A. & Huch, M. Disease modelling in human organoids. *DMM Dis. Model. Mech.* **12**, dmm039347 (2019).
39. Muotri, A. R. Brain organoids and insights on human evolution [version 1; peer review: 4

approved]. *F1000Research* **8**, (2019).
40. Bubnys, A. & Tsai, L. H. Harnessing cerebral organoids for Alzheimer's disease research. *Current Opinion in Neurobiology* **72**, 120–130 (2022).
41. Choi, S. H. *et al.* A three-dimensional human neural cell culture model of Alzheimer's disease. *Nature* **515**, 274–278 (2014).
42. Mohamed, N. V. *et al.* Midbrain organoids with an SNCA gene triplication model key features of synucleinopathy. *Brain Commun.* **3**, (2021).
43. Kim, H. *et al.* Modeling G2019S-LRRK2 Sporadic Parkinson's Disease in 3D Midbrain Organoids. *Stem Cell Reports* **12**, 518–531 (2019).
44. Mariani, J. *et al.* FOXG1-Dependent Dysregulation of GABA/Glutamate Neuron Differentiation in Autism Spectrum Disorders. *Cell* **162**, 375–390 (2015).
45. Stachowiak, E. K. *et al.* Cerebral organoids reveal early cortical maldevelopment in schizophrenia—computational anatomy and genomics, role of FGFR1. *Transl. Psychiatry* **7**, 1–24 (2017).
46. Zhang, W. *et al.* Cerebral organoid and mouse models reveal a RAB39b-PI3K-mTOR pathway-dependent dysregulation of cortical development leading to macrocephaly/ autism phenotypes. *Genes Dev.* **34**, 580–597 (2020).
47. Krenn, V. *et al.* Organoid modeling of Zika and herpes simplex virus 1 infections reveals virus-specific responses leading to microcephaly. *Cell Stem Cell* **28**, 1362-1379.e7 (2021).
48. Park, S. E., Georgescu, A. & Huh, D. Organoids-on-a-chip. *Science (80-.).* **364**, 960–965 (2019).
49. Yoon, S. J. *et al.* Reliability of human cortical organoid generation. *Nat. Methods* **16**, 75–78 (2019).
50. Qian, X. *et al.* Sliced Human Cortical Organoids for Modeling Distinct Cortical Layer Formation. *Cell Stem Cell* **26**, 766-781.e9 (2020).
51. Pham, M. T. *et al.* Generation of human vascularized brain organoids. *Neuroreport* **29**, 588 (2018).
52. Sakaguchi, H. *et al.* Generation of functional hippocampal neurons from self-organizing human embryonic stem cell-derived dorsomedial telencephalic tissue. *Nat. Commun.* **6**, 1–11 (2015).
53. Watanabe, M. *et al.* Self-Organized Cerebral Organoids with Human-Specific Features Predict Effective Drugs to Combat Zika Virus Infection. *Cell Rep.* **21**, 517–532 (2017).
54. Qian, X., Song, H. & Ming, G. Brain organoids: advances, applications and challenges. *Development* **146**, (2019).
55. Raja, W. K. *et al.* Self-organizing 3D human neural tissue derived from induced pluripotent stem cells recapitulate Alzheimer's disease phenotypes. *PLoS One* **11**, e0161969 (2016).
56. Cederquist, G. Y. *et al.* Specification of positional identity in forebrain organoids. *Nat. Biotechnol. 2019 374* **37**, 436–444 (2019).
57. Sakaguchi, H. *et al.* Self-Organized Synchronous Calcium Transients in a Cultured Human Neural Network Derived from Cerebral Organoids. *Stem Cell Reports* **13**, 458–473 (2019).
58. Sabate-Soler, S. *et al.* Microglia integration into human midbrain organoids leads to increased neuronal maturation and functionality. *Glia* **70**, 1267–1288 (2022).
59. Mohamed, N. V. *et al.* Microfabricated disk technology: Rapid scale up in midbrain

organoid generation. *Methods* **203**, 465–477 (2022).
60. Chen, C., Rengarajan, V., Kjar, A. & Huang, Y. A matrigel-free method to generate matured human cerebral organoids using 3D-Printed microwell arrays. *Bioact. Mater.* **6**, 1130 (2021).
61. Zhu, Y., Zhang, X., Sun, L., Wang, Y. & Zhao, Y. Engineering Human Brain Assembloids by Microfluidics. *Adv. Mater.* 2210083 (2023). doi:10.1002/adma.202210083
62. Miura, Y. *et al.* Engineering brain assembloids to interrogate human neural circuits. *Nature Protocols* **17**, 15–35 (2022).
63. Marton, R. M. & Pașca, S. P. Organoid and Assembloid Technologies for Investigating Cellular Crosstalk in Human Brain Development and Disease. *Trends Cell Biol.* **30**, 133–143 (2020).
64. Vogt, N. Assembloids. *Nature Methods* **18**, 27 (2021).
65. Kim, E. *et al.* Creation of bladder assembloids mimicking tissue regeneration and cancer. *Nature* **588**, 664–669 (2020).
66. Rawlings, T. M. *et al.* Modelling the impact of decidual senescence on embryo implantation in human endometrial assembloids. *Elife* **10**, (2021).
67. Sun, X. Y. *et al.* Generation of Vascularized Brain Organoids to Study Neurovascular Interactions. *Elife* **11**, (2022).
68. Abud, E. M. *et al.* iPSC-Derived Human Microglia-like Cells to Study Neurological Diseases. *Neuron* **94**, 278-293.e9 (2017).
69. Xu, R. *et al.* Developing human pluripotent stem cell-based cerebral organoids with a controllable microglia ratio for modeling brain development and pathology. *Stem Cell Reports* **16**, 1923–1937 (2021).
70. Cakir, B. *et al.* Engineering of human brain organoids with a functional vascular-like system. *Nat. Methods 2019 1611* **16**, 1169–1175 (2019).
71. Ahn, Y. *et al.* Human blood vessel organoids penetrate human cerebral organoids and form a vessel-like system. *Cells* **10**, 2036 (2021).
72. Bergmann, S. *et al.* Blood–brain-barrier organoids for investigating the permeability of CNS therapeutics. *Nat. Protoc. 2018 1312* **13**, 2827–2843 (2018).
73. Simonneau, C. *et al.* Investigating receptor-mediated antibody transcytosis using blood–brain barrier organoid arrays. *Fluids Barriers CNS* **18**, 1–17 (2021).
74. Linkous, A. *et al.* Modeling Patient-Derived Glioblastoma with Cerebral Organoids. *Cell Rep.* **26**, 3203-3211.e5 (2019).
75. Appelt-Menzel, A. *et al.* Establishment of a Human Blood-Brain Barrier Co-culture Model Mimicking the Neurovascular Unit Using Induced Pluri- and Multipotent Stem Cells. *Stem Cell Reports* **8**, 894–906 (2017).
76. de Jongh, R., Spijkers, X. M., Pasteuning-Vuhman, S., Vulto, P. & Pasterkamp, R. J. Neuromuscular junction-on-a-chip: ALS disease modeling and read-out development in microfluidic devices. *J. Neurochem.* **157**, 393–412 (2021).
77. Takebe, T., Zhang, B. & Radisic, M. Synergistic Engineering: Organoids Meet Organs-on-a-Chip. *Cell Stem Cell* **21**, 297–300 (2017).
78. Jin, Y. *et al.* Vascularized Liver Organoids Generated Using Induced Hepatic Tissue and Dynamic Liver-Specific Microenvironment as a Drug Testing Platform. *Adv. Funct. Mater.* **28**, 1801954 (2018).

79. Skardal, A. *et al.* Multi-tissue interactions in an integrated three-tissue organ-on-a-chip platform. *Sci. Reports 2017 71* **7**, 1–16 (2017).
80. Kratochvil, M. J. *et al.* Engineered materials for organoid systems. *Nat. Rev. Mater.* **4**, 606–622 (2019).
81. Vining, K. H. & Mooney, D. J. Mechanical forces direct stem cell behaviour in development and regeneration. *Nat. Rev. Mol. Cell Biol.* **18**, 728–742 (2017).
82. Barnes, J. M., Przybyla, L. & Weaver, V. M. Tissue mechanics regulate brain development, homeostasis and disease. *J. Cell Sci.* **130**, 71–82 (2017).
83. Caiazzo, M. *et al.* Defined three-dimensional microenvironments boost induction of pluripotency. *Nat. Mater.* **15**, 344–352 (2016).
84. Ayad, N. M. E. E., Kaushik, S. & Weaver, V. M. Tissue mechanics, an important regulator of development and disease. *Philos. Trans. R. Soc. B Biol. Sci.* **374**, 20180215 (2019).
85. Watt, F. M. & Huck, W. T. S. Role of the extracellular matrix in regulating stem cell fate. *Nat. Rev. Mol. Cell Biol.* **14**, 467–473 (2013).
86. Anlaş, A. A. & Nelson, C. M. Tissue mechanics regulates form, function, and dysfunction. *Curr. Opin. Cell Biol.* **54**, 98–105 (2018).
87. Nowlan, N. C., Francis-West, P. & Nelson, C. Mechanics of development. *Philosophical Transactions of the Royal Society B: Biological Sciences* **373**, (2018).
88. Mammoto, T. & Ingber, D. E. Mechanical control of tissue and organ development. *Development* **137**, 1407–1420 (2010).
89. Saraswathibhatla, A., Indana, D. & Chaudhuri, O. Cell–extracellular matrix mechanotransduction in 3D. *Nature Reviews Molecular Cell Biology* 1–22 (2023). doi:10.1038/s41580-023-00583-1
90. Crest, J., Diz-Muñoz, A., Chen, D. Y., Fletcher, D. A. & Bilder, D. Organ sculpting by patterned extracellular matrix stiffness. *Elife* **6**, 1–16 (2017).
91. Etournay, R. *et al.* Interplay of cell dynamics and epithelial tension during morphogenesis of the Drosophila pupal wing. *Elife* **4**, e07090 (2015).
92. Taber, L. A. Morphomechanics: Transforming tubes into organs. *Curr. Opin. Genet. Dev.* **27**, 7–13 (2014).
93. Mandrycky, C. J. *et al.* Engineering Heart Morphogenesis. *Trends Biotechnol.* **38**, 835–845 (2020).
94. Mishra, N. & Heisenberg, C. P. Dissecting Organismal Morphogenesis by Bridging Genetics and Biophysics. *Annual Review of Genetics* **55**, 209–233 (2021).
95. Stooke-Vaughan, G. A. & Campàs, O. Physical control of tissue morphogenesis across scales. *Current Opinion in Genetics and Development* **51**, 111–119 (2018).
96. Galea, G. L. *et al.* Vangl2 disruption alters the biomechanics of late spinal neurulation leading to spina bifida in mouse embryos. *Dis. Model. Mech.* **11**, (2018).
97. Galea, G. L. *et al.* Biomechanical coupling facilitates spinal neural tube closure in mouse embryos. *Proc. Natl. Acad. Sci. U. S. A.* **114**, E5177–E5186 (2017).
98. Paszek, M. J. *et al.* Tensional homeostasis and the malignant phenotype. *Cancer Cell* **8**, 241–254 (2005).
99. Lee, J. Y. & Chaudhuri, O. Regulation of Breast Cancer Progression by Extracellular Matrix Mechanics: Insights from 3D Culture Models. *ACS Biomater. Sci. Eng.* **4**, 302–313 (2018).
100. Lee, J. Y. *et al.* YAP-independent mechanotransduction drives breast cancer progression.

Nat. Commun. 2019 101 **10**, 1–9 (2019).
101. Murphy, M. C., Huston, J. & Ehman, R. L. MR elastography of the brain and its application in neurological diseases. *Neuroimage* 1–8 (2017). doi:10.1016/j.neuroimage.2017.10.008
102. Engler, A. J., Sen, S., Sweeney, H. L. & Discher, D. E. Matrix Elasticity Directs Stem Cell Lineage Specification. *Cell* **126**, 677–689 (2006).
103. Georges, P. C., Miller, W. J., Meaney, D. F., Sawyer, E. S. & Janmey, P. A. Matrices with compliance comparable to that of brain tissue select neuronal over glial growth in mixed cortical cultures. *Biophys. J.* **90**, 3012–3018 (2006).
104. Flanagan, L. A., Ju, Y.-E., Marg, B., Osterfield, M. & Janmey, P. A. Neurite branching on deformable substrates. *Neuroreport* **13**, 2411 (2002).
105. Kim, H. N. & Choi, N. Consideration of the Mechanical Properties of Hydrogels for Brain Tissue Engineering and Brain-on-a-chip. *BioChip J.* **13**, 8–19 (2019).
106. Saha, K. *et al.* Substrate modulus directs neural stem cell behavior. *Biophys. J.* **95**, 4426–4438 (2008).
107. Tanaka, A., Fujii, Y., Kasai, N., Okajima, T. & Nakashima, H. Regulation of neuritogenesis in hippocampal neurons using stiffness of extracellular microenvironment. *PLoS One* **13**, e0191928 (2018).
108. Gunn, J. W., Turner, S. D. & Mann, B. K. Adhesive and mechanical properties of hydrogels influence neurite extension. *J. Biomed. Mater. Res.* **72A**, 91–97 (2005).
109. Madl, C. M. *et al.* Maintenance of neural progenitor cell stemness in 3D hydrogels requires matrix remodelling. *Nat. Mater.* **16**, 1233–1242 (2017).
110. DiMarco, R. L., Dewi, R. E., Bernal, G., Kuo, C. & Heilshorn, S. C. Protein-engineered scaffolds for in vitro 3D culture of primary adult intestinal organoids. *Biomater. Sci.* **3**, 1376–1385 (2015).
111. Gjorevski, N. *et al.* Designer matrices for intestinal stem cell and organoid culture. *Nature* **539**, 560–564 (2016).
112. Candiello, J. *et al.* 3D heterogeneous islet organoid generation from human embryonic stem cells using a novel engineered hydrogel platform. *Biomaterials* **177**, 27–39 (2018).
113. Cruz-Acuña, R. *et al.* Synthetic hydrogels for human intestinal organoid generation and colonic wound repair. *Nat. Cell Biol.* **19**, 1326–1335 (2017).
114. Capeling, M. M. *et al.* Nonadhesive Alginate Hydrogels Support Growth of Pluripotent Stem Cell-Derived Intestinal Organoids. *Stem Cell Reports* **12**, 381–394 (2019).
115. Ranga, A. *et al.* Neural tube morphogenesis in synthetic 3D microenvironments. *Proc. Natl. Acad. Sci.* **113**, E6831–E6839 (2016).
116. Keller, R., Davidson, L. A. & Shook, D. R. How we are shaped: The biomechanics of gastrulation. *Differentiation* **71**, 171–205 (2003).
117. Heisenberg, C.-P. & Bellaïche, Y. Forces in Tissue Morphogenesis and Patterning. *Cell* **153**, 948–962 (2013).
118. Tozluoğlu, M. & Mao, Y. On folding morphogenesis, a mechanical problem. *Philos. Trans. R. Soc. Lond. B. Biol. Sci.* **375**, 20190564 (2020).
119. Smith, J. L. & Schoenwolf, G. C. Neurulation: coming to closure. *Trends Neurosci.* **20**, 510–517 (1997).
120. Bolaños Quiñones, V. A., Zhu, H., Solovev, A. A., Mei, Y. & Gracias, D. H. Origami Biosystems: 3D Assembly Methods for Biomedical Applications. *Adv. Biosyst.* **2**, 1800230

(2018).
121. Gilbert, S. F. The central nervous system and the epidermis. in *Developmental Biology* (Sinauer Associates, 2000).
122. Vijayraghavan, D. S. & Davidson, L. A. Mechanics of neurulation: From classical to current perspectives on the physical mechanics that shape, fold, and form the neural tube. *Birth defects Res.* **109**, 153–168 (2017).
123. Alvarez, I. S. & Schoenwolf, G. C. Expansion of surface epithelium provides the major extrinsic force for bending of the neural plate. *J. Exp. Zool.* **261**, 340–348 (1992).
124. Jacobson, A. G. & Moury, J. D. Tissue boundaries and cell behavior during neurulation. *Developmental Biology* **171**, 98–110 (1995).
125. Moury, J. D. & Schoenwolf, G. C. Cooperative model of epithelial shaping and bending during avian neurulation: Autonomous movements of the neural plate, autonomous movements of the epidermis, and interactions in the neural plate/epidermis transition zone. *Dev. Dyn.* **204**, 323–337 (1995).
126. Copp, A. J. & Greene, N. D. E. Neural tube defects-disorders of neurulation and related embryonic processes. *Wiley Interdiscip. Rev. Dev. Biol.* **2**, 213–227 (2013).
127. Blencowe, H., Kancherla, V., Moorthie, S., Darlison, M. W. & Modell, B. Estimates of global and regional prevalence of neural tube defects for 2015: a systematic analysis. *Ann. N. Y. Acad. Sci.* **1414**, 31–46 (2018).
128. Kumar, A., Placone, J. K. & Engler, A. J. Understanding the extracellular forces that determine cell fate and maintenance. *Development* **144**, 4261–4270 (2017).
129. Song, G., Ju, Y., Soyama, H., Ohashi, T. & Sato, M. *Regulation of Cyclic Longitudinal Mechanical Stretch on Proliferation of Human Bone Marrow Mesenchymal Stem Cells*. *MCB* **4**, (2007).
130. Yoon, J. K. *et al.* Stretchable Piezoelectric Substrate Providing Pulsatile Mechanoelectric Cues for Cardiomyogenic Differentiation of Mesenchymal Stem Cells. *ACS Appl. Mater. Interfaces* **9**, 22101–22111 (2017).
131. Miyashita, S. *et al.* Mechanical forces induce odontoblastic differentiation of mesenchymal stem cells on three-dimensional biomimetic scaffolds. *J. Tissue Eng. Regen. Med.* **11**, 434–446 (2017).
132. Sivarapatna, A. *et al.* Arterial specification of endothelial cells derived from human induced pluripotent stem cells in a biomimetic flow bioreactor. *Biomaterials* **53**, 621–633 (2015).
133. Copp, A. J., Stanier, P. & Greene, N. D. E. Neural tube defects: Recent advances, unsolved questions, and controversies. *Lancet Neurol.* **12**, 799–810 (2013).
134. Tallinen, T., Chung, J. Y., Biggins, J. S. & Mahadevan, L. Gyrification from constrained cortical expansion. *Proc. Natl. Acad. Sci. U. S. A.* **111**, 12667–12672 (2014).
135. Fletcher, A. G., Osterfield, M., Baker, R. E. & Shvartsman, S. Y. Vertex models of epithelial morphogenesis. *Biophys. J.* **106**, 2291–2304 (2014).
136. Okuda, S., Inoue, Y. & Adachi, T. Three-dimensional vertex model for simulating multicellular morphogenesis. *Biophys. Physicobiology* **12**, 13 (2015).
137. Alt, S., Ganguly, P. & Salbreux, G. Vertex models: From cell mechanics to tissue morphogenesis. *Philosophical Transactions of the Royal Society B: Biological Sciences* **372**, 20150520 (2017).

138. Kiehart, D. P., Galbraith, C. G., Edwards, K. A., Rickoll, W. L. & Montague, R. A. Multiple forces contribute to cell sheet morphogenesis for dorsal closure in Drosophila. *J. Cell Biol.* **149**, 471–490 (2000).
139. Zhou, J., Kim, H. Y. & Davidson, L. A. Actomyosin stiffens the vertebrate embryo during crucial stages of elongation and neural tube closure. *Development* **136**, 677–688 (2009).
140. Chien, Y. H., Keller, R., Kintner, C. & Shook, D. R. Mechanical strain determines the axis of planar polarity in ciliated epithelia. *Curr. Biol.* **25**, 2774–2784 (2015).
141. Lowery, L. A. & Sive, H. Strategies of vertebrate neurulation and a re-evaluation of teleost neural tube formation. *Mech. Dev.* **121**, 1189–1197 (2004).
142. Homan, K. A. *et al.* Flow-enhanced vascularization and maturation of kidney organoids in vitro. *Nat. Methods 2019 163* **16**, 255–262 (2019).
143. Tao, T. *et al.* Engineering human islet organoids from iPSCs using an organ-on-chip platform. *Lab Chip* **19**, 948–958 (2019).
144. Workman, M. J. *et al.* Enhanced Utilization of Induced Pluripotent Stem Cell–Derived Human Intestinal Organoids Using Microengineered Chips. *CMGH* **5**, 669-677.e2 (2018).
145. Abdel Fattah, A. R. *et al.* Actuation enhances patterning in human neural tube organoids. *Nat. Commun.* **12**, 3192 (2021).
146. Mammoto, T., Mammoto, A. & Ingber, D. E. Mechanobiology and Developmental Control. *Annu. Rev. Cell Dev. Biol.* **29**, 27–61 (2013).
147. Schittny, J. C. Development of the lung. *Cell Tissue Res.* **367**, 427–444 (2017).
148. Metzger, R. J., Klein, O. D., Martin, G. R. & Krasnow, M. A. The branching programme of mouse lung development. *Nat. 2008 4537196* **453**, 745–750 (2008).
149. *Oxford Surveys in Evolutionary Biology*. *Oxford University Press* **8**, (Oxford University Press, 1992).
150. Warmflash, A., Sorre, B., Etoc, F., Siggia, E. D. & Brivanlou, A. H. A method to recapitulate early embryonic spatial patterning in human embryonic stem cells. *Nat. Methods* **11**, 847–854 (2014).
151. Tran, R., Moraes, C. & Hoesli, C. A. Controlled clustering enhances PDX1 and NKX6.1 expression in pancreatic endoderm cells derived from pluripotent stem cells. *Sci. Rep.* **10**, (2020).
152. Knight, G. T. *et al.* Engineering induction of singular neural rosette emergence within hPSC-derived tissues. *Elife* **7**, (2018).
153. Haremaki, T. *et al.* Self-organizing neuruloids model developmental aspects of Huntington's disease in the ectodermal compartment. *Nat. Biotechnol. 2019 3710* **37**, 1198–1208 (2019).
154. Lancaster, M. A. *et al.* Guided self-organization and cortical plate formation in human brain organoids. *Nat. Biotechnol.* **35**, 659–666 (2017).
155. Nelson, C. M., VanDuijn, M. M., Inman, J. L., Fletcher, D. A. & Bissell, M. J. Tissue Geometry Determines Sites of Mammary Branching Morphogenesis in Organotypic Cultures. *Science* **314**, 298 (2006).
156. Boghaert, E. *et al.* Host epithelial geometry regulates breast cancer cell invasiveness. *Proc. Natl. Acad. Sci. U. S. A.* **109**, 19632–19637 (2012).
157. Gjorevski, N. & Nelson, C. M. Endogenous patterns of mechanical stress are required for branching morphogenesis. *Integr. Biol.* **2**, 424–434 (2010).

158. Rodenhizer, D., Cojocari, D., Wouters, B. G. & McGuigan, A. P. Development of TRACER: Tissue roll for analysis of cellular environment and response. *Biofabrication* **8**, 45008 (2016).
159. Karzbrun, E., Kshirsagar, A., Cohen, S. R., Hanna, J. H. & Reiner, O. Human brain organoids on a chip reveal the physics of folding. *Nat. Phys.* **14**, 515–522 (2018).
160. He, Q. *et al.* Origami-based self-folding of co-cultured NIH/3T3 and HepG2 cells into 3D microstructures. *Sci. Reports 2018 81* **8**, 1–7 (2018).
161. Hughes, A. J. *et al.* Engineered Tissue Folding by Mechanical Compaction of the Mesenchyme. *Dev. Cell* **44**, 165-178.e6 (2018).
162. Kalashnikov, N. & Moraes, C. Morphodynamic Tissues via Integrated Programmable Shape Memory Actuators. *Adv. Funct. Mater.* **1903327**, 1–12 (2019).
163. Karzbrun, E. *et al.* Human neural tube morphogenesis in vitro by geometric constraints. *Nature* **599**, 268–272 (2021).
164. Sousa, A. M. M., Meyer, K. A., Santpere, G., Gulden, F. O. & Sestan, N. Evolution of the Human Nervous System Function, Structure, and Development. *Cell* **170**, 226–247 (2017).
165. Lui, J. H., Hansen, D. V. & Kriegstein, A. R. Development and evolution of the human neocortex. *Cell* **146**, 18–36 (2011).
166. Brown, J., Quadrato, G. & Arlotta, P. Studying the Brain in a Dish: 3D Cell Culture Models of Human Brain Development and Disease. in *Current Topics in Developmental Biology* **129**, 99–122 (Academic Press Inc., 2018).
167. Hughes, C. S., Postovit, L. M. & Lajoie, G. A. Matrigel: A complex protein mixture required for optimal growth of cell culture. *Proteomics* **10**, 1886–1890 (2010).
168. Yin, X. *et al.* Engineering Stem Cell Organoids. *Cell Stem Cell* **18**, 25–38 (2016).
169. Davidson, M. D., Burdick, J. A. & Wells, R. G. Engineered Biomaterial Platforms to Study Fibrosis. *Adv. Healthc. Mater.* **9**, 1901682 (2020).
170. Aisenbrey, E. A. & Murphy, W. L. Synthetic alternatives to Matrigel. *Nat. Rev. Mater.* **5**, 539–551 (2020).
171. Carrow, J. K., Kerativitayanan, P., Jaiswal, M. K., Lokhande, G. & Gaharwar, A. K. Polymers for bioprinting. in *Essentials of 3D Biofabrication and Translation* 229–248 (Elsevier Inc., 2015). doi:10.1016/B978-0-12-800972-7.00013-X
172. Chaudhuri, O. *et al.* Extracellular matrix stiffness and composition jointly regulate the induction of malignant phenotypes in mammary epithelium. *Nat. Mater.* **13**, 970–978 (2014).
173. Cavo, M. *et al.* A new cell-laden 3D Alginate-Matrigel hydrogel resembles human breast cancer cell malignant morphology, spread and invasion capability observed 'in vivo'. *Sci. Rep.* **8**, 1–12 (2018).
174. Tekin, H. *et al.* Effects of 3D culturing conditions on the transcriptomic profile of stem-cell-derived neurons. *Nat. Biomed. Eng.* **2**, 540–554 (2018).
175. Li, Y. *et al.* 3D printable Sodium alginate-Matrigel (SA-MA) hydrogel facilitated ectomesenchymal stem cells (EMSCs) neuron differentiation. *J. Biomater. Appl.* **35**, 709–719 (2021).
176. Wisdom, K. & Chaudhuri, O. Chapter 3: 3D Cell Culture in Interpenetrating Networks of Alginate and rBM Matrix. *Methods Mol. Biol.* **1612**, 29–37 (2017).
177. Branco da Cunha, C. *et al.* Influence of the stiffness of three-dimensional

alginate/collagen-I interpenetrating networks on fibroblast biology. *Biomaterials* **35**, 8927–8936 (2014).
178. Chaudhuri, O. Viscoelastic hydrogels for 3D cell culture. *Biomaterials Science* **5**, 1480–1490 (2017).
179. Rowley, J. A., Madlambayan, G. & Mooney, D. J. Alginate hydrogels as synthetic extracellular matrix materials. *Biomaterials* **20**, 45–53 (1999).
180. Ort, C., Chen, Y., Ghagre, A., Ehrlicher, A. & Moraes, C. Bioprintable, Stiffness-Tunable Collagen-Alginate Microgels for Increased Throughput 3D Cell Culture Studies. *ACS Biomater. Sci. Eng.* **7**, 2814–2822 (2021).
181. Trappmann, B. *et al.* Extracellular-matrix tethering regulates stem-cell fate. *Nat. Mater.* **11**, 642–649 (2012).
182. Rasband, W. S. ImageJ, U. S. National Institutes of Health. (2018). Available at: https://imagej.nih.gov/ij/.
183. Chen, C. X.-Q. *et al.* Standardized Quality Control Workflow to Evaluate the Reproducibility and Differentiation Potential of Human iPSCs into Neurons. *bioRxiv* 426620 (2021). doi:10.1101/2021.01.13.426620
184. Thomas, R. A. & Cai, E. OrgM: A Fiji macro for automated measurement of object area, diameter and roundness from bright field images. *Github* (2019). Available at: https://github.com/neuroeddu/OrgM%0A.
185. McQuin, C. *et al.* CellProfiler 3.0: Next-generation image processing for biology. *PLOS Biol.* **16**, e2005970 (2018).
186. Libby, A. R. G. *et al.* Axial elongation of caudalized human organoids mimics aspects of neural tube development. *Dev.* **148**, (2021).
187. R Core Team. R: A language and environment for statistical computing. (2017).
188. JASPTeam. JASP (Version 0.14.1) [Computer software]. (2020).
189. Matricardi, P., Di Meo, C., Coviello, T., Hennink, W. E. & Alhaique, F. Interpenetrating polymer networks polysaccharide hydrogels for drug delivery and tissue engineering. *Adv. Drug Deliv. Rev.* **65**, 1172–1187 (2013).
190. Doumèche, B., Picard, J. & Larreta-Garde, V. Enzyme-catalyzed phase transition of alginate gels and gelatin - Alginate interpenetrated networks. *Biomacromolecules* **8**, 3613–3618 (2007).
191. Matricardi, P., Pontoriero, M., Coviello, T., Casadei, M. A. & Alhaique, F. In situ cross-linkable novel alginate-dextran methacrylate IPN hydrogels for biomedical applications: Mechanical characterization and drug delivery properties. *Biomacromolecules* **9**, 2014–2020 (2008).
192. Pescosolido, L. *et al.* Injectable and in situ gelling hydrogels for modified protein release. *Eur. Biophys. J.* **39**, 903–909 (2010).
193. Hoffman, A. S. Hydrogels for biomedical applications. *Adv. Drug Deliv. Rev.* **54**, 3–12 (2002).
194. Akhmanova, M., Osidak, E., Domogatsky, S., Rodin, S. & Domogatskaya, A. Physical, Spatial, and Molecular Aspects of Extracellular Matrix of in Vivo Niches and Artificial Scaffolds Relevant to Stem Cells Research. *Stem Cells Int.* **2015**, 167025 (2015).
195. Moraes, C. *et al.* On being the right size: Scaling effects in designing a human-on-a-chip. *Integr. Biol. (United Kingdom)* **5**, 1149–1161 (2013).

196. Raeber, G. P., Lutolf, M. P. & Hubbell, J. A. Molecularly Engineered PEG Hydrogels: A Novel Model System for Proteolytically Mediated Cell Migration. *Biophys. J.* **89**, 1374 (2005).
197. Moraes, C., Simon, A. B., Putnam, A. J. & Takayama, S. Aqueous two-phase printing of cell-containing contractile collagen microgels. *Biomaterials* **34**, 9623–9631 (2013).
198. Soofi, S. S., Last, J. A., Liliensiek, S. J., Nealey, P. F. & Murphy, C. J. The elastic modulus of Matrigel™ as determined by atomic force microscopy. *J. Struct. Biol.* **167**, 216–219 (2009).
199. Nguyen, E. H. *et al.* Versatile synthetic alternatives to Matrigel for vascular toxicity screening and stem cell expansion. *Nat. Biomed. Eng.* **1**, 96 (2017).
200. Mok, S. *et al.* Mapping cellular-scale internal mechanics in 3D tissues with thermally responsive hydrogel probes. *Nat. Commun.* **11**, 1–11 (2020).
201. Reed, J., Walczak, W. J., Petzold, O. N. & Gimzewski, J. K. In Situ Mechanical Interferometry of Matrigel™ Films. *Langmuir* **25**, 36 (2009).
202. Jayawardena, I. *et al.* Evaluation of techniques used for visualisation of hydrogel morphology and determination of pore size distributions. *Mater. Adv.* **4**, 669–682 (2023).
203. Moroni, L. *et al.* Biofabrication: A Guide to Technology and Terminology. *Trends in Biotechnology* **36**, 384–402 (2018).
204. Ino, K. *et al.* Biofabrication Using Electrochemical Devices and Systems. *Adv. Biosyst.* **4**, 1900234 (2020).
205. Bajaj, P., Schweller, R. M., Khademhosseini, A., West, J. L. & Bashir, R. 3D Biofabrication Strategies for Tissue Engineering and Regenerative Medicine. *Annu. Rev. Biomed. Eng.* **16**, 247 (2014).
206. Castilho, M. *et al.* Multitechnology Biofabrication: A New Approach for the Manufacturing of Functional Tissue Structures? *Trends in Biotechnology* **38**, 1316–1328 (2020).
207. Bajaj, P., Tang, X., Saif, T. A. & Bashir, R. Stiffness of the substrate influences the phenotype of embryonic chicken cardiac myocytes. *J. Biomed. Mater. Res. - Part A* **95**, 1261–1269 (2010).
208. Brassard, J. A., Nikolaev, M., Hübscher, T., Hofer, M. & Lutolf, M. P. Recapitulating macro-scale tissue self-organization through organoid bioprinting. *Nat. Mater.* **20**, 22–29 (2021).
209. Skylar-Scott, M. A. *et al.* Biomanufacturing of organ-specific tissues with high cellular density and embedded vascular channels. *Sci. Adv.* **5**, (2019).
210. Sato, T. *et al.* Single Lgr5 stem cells build crypt-villus structures in vitro without a mesenchymal niche. *Nature* **459**, 262–265 (2009).
211. Sachs, N., Tsukamoto, Y., Kujala, P., Peters, P. J. & Clevers, H. Intestinal epithelial organoids fuse to form self-organizing tubes in floating collagen gels. *Dev.* **144**, 1107–1112 (2017).
212. Reid, J. A., Mollica, P. A., Bruno, R. D. & Sachs, P. C. Consistent and reproducible cultures of large-scale 3D mammary epithelial structures using an accessible bioprinting platform. *Breast Cancer Res.* **20**, 1–13 (2018).
213. Martínez-Ara, G., Stapornwongkul, K. S. & Ebisuya, M. Scaling up complexity in synthetic developmental biology. *Science (80-.).* **378**, 864–868 (2022).
214. Park, S. E. *et al.* Geometric engineering of organoid culture for enhanced organogenesis

in a dish. *Nat. Methods* **19**, (2022).
215. Ferreira, N. N. *et al.* Recent advances in smart hydrogels for biomedical applications: From self-assembly to functional approaches. *Eur. Polym. J.* **99**, 117–133 (2018).
216. Shang, J., Le, X., Zhang, J., Chen, T. & Theato, P. Trends in polymeric shape memory hydrogels and hydrogel actuators. *Polym. Chem.* **10**, 1036–1055 (2019).
217. Cheng, F. M., Chen, H. X. & Li, H. D. Recent progress on hydrogel actuators. *J. Mater. Chem. B* **9**, 1762–1780 (2021).
218. Choi, E. J., Ha, S., Lee, J., Premkumar, T. & Song, C. UV-mediated synthesis of pNIPAM-crosslinked double-network alginate hydrogels: Enhanced mechanical and shape-memory properties by metal ions and temperature. *Polymer (Guildf).* **149**, 206–212 (2018).
219. Luo, R., Wu, J., Dinh, N. D. & Chen, C. H. Gradient Porous Elastic Hydrogels with Shape-Memory Property and Anisotropic Responses for Programmable Locomotion. *Adv. Funct. Mater.* **25**, 7272–7279 (2015).
220. Romo-Uribe, A. & Albanil, L. POSS-Induced Dynamic Cross-Links Produced Self-Healing and Shape Memory Physical Hydrogels When Copolymerized with N-Isopropyl acrylamide. *ACS Appl. Mater. Interfaces* **11**, 24447–24458 (2019).
221. Halperin, A., Kröger, M. & Winnik, F. M. Poly(N-isopropylacrylamide) Phase Diagrams: Fifty Years of Research. *Angew. Chemie Int. Ed.* **54**, 15342–15367 (2015).
222. Capella, V. *et al.* Cytotoxicity and bioadhesive properties of poly-N-isopropylacrylamide hydrogel. *Heliyon* **5**, 1–19 (2019).
223. Zhao, L., Mok, S. & Moraes, C. Micropocket hydrogel devices for all-in-one formation, assembly, and analysis of aggregate-based tissues. *Biofabrication* **11**, 045013 (2019).
224. Chen, C. X. Q. *et al.* A multistep workflow to evaluate newly generated ipscs and their ability to generate different cell types. *Methods Protoc.* **4**, 50 (2021).
225. Schindelin, J. *et al.* Fiji: An open-source platform for biological-image analysis. *Nature Methods* **9**, 676–682 (2012).
226. Preibisch, S., Saalfeld, S. & Tomancak, P. Globally optimal stitching of tiled 3D microscopic image acquisitions. *Bioinformatics* **25**, 1463–1465 (2009).
227. Okajima, T., Harada, I., Nishio, K. & Hirotsu, S. Kinetics of volume phase transition in poly(N-isopropylacrylamide) gels. *J. Chem. Phys.* **116**, 9068–9077 (2002).
228. Xia, L. W. *et al.* Nano-structured smart hydrogels with rapid response and high elasticity. *Nat. Commun.* **4**, 1–11 (2013).
229. Lee, W. *et al.* Dispersible hydrogel force sensors reveal patterns of solid mechanical stress in multicellular spheroid cultures. *Nat. Commun.* **10**, 1–14 (2019).
230. Lubarsky, B. & Krasnow, M. A. Tube Morphogenesis: Making and Shaping Biological Tubes. *Cell* **112**, 19–28 (2003).
231. Cassel de Camps, C. *et al.* Hydrogel Mechanics Influence the Growth and Development of Embedded Brain Organoids. *ACS Appl. Bio Mater.* **5**, 214–224 (2022).
232. Kumar, S. & Weaver, V. M. Mechanics, malignancy, and metastasis: the force journey of a tumor cell. *Cancer Metastasis Rev.* **28**, 113–127 (2009).
233. Ma, Z., Sagrillo-Fagundes, L., Mok, S., Vaillancourt, C. & Moraes, C. Mechanobiological regulation of placental trophoblast fusion and function through extracellular matrix rigidity. *Sci. Rep.* **10**, (2020).

234. Hayward, M. K., Muncie, J. M. & Weaver, V. M. Tissue mechanics in stem cell fate, development, and cancer. *Dev. Cell* **56**, 1833–1847 (2021).
235. Ort, C., Lee, W., Kalashnikov, N. & Moraes, C. Disentangling the fibrous microenvironment: designer culture models for improved drug discovery. *Expert Opin. Drug Discov.* **00**, 1–13 (2020).
236. Khalilgharibi, N. & Mao, Y. To form and function: On the role of basement membrane mechanics in tissue development, homeostasis and disease. *Open Biol.* **11**, (2021).
237. Grossman, D. & Joanny, J. F. Instabilities and Geometry of Growing Tissues. *Phys. Rev. Lett.* **129**, (2022).
238. Goodwin, K. & Nelson, C. M. Mechanics of Development. *Dev. Cell* **56**, 240–250 (2021).
239. Ma, Z. *et al.* Biomimetic Micropatterned Adhesive Surfaces to Mechanobiologically Regulate Placental Trophoblast Fusion. *ACS Appl. Mater. Interfaces* **11**, 47810–47821 (2019).
240. Kim, H. Y. *et al.* Localized Smooth Muscle Differentiation Is Essential for Epithelial Bifurcation during Branching Morphogenesis of the Mammalian Lung. *Dev. Cell* **34**, 719–726 (2015).
241. Goodwin, K. *et al.* Smooth muscle differentiation shapes domain branches during mouse lung development. *Dev.* **146**, (2019).
242. Nelson, C. M., Inman, J. L. & Bissell, M. J. Three-dimensional lithographically defined organotypic tissue arrays for quantitative analysis of morphogenesis and neoplastic progression. *Nat. Protoc.* **3**, 674–678 (2008).
243. Nikolopoulou, E., Galea, G. L., Rolo, A., Greene, N. D. E. & Copp, A. J. Neural tube closure: Cellular, molecular and biomechanical mechanisms. *Dev.* **144**, 552–566 (2017).
244. Xue, X. *et al.* Mechanics-guided embryonic patterning of neuroectoderm tissue from human pluripotent stem cells. *Nat. Mater.* **17**, 633–641 (2018).
245. Stoeckli, E. T. Understanding axon guidance: Are we nearly there yet? *Dev.* **145**, (2018).
246. Huberman, A. D., Clandinin, T. R. & Baier, H. Molecular and Cellular Mechanisms of Lamina-specific Axon Targeting. *Cold Spring Harb. Perspect. Biol.* **2**, a001743 (2010).
247. Accogli, A., Addour-Boudrahem, N. & Srour, M. Neurogenesis, neuronal migration, and axon guidance. *Handb. Clin. Neurol.* **173**, 25–42 (2020).
248. Gomez, E. W., Chen, Q. K., Gjorevski, N. & Nelson, C. M. Tissue geometry patterns epithelial-mesenchymal transition via intercellular mechanotransduction. *J. Cell. Biochem.* **110**, 44 (2010).
249. Raghavan, S., Nelson, C. M., Baranski, J. D., Lim, E. & Chen, C. S. Geometrically controlled endothelial tubulogenesis in micropatterned gels. *Tissue Eng. - Part A* **16**, 2255–2263 (2010).
250. Nelson, C. M. *et al.* Emergent patterns of growth controlled by multicellular form and mechanics. *Proc. Natl. Acad. Sci. U. S. A.* **102**, 11594–11599 (2005).
251. Boghdady, C. M., Kalashnikov, N., Mok, S., McCaffrey, L. & Moraes, C. Revisiting tissue tensegrity: Biomaterial-based approaches to measure forces across length scales. *APL Bioeng.* **5**, 41501 (2021).
252. Moraes, C., Sun, Y. & Simmons, C. A. Solving the shrinkage-induced PDMS alignment registration issue in multilayer soft lithography. *J. Micromechanics Microengineering* **19**, 065015 (2009).

253. Park, S. E., Georgescu, A., Oh, J. M., Kwon, K. W. & Huh, D. Polydopamine-Based Interfacial Engineering of Extracellular Matrix Hydrogels for the Construction and Long-Term Maintenance of Living Three-Dimensional Tissues. *ACS Appl. Mater. Interfaces* **11**, 23919–23925 (2019).
254. Azizipour, N., Avazpour, R., Sawan, M., Rosenzweig, D. H. & Ajji, A. Uniformity of spheroids-on-a-chip by surface treatment of PDMS microfluidic platforms. *Sensors & Diagnostics* **1**, 750–764 (2022).
255. Boxshall, K. *et al.* Simple surface treatments to modify protein adsorption and cell attachment properties within a poly(dimethylsiloxane) micro-bioreactor. in *Surface and Interface Analysis* **38**, 198–201 (2006).
256. Cassel de Camps, C. *et al.* Compressive molding of engineered tissues via thermoresponsive hydrogel devices. *Lab Chip* (2023). doi:10.1039/D3LC00007A
257. Yeap, Y. J., Teddy, T. J. W., Lee, M. J., Goh, M. & Lim, K. L. From 2D to 3D: Development of Monolayer Dopaminergic Neuronal and Midbrain Organoid Cultures for Parkinson's Disease Modeling and Regenerative Therapy. *Int. J. Mol. Sci.* **24**, 2523 (2023).
258. Binder, L. I., Frankfurter, A. & Rebhun, L. I. The distribution of tau in the mammalian central nervous central nervous. *J. Cell Biol.* **101**, 1371–1378 (1985).
259. Papasozomenos, S. C. & Binder, L. I. Phosphorylation determines two distinct species of Tau in the central nervous system. *Cell Motil. Cytoskeleton* **8**, 210–226 (1987).
260. Gervasi, N. M. *et al.* The local expression and trafficking of tyrosine hydroxylase mRNA in the axons of sympathetic neurons. *RNA* **22**, 883–895 (2016).
261. Prakash, N. & Wurst, W. Development of dopaminergic neurons in the mammalian brain. *Cell. Mol. Life Sci.* **63**, 187–206 (2006).
262. Tidball, A. M. *et al.* Self-Organizing Single-Rosette Brain Organoids From Human Pluripotent Stem Cells. *bioRxiv* (2022). doi:10.2139/ssrn.3925254
263. Zhou, J., Kim, H. Y., Wang, J. H. C. & Davidson, L. A. Macroscopic stiffening of embryonic tissues via microtubules, RhoGEF and the assembly of contractile bundles of actomyosin. *Development* **137**, 2785–2794 (2010).
264. Herrera-Perez, R. M. & Kasza, K. E. Manipulating the patterns of mechanical forces that shape multicellular tissues. *Physiology* **34**, 381–391 (2019).